Characterisation of Mesozoic Depositional Systems along the Atlantic Passive Margin of Morocco. North Aaiun-Tarfaya Basin

A thesis submitted to the University of Manchester for the degree of Doctor of Philosophy in the Faculty of Science and Engeneering

2018

Angel I. Arantegui

School of Earth and Environmental Sciences

List of contents

Final Word Count: 38195

List of figures

List of tables

Abstract

Passive margin coastal basins are recipients of thick sedimentary successions with significant economic interest. Natural resources hosted in these sequences are being targeted around the globe. The evolution of passive margins predicted by classic thermal sag models is being challenged by a relatively recent body of studies highlighting “unexpected” vertical movements in the hinterland and basin during late syn- and post-rift stages. This new element of complexity has direct implications in predicting facies distribution and the volume, routing and type of sediment delivered to the basins.

The depositional style and evolution of the post-rift sedimentary sequences exposed onshore the Aaiun-Tarfaya Basin (ATB), Morocco, have been studied to characterise the early post rift depositional sequences to assess the relative control of eustacy versus local and regional tectonic movements in the hinterland.

The research has resulted in re-dating of a significant part of the northern ATB outcrops using bivalves and gastropods, previously ascribed to the Cretaceous, to a new Jurassic (Bathonian) and older age, which has implications for the prediction of offshore deepwater packages. Three depositional sequences have been described in this interval, with the overall succession exhibiting a deepening-upward transgressive profile from continental conglomerates and sandstones to shallow marine carbonates and fine-grined clastics. Each sequence shows a similar evolution from basal alluvial fan conglomerates to peritidal fine-grained sandstones, silts and interbedded microbial mats and shallow subtidal carbonates. Finally, they are capped by mixed carbonate-clastic shallow marine lagoon to ramp facies. A minimum thickness of 300 m containing age-diagnostic fossil groups was deposited during the Bathonian. This is coeval with a global eustatic sea-level fall evidencing the strong tectonic control on deposition.

The lower Cretaceous post-rift successions comprising proximal fluvial to shallow marine extensively exposed onshore Morocco have been logged along two dip profiles. This has been correlated with distal deep water turbiditic equivalent examined in Fuerteventura. The early Cretaceous was the time of onset and evolution of the large Tantan delta. The first outcrop-based sequence stratigraphic framework has been established for the area.

The pre-Aptian progradation of the Tantan delta was followed by subsequent regression and reworking. Four depositional sequences, bounded by amalgamated sequence boundary and transgressive surface, have been identified onshore. Offshore, in the inverted sections exposed in Fuerteventura, a Berriasian sand-prone deep-water fan facies is interpreted to record a Falling Stage System Tract, confidently dated with the discovery of ammonite fauna. The proximal onshore equivalent is represented by alluvial fan conglomerates exposed in extensive outcrops onshore and also penetrated by wells. The fans can be associated with faulted contacts with the basement and represent local sediment input on the basin margin. The thick stacked fluvial packages have a mean NNE palaeocurrent, and suggest a long distance regional drainage provenance from the Reguibat Shield. The Pre-Aptian sand-prone fluvial deposits show a significant thickness variation between transects, suggesting a possible structural control on differential subsidence.

The third sequence is represented by marine facies interpreted to record a regional transgression (TST) that can be traced across the entire area. This Aptian transgression is followed by aggradational/progradational fluvial (south) and peritidal to shoreface (north) units ascribed to a HST deposited in a homogeneously subsiding basin at this time. In the equivalent deep offshore sediments outcropping on Fuerteventura a large-scale fining-upward cycle of mud-prone turbidites with increasing carbonate and mud content upwards correlates with the sequence onshore.

The last sequences studied onshore are Albian peritidal to shoreface units. These show more distal facies towards the north, associated with the widespread Albian sea-level rise.

The results show an important tectonic-control on sedimentation during Middle Jurassic, when active faulting and local tectonics uplifted basement massifs that played a role in sediment distribution and provenance areas, followed by a complex interplay between tectonics and eustatic sea-level change during early Cretaceous.

Sand-dominated onshore sections contrast with the relatively sand-starved record offshore penetrated by exploration wells. Significant volumes of sediment were delivered to the basin as evidenced by km-scale sequences onshore and offshore. Enhanced subsidence on the proximal shelf may have trapped the coarser fraction, allowing mainly fine-grained sediment to be accumulated offshore.

Declaration

No portion of the work referred to in the thesis has been submitted in support of an application for another degree or qualification of this or any other university or other institute of learning.

Angel I. Arantegui

Copyright statement

Acknowledgments

I would like to thank the North Africa Research Group and the consortium of companies supporting it for the great opportunity I was offered with this project. Office National des Hydrocarbures et des Mines du Maroc (ONHYM) is also thanked for the logistic support in the numerous field seasons in Morocco.

I would like to express my gratitude to Professor Jonathan Redfern for giving me the opportunity of taking part in this research adventure and for his constant support and guidance. I would also like to thank my co-supervisor Dr Stefan Schröder for his patience with the carbonates, insightful comments and hours spent together at the microscope.

This PhD would not have been possible without the tremendous help and teaching skills in the field of Dr Rhodri Jerrett and all the time taken for constructive discussions that followed.

I want to express my sincere gratitude to Dr Luc Bulot for his palaeontological expertise, help in the field and for convincing me that the answer might was in the *Trigonias*…

Many thanks to Mike Simmons for his valuable comments on the foraminifers and Bruno Granier for his help with the algae.

I would like to grant a special acknowledge to my two office mates Aude and Tim for all the time we have spent together inside those walls. Thank you for your support, the good (and bad) banter and making the long hours a bit shorter. So much lived in 1.62… And although he has been far from Manchester, I wanted also some words for Remi… we will always have La Belle Vue.

I would like to thank all my field assistants for their effort, helpful discussions, enthusiasm and all the good moments and adventures in the field. Tim, Remi, Pablo, Nathan, Arne and Jianpeng, I could not have done it without your help.

I would not like to forget all my colleagues and friends I have been lucky enough to have during my time in Manchester and that have been there at some point during this trip to make it easier. Luz, Miquel, Eoin, Marcello, Sarah, Dan, Kevin, Leonardo, Chiara, Javi, Gianfranco, Georgina, Richard, Jonathan, Agus, Fabi, Rebeca, Michele Nawwar, Emmanuel, Max, Rashad, Brian, Gina, Julien, Lin, Francisco, Javier and Graciela. Thank you all for being there. My apologies to the ones I am certainly forgetting.

Last but not least; I would like to thank my family for their support and above all, my parents for always being there for me whenever I needed them. And finally Cristina for being strong until we finally reunited, easing the tough moments and making the good ones even better. *You're simply the best*…

Chapter 1

INTRODUCTION

1.1 Introduction

This thesis integrates extensive new outcrop descriptions and new biostratigraphic dating with available subsurface data to characterise the facies associations and produce a series of cross sections and depositional environment maps to constrain the Mesozoic early post-rift evolution and depositional systems along the eastern Central Atlantic Margin. It is a contribution to an on-going large-scale source-to-sink project along the Atlantic margin of NW Africa, involving the University of Manchester and the Technical University of Delft (The Netherlands) within the North Africa Research Group (NARG) consortium, sponsored by several oil companies.

Along the NW African margin several coastal basins were created after the breakup of Pangaea during the Mesozoic. These basins developed into a passive margin and are filled with km-thick syn- and post-rift sedimentary sequences. These Mesozoic sequences have been the target of intense hydrocarbon exploration from Morocco to Liberia. New hydrocarbon provinces are constantly being discovered, of which a significant gas discovery offshore Mauritania and Senegal (Great Tortue Complex) in early 2017, with more than 25 trillion cubic feet of gas, is the most recent example. However the offshore Morocco basins to-date have been less prolific, in part due to the available subsurface data and limited studies undertaken.

One of these under-explored basins is the Aaiun-Tarfaya Basin (Figure 1.1 and Figure 1.2). Thick depocenters in excess of 10 km (Ranke et al., 1982) accumulated offshore, where several oil shows and non-commercial discoveries (Figure 1.2) suggest future potential. Although subsurface data (wells) are sparse, this onshore part of the basin has extensive exposures of Palaeozoic and Mesozoic sections, which offer a valuable resource to better understand the depositional systems, control on the evolution of the system and develop regional depositional models.

1.1.1 Rationale for the project

The Mesozoic in the Aaiun-Tarfaya Basin became an important target as a potential host of reservoir facies in the 1950's. Between 1960-1962 the first three exploration wells (Figure 1.1) were drilled in the onshore Aaiun-Tarfaya Basin. Since then, a limited, but relatively steady and constant exploration activity in the area has yielded only poor results. The post-rift succession onshore and offshore can be broadly characterized as Jurassic carbonate platforms overlain by lower Cretaceous prograding

clastic deltas (i.e. Tantan and West Saharan/Boujdour deltas) and deep water equivalent. Jurassic carbonates and Cretaceous clastics plays have been systematically targeted, but only three sub-commercial discoveries (Figure 1.2) have been found to-date in the basin. This confirms a working petroleum system, but a better understanding is needed to unlock commercial quantities.

There are two proven reservoirs for the offshore discoveries. In the northern part of the Aaiun-Tarfaya Basin the oldest are Jurassic carbonates, with oil shows encountered in the Cap Juby and Sidi Moussa wells (Figure 1.1). These are fractured and brecciated upper Jurassic carbonates belonging to the Puerto Cansado Formation (defined from the Puerto Cansado-1 onshore well; Martinis and Visintin (1966)). The Jurassic succession was dated using microfossil assemblages from the Puerto Cansado-1 well (Viotti, 1966, 1965).

Cap Boujdour-1well offshore Boujdour encountered gas and condensate in the other main reservoir, the Cretaceous clastics (Figure 1.2) of the Jreibichat Formation associated with the development of the West Saharan Deltas (Ranke et al., 1982). The sand-prone facies offshore, associated with the development of the Tantan Delta in the area, have been one of the main targets of hydrocarbon exploration, but to-date sand-prone intervals are very scarce and thin in all the wells drilled offshore Morocco and their distribution remains poorly understood.

The lower Cretaceous proximal equivalents of the deep-water facies being targeted offshore are exposed onshore Morocco in the northern part of the Aaiun-Tarfaya Basin. Further outcrop-based works focused on mapping the Cretaceous successions (Choubert et al., 1966) and dating (Collignon, 1967, 1966). No previous onshore detailed sedimentological studies were performed in the area, with no previous vertical and lateral facies descriptions.

Kilometre-scale post-rift Mesozoic successions have been recorded in onshore wells in relatively proximal areas of the basin (3100 m in Chebeika-1 for instance; Figure 1.1). Understanding the mechanisms and interplay between tectonics, eustacy and climate that influence the sedimentary filling of coastal basins in passive margins was a key question to be addressed.

1.1.2 Aims of the project

Due to excellent exposures onshore Morocco of the lower Cretaceous succession (Tantan Formation; Martinis & Visintin, 1966), this project aims to re-evaluate the sedimentology of the coastal sections, and two transects inland following the main rivers (including revisiting sections first studied in the 1960's) in order to refine litho-, bio- and sequence stratigraphy.

The main aims include i) characterization of the entire Tantan Fm. in order to re-interpret the vertical and lateral succession of facies; ii) improve the biostratigraphic constrains in order to define the age of the sections and any key surfaces; iii) develop a sequence stratigraphic framework, defining progradational and retrogradational packages; iv) develop a model for the evolution of depositional environments and facies types; v) assess the controls on depositional systems, and vi) correlate the onshore section with available subsurface data offshore and Fuerteventura, in order to develop a predictive model for facies development offshore.

1.1.3 Objectives

The main objectives for this thesis are:

- Reinterpret the coastal sections in the northern tip of the Aaiun-Tarfaya Basin, next to Sidi Ifni, and sample extensively for biostratigraphy.
- Re-date the successions with new collections of macro and microfossils, pollen and spores.
- Construct a vertical composite sedimentary log along two parallel transects, Oued Draa and Oued Chebeika (Figure 1.1), and compare with the original descriptions and interpretations.
- Correlate the two transects assisted by biostratigraphic markers and sequence stratigraphy.
- Re-visit the distal deep-water equivalent of the Tantan Fm. exposed in Fuerteventura.

Figure 1.1. (Next page). Geographic overview of the study area. Sedimentary logs used on this thesis were collected at the green squares. Satellite image taken from GoogleEarth™.

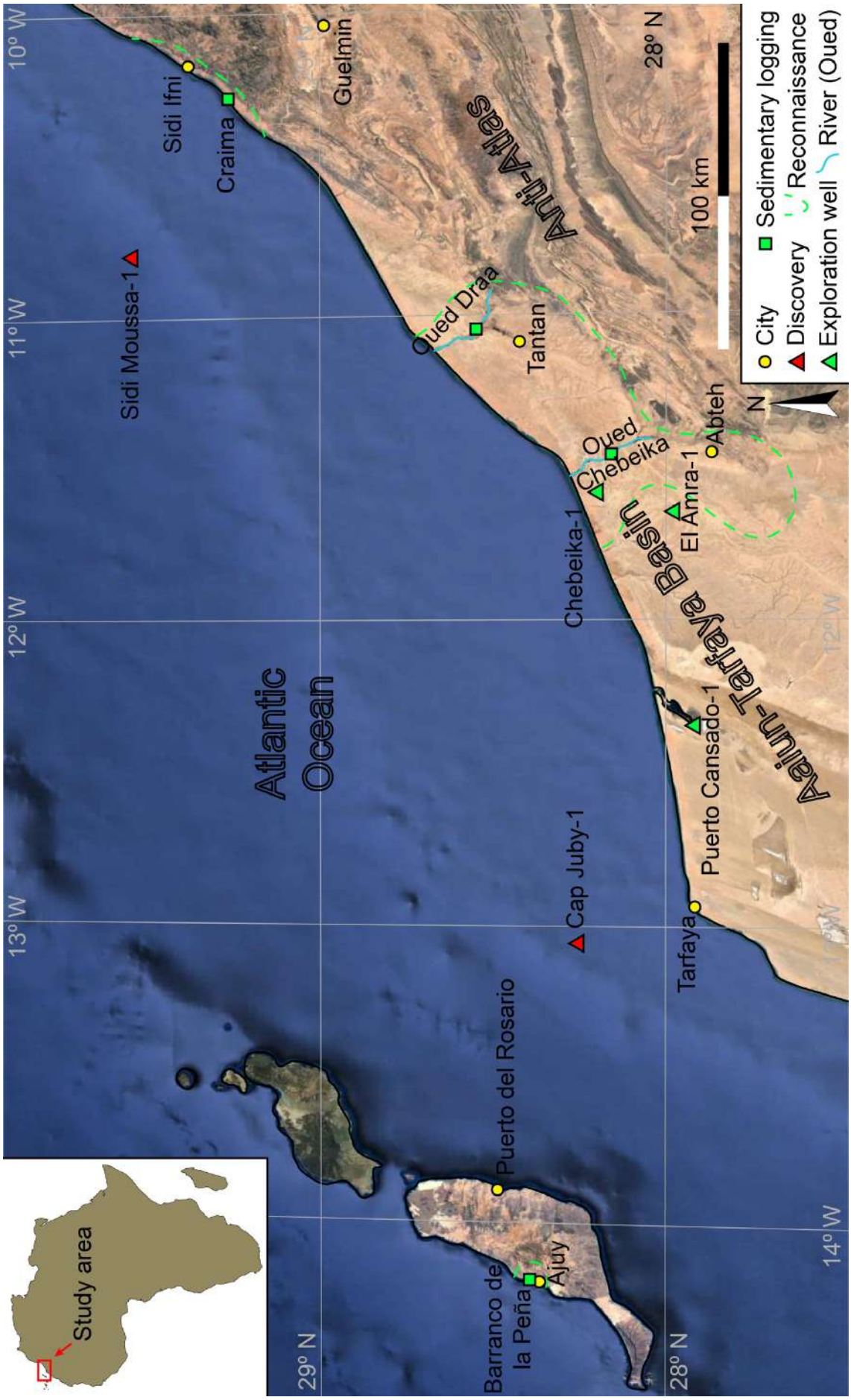
Atlantic Ocean
Anti-Atlas
Aaiun-Tarfaya Basin
Sidi Ifni
Craima
Guelmin
Sidi Moussa-1
Oued Draa
Tantan
Oued Chebeika
Abteh
El Amra-1
Chebeika-1
Cap Juby-1
Puerto Cansado-1
Tarfaya
Puerto del Rosario
Barranco de la Peña
Ajuy
Study area
City
Discovery
Exploration well
Sedimentary logging
Reconnaissance
River (Oued)
100 km
N
10° W
11° W
12° W
13° W
14° W
28° N
29° N

1.1.4 Methods and Datasets

The initial stage of the project involved an extensive literature review and search of geological maps of the study area. This was aided by remote reconnaissance sensing using GoogleEarth™ and ArcGIS® satellite imagery in order to define suitable locations to study. The final stage involved a reconnaissance in the field (Figure 1.1) in order to assess accessibility and quality of the successions.

The fieldwork focused on two areas onshore Morocco (Figure 1.1); one in the north, along coastal outcrops that were easily accessible, close to the town of Sidi Ifni; and the second in the south, inland, where the terrain is more remote, with the main outcrops located in wadis along two main rivers (i.e. Oued Draa and Oued Chebeika). The majority of the inland fieldwork was performed in very remote areas with difficult access requiring off-road driving and camping.

A third field locality was in Fuerteventura, which was visited in Year 1, as it allowed access to outcrops of equivalent age from the deep water environments. The 1 week fieldwork was undertaken north of the village of Ajuy, at the Barranco de la Peña (Figure 1.1).

Tectonic tilt of the sections is low to moderate around Sidi Ifni (0-30 degrees), low along both rivers in the south (0-10 degrees) and sub-vertical and overturned in Fuerteventura. Exposures around the Tantan area range from a few meters up to 80 m of stratigraphy. The low dip of the beds and near complete exposure allowed tracing of the section and generation of a vertical profile by moving up section, with allowance for the lateral displacement, in order to cover as much stratigraphy as possible and produce composite logs.

Fieldwork was performed by traditional sedimentary logging complemented with palaeocurrent measurements, sampling for petrographic and biostratigraphic purposes. Six field seasons were undertaken from 2014 to 2016, with a total of 18.5 weeks in the field.

121 samples for petrographic observations of stained thin sections under transmitted light microscope were examined in order to aid facies descriptions and identification of microfauna and cements. The majority of thin sections were prepared by Independent Petrographic Services Ltd (Aberdeen) and a few of them were prepared at the University of Manchester and at Keele University.

32 samples collected for palynological studies were prepared in Manchester and sent for identification to Palynological Laboratory Services Ltd (Wales), PetroStrat Ltd (Wales) and the National History Museum (London).

Data and interpretations generated by this PhD have contributed to and benefited from the low-temperature thermochronology and time-temperature modelling carried out by a parallel PhD project at the TU Delft University.

1.1.5 Thesis structure

This PhD thesis is presented in alternative format and includes five chapters. Chapters 2-4 have been prepared in paper-format and contributions of authors are outlined below.

Chapter 2: Constraining Mesozoic early post-rift evolution and depositional systems along the eastern Central Atlantic Margin

Prof. Jonathan Redfern (filed assistance, main-supervisor; discussion and manuscript review) Dr. Rhodri Jerrett (field assistance, discussion and manuscript review), Dr. Stefan Schröder (co-supervisor; discussion and manuscript review), Dr. Luc Bulot (discussion and field assistance), Dr. Stefano Monari and Dr. Roberto Gatto (gastropods and bivalve identification).

Chapter 3: Sedimentology of Lower Cretaceous fluvial to shallow marine deposits on the Central Atlantic passive margin; a case study in the Aaiun-Tarfaya Basin, Morocco

Prof. Jonathan Redfern (main-supervisor; discussion and manuscript review), Dr. Rhodri Jerrett (field assistance, discussion and manuscript review), Dr. Luc Bulot (discussion, fossil identification).

Chapter 4: Predicting Early Cretaceous deepwater turbiditic successions in the offshore Aaiun-Tarfaya Basin, southern Morocco: constraints from new data from Fuerteventura

Prof. Jonathan Redfern (main-supervisor; discussion and manuscript review), Dr. Tim Luber (field assistance, discussion), Dr. Luc Bulot (ammonite identification, discussion).

1.2 Geological setting

1.2.1 Tectono-stratigraphic history of NW Africa

The majority of northwest Africa comprises the West African Craton (WAC; Figure 1.2). The exact limits of the different terranes involved in the assembly of the WAC during the geological history of the Earth are still debated, however a good review of the role they played in the different orogenic cycles can be seen in (Ennih and Liégeois, 2008).

The WAC is a landmass that was mainly assembled in the Precambrian by different orogenic episodes (Eburnean and Pan-African I and II mainly). At the end of the Proterozoic it was part of the supercontinent Gondwana. The Palaeozoic witnessed the dismantling of Gondwana, drifting of cratonic shields and the assemblage again to form a new supercontinent, Pangaea. A number of orogenic phases, from the Ordovician onwards, resulted in collision of terranes that continued until Permian, culminating in the Variscan (Hercynian) Orogeny to form the supercontinent Pangaea. During this final event the western part of the WAC collided with the supercontinent Laurasia giving rise to the Variscan Ouachita-Appalachian-Mauritanides orogenic belt (Figure 1.3) whose effects on the African side can be observed from Morocco (Mesetas and Anti-Atlas) to Sierra Leone (Figure 1.2). This new supercontinent was short-lived and started to dismember soon after it was assembled at beginning of the Mesozoic.

This forms the underlying basement and tectonic framework that later influenced the west Moroccan basins' geometry, and provided the clastic input from the uplifted terranes.

The Mesozoic breakup of Pangaea along northwest Africa led to the opening of the Atlantic Ocean, closing of the Tethys Ocean and opening of the Mediterranean (Jansa and Wiedmann, 1982; Lehner and De Ruiter, 1977). The separation of Africa from North and South America evolved from a Triassic rift to Jurassic to recent passive margin. This tectonically stable passive margin was later affected by the Atlasic Orogeny along the northern edge of Africa during the Cenozoic (Figure 1.2).

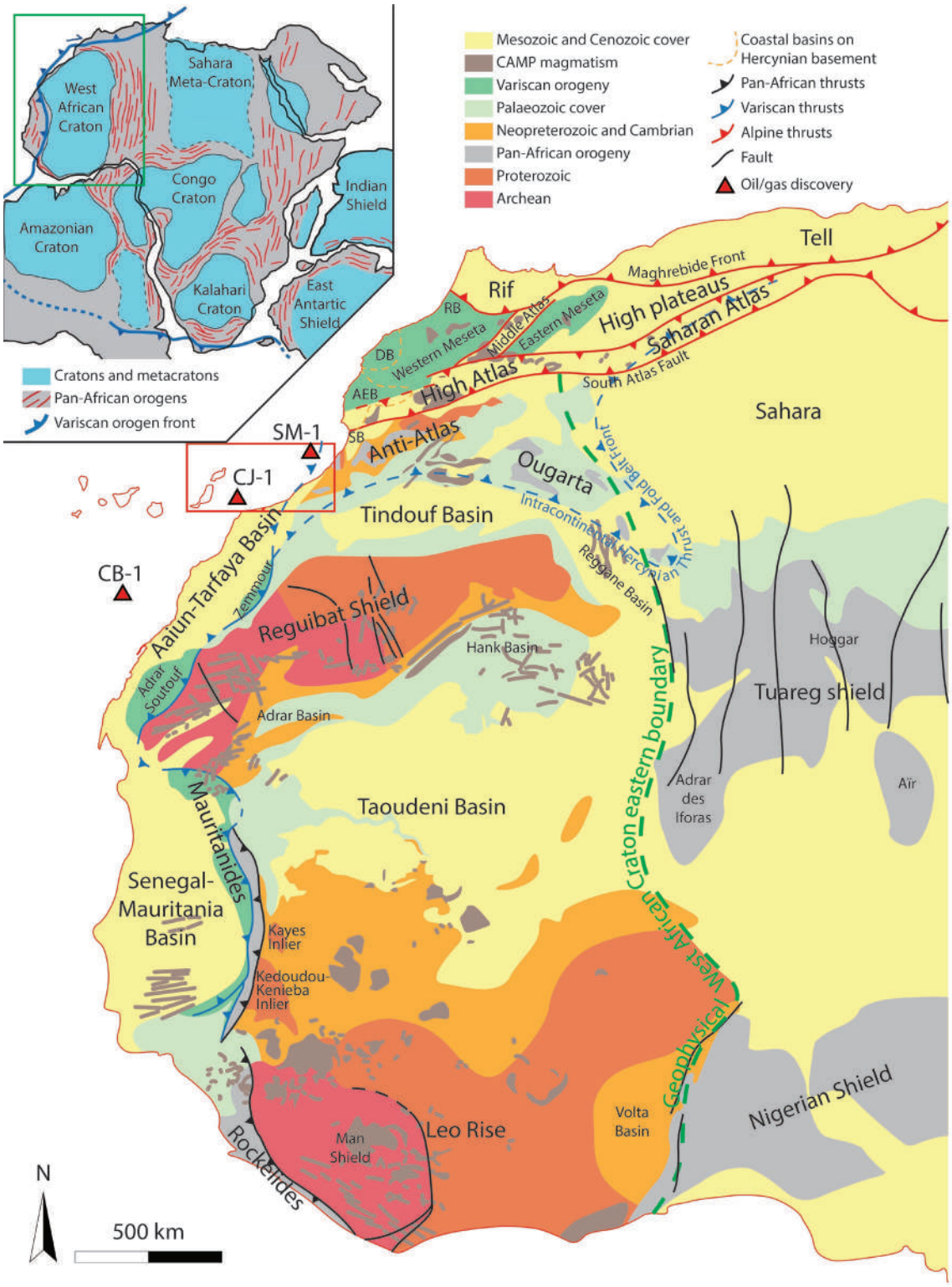

Figure 1.2. Main structural domains of northwest Africa (compiled after Boher et al., 1992; Bradley et al., 2015; Davison, 2005; Frizon de Lamotte et al., 2009; Hollard et al., 1985; Leprêtre et al., 2013; Meddah et al., 2017; Michard et al., 2008a; Schlüter, 2006; Villeneuve, 2005). Red rectangle represents the study area of this project. Inset: West African Craton (WAC) within the context of Africa and Gondwana supercontinent (modified after Michard, Frizon de Lamotte, Liégeois, Saddiqi, & Chalouan, 2008). The green rectangle in the inset highlights the expanded image in the figure.

The hinterland of northwest Africa has experienced syn- and post-rift km-scale vertical movements from the Jurassic to recent (e.g. Bertotti and Gouiza, 2012; Charton et al., 2017; Gouiza et al., 2017; Leprêtre et al., 2017, 2013), suggesting a more complex tectonic history that might be expected from a "classical" passive margin model, and these movements have a direct impact of sediment sourcing into the study area.

The segment between northwest Africa and north America (i.e. Central Atlantic) was the first to rift in the Triassic (Davison, 2005), followed by the south Atlantic in the early Cretaceous and North Atlantic. It led, along the northwest margin of Africa, to the development of grabens and half-grabens approximately oriented NE-SW (Bouatmani et al., 2004) and sub-parallel to the Variscan thrust and fold belt (Jansa and Wiedmann, (1982); Figure 1.2 and Figure 1.3). These restricted basins were filled with red coarse alluvial and fluvial syn-rift deposits and evaporites (Abou Ali et al., 2005, 2004; Brown, 1980; van Houten, 1977). Rifting progressed, and towards the end of the Triassic/beginning of the Jurassic extensive tholeiitic magmatic activity occurred belonging to the Central Atlantic Magmatic Province (CAMP; Figure 1.2; Davies et al., 2017; Marzoli et al., 2004; Nomade et al., 2007; Verati et al., 2007; Wilson and Guiraud, 1998). During the Jurassic, marine conditions were established in the Central Atlantic (Jansa and Wiedmann, 1982) although restricted conditions continued in some basins like Agadir-Essaouira Basin, and evaporite deposition extended into the Early Jurassic.

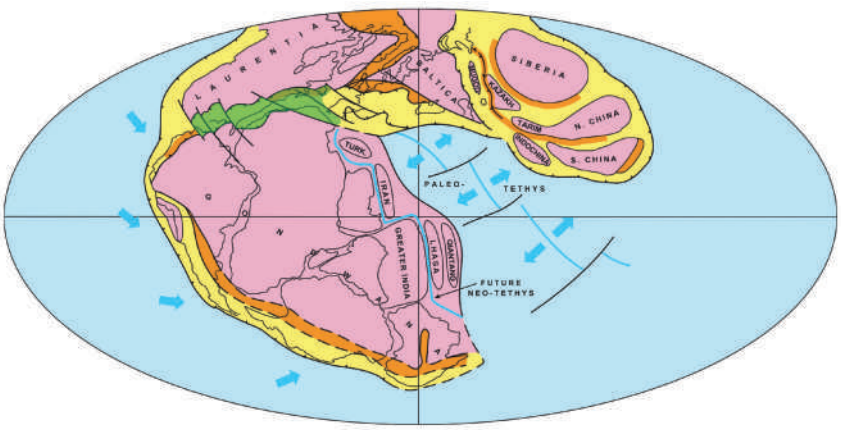

Figure 1.3. Permian (280 Ma) reconstruction of Pangaea with Palaeozoic orogens (from Matte, 2001). Orange: Ordovician to Devonian belts. Yellow: Devonian to Permian belts. The area shaded in green correspond approximately to the extension of the Ouachita-Appalachian-Mauritanide Variscan belt, part of which is bounding nowadays the eastern side of the Aaiun-Tarfaya Basin (see Figure 1.2).

The time of the end of rifting and onset of the drift phase and creation of the first oceanic crust is still unclear and debated (Biari et al., 2017; Davison, 2005; Klitgord and Schouten, 1986; Labails et al., 2010; Sahabi et al., 2004; Schettino and Turco, 2009; Scotese, 1991; Steiner et al., 1998 and references therein). The spreading was asymmetric and started earlier in the southern part of the Central Atlantic and progressed towards the north (Heyman, 1989). The first oceanic crust on the African side probably occurred at some point before the oldest magnetic anomaly (M25) registered in the Central Atlantic, within the Jurassic Magnetic Quiet Zone. Depending on plate reconstructions models, input parameters, dating of break-up unconformity, etc. an Early to Middle Jurassic age is obtained with an age as old as 200 Ma for the southern Central Atlantic (Sahabi et al., 2004; Schettino and Turco, 2009).

During the Jurassic open marine conditions were established in the Central Atlantic and a connection with the Pacific Ocean is speculated (Westermann, 1993). Overall, there is an increase in carbonate production throughout the Jurassic and sequences can reach more than 2 km in thickness in some segments of the margin. Carbonate platforms are widespread from the Middle Jurassic to late Jurassic/early Cretaceous (Jansa and Wiedmann, 1982) and more or less continuous carbonate build-ups extend from north to south along the northwest African margin defining the Jurassic palaeoshelf. In the deep basins marls, fine clastics and calciturbidites were deposited (Steiner et al., 1998). During the Berriasian lowstand terrigenous delivery increased into the basins, with a decrease in carbonate production during the early Cretaceous. Large prograding deltas were established along the margin, such as the Tan Tan and Boujdour systems (Choubert et al., 1966; Davison, 2005; Einsele and von Rad, 1979; Martinis and Visintin, 1966; Ranke et al., 1982) and the carbonate shelves became discontinuous. Towards the end of the early Cretaceous sea level started to rise and finer-grained sediments were deposited in the basins. The Late Cretaceous is a time of global high sea-level (Haq, 2014; Haq et al., 1987; Snedden and Liu, 2010). The Cenomanian-Turonian also coincides with low oxygen levels in oceanic waters and wide spread deposition of black shales occur in basin of northwest Africa (Macgregor and Moody, 1998).

The African plate experienced an overall eastward translation and anticlockwise movement during the Mesozoic, due to the opening of the South Atlantic Ocean (Klitgord and Schouten, 1986; Savostin et al., 1986; Schettino and Turco, 2009). Aptian

to Albian is the onset of a NNE-SSW convergence movement between the African and European plates (Schettino and Turco, 2011) that continued into the Cenozoic. The direct effect of this convergence in northwest Africa is the rising of the Rif and Tell mountain belts along the northern margin of Morocco and Algeria and the inversion of the Atlas basins during the Atlasic (Alpine) Orogeny. Triassic and Jurassic rift basins inverted in the Atlas system (including its prolongation towards the Tethys) to build the Atlas Orogen (Morocco, Algeria and Tunisia) during Oligocene to Early Miocene. Inversion ended in the early Burdigalian (Schettino and Turco, 2009).

1.2.2 The Aaiun-Tarfaya Basin

The opening of the Central Atlantic Ocean during the Triassic / Jurassic led to the development of a series of linked coastal passive margin basins along the west margin of Morocco in which sediments were deposited through the Mesozoic and Cenozoic (Figure 1.2).

The Aaiun-Tarfaya Basin (ATB; Figure 1.2) stretches along the present day Moroccan coastal margin for more than 1000 km, trending NE-SW with an approximate onshore area of 170000 km^2. It is bounded to the east by three important physiographic and geologic domains (Figure 1.2); i) the western termination of the Pan-African and Variscan Anti-Atlas mountain belt to the NE, ii) the Precambrian and Palaeozoic Tindouf/Zag Basin to the E and iii) the Precambrian terrains of the Reguibat Shield to the SE. Atlasian compression in northwest Africa from Late Cretaceous did not result in any significant deformation south of the South Atlas Fault. The Mesozoic sedimentary fill of the ATB largely lies gently tilted or even horizontal. Consequently, most of the sediments exposed onshore are Jurassic and Cretaceous.

Since the pioneering work in the 1940's to 1960's on the regional geology (e.g. Alia Medina, 1952, 1945; Choubert and Marçais, 1956; Martinis and Visintin, 1966; Querol, 1966), few outcrop-based studies have been published on the Mesozoic in the ATB.

A general overview of the stratigraphy and evolution of the Aaiun-Tarfaya Basin follows, although differences from north to south exist and will be highlighted later (Figure 2.2).

Definition of the Triassic to upper Jurassic stratigraphy had been limited to data from onshore and offshore exploration wells, drilled from the 1960´s onwards. Ages are mostly derived from the micropaleontological survey of the Puerto Cansado-1 well

(Figure 1.1; Viotti, 1966) and subsequent reinterpretation by du Dresnay (1988) and Bouaouda (2004). The oldest Mesozoic sediments are coarse alluvial and fluvial terrigenous deposits delivered to the basin during the rift stage (AbouAli et al., 2005, 2004; Choubert et al., 1966; Martinis and Visintin, 1966). These are associated with thick evaporite sequences deposited offshore during Early Norian.

Within this study new age dating for the coastal sections will be presented that allows much improved definition and reassignment of previously mapped Cretaceous undifferentiated section as Middle Jurassic or older. Open marine conditions were only established in the Sinemurian (AbouAli et al., 2005; Davison, 2005; du Dresnay, 1988; Zühlke et al., 2004), followed in the Pliensbachian to Callovian by establishment of a carbonate platform, then regressive marine sandstones and finally a renewed transgression leading to deposition of open marine carbonates. Offshore, well and seismic data indicate the late Jurassic Puerto Cansado Fm. is represented by an extensive carbonate platform with reefal build-ups along the platform margin (AbouAli et al., 2005; Michard et al., 2008b). Salt remobilisation started in the early Cretaceous, representing the dominant structural driving force in this period (Michard et al., 2008b; Zühlke et al., 2004). The platform margin slope collapsed during the Berriasian eustatic lowstand, and at this time some of the Jurassic succession was eroded and redeposited in the deep basin (Steiner et al., 1998).

The precise extent and subdivision of the lower Cretaceous section is poorly constrained in the literature due to the almost total lack of diagnostic fossils (Grosheny et al., 2012; Viotti, 1966). The Berriasian to Aptian in the Aaiun-Tarfaya Basin is dominated by the Tantan and Boujdour fluvio-deltaic systems (Tantan and Jreibichat Formations) which prograded towards the NW (AbouAli et al., 2005; Ranke et al., 1982).

In the NW outer shelf area the lower Cretaceous succession consists of carbonates to fine clastic deposits. The southern outer shelf is divided into a Berriasian to middle Barremian carbonate succession followed by clastic deposits of Upper Barremian to Aptian age. The overlying upper Aptian to upper Campanian interval is much better dated by the macro- and microfaunal succession from the onshore sections from Tantan to the south of Tarfaya (Collignon, 1967, 1966; El Albani, 1995; El Albani et al., 1999; Freneix, 1972; Grosheny et al., 2012; Kuhnt et al., 2009; Wiedmann et al., 1982, 1978).

An open marine outer shelf to shelf margin environment developed during the Albian (Aguidir Fm.; Martinis and Visintin, 1966) coinciding with the beginning of a general

transgression. Increasing paleobathymetry during the Cenomanian to Coniacian (Snedden and Liu, 2010) coincided with oceanic anoxic conditions, and deposition of organic rich clay and marls. The Upper Cretaceous Lower Lebtaina Fm. comprises mudstones deposited in a deep open marine outer shelf environment in the Tarfaya Basin (AbouAli et al., 2005; Davison, 2005).

The end of the Cretaceous marks the onset of the convergence between the African and European plates, which resulted in the inversion of the Atlas basins and development of the Atlas Mountain Range. The Tertiary Atlasic compression did not result in any significant deformation south of the South Atlas Fault, and as such the Mesozoic sedimentary fill of the Aaiun-Tarfaya Basin remains largely horizontal or only gently tilted.

1.3 References

AbouAli, N., Chellaie, E.H., Nahim, M., 2004. Anatomie d'une marge passive hybride. Marge Ifni/Tan-Tan (sud du Maroc) au Mesozoique: apports des donnees geophysiques. Estud. Geológicos 60, 111–121. doi:10.3989/egeol.04603-683

AbouAli, N., Hafid, M., Chellaï, E.H., Nahim, M., Zizi, M., 2005. Structure de socle, sismostratigraphie et héritage structural au cours du rifting au niveau de la marge d'Ifni/Tan-Tan (Maroc sud-occidental). Comptes Rendus Geosci. 337, 1267–1276. doi:10.1016/j.crte.2005.07.003

Alia Medina, M., 1952. Bosquejo geológico del Sahara Español. Mapa. Consejo Superior de Investigaciones Cientificas, Madrid.

Alia Medina, M., 1945. Características morfográficas y geológicas de la zona septentrional del Sahara español. Consejo Superior de Investigaciones Cientificas, Madrid.

Bertotti, G., Gouiza, M., 2012. Post-rift vertical movements and horizontal deformations in the eastern margin of the Central Atlantic: Middle Jurassic to Early Cretaceous evolution of Morocco. Int. J. Earth Sci. 101, 2151–2165. doi:10.1007/s00531-012-0773-4

Biari, Y., Klingelhoefer, F., Sahabi, M., Funck, T., Benabdellouahed, M., Schnabel, M., Reichert, C., Gutscher, M.-A., Bronner, A., Austin, J.A., 2017. Opening of the Central Atlantic Ocean: implications for geometric rifting and asymmetric initial

seafloor spreading after continental breakup. Tectonics 1–22. doi:10.1002/2017TC004596

Boher, M., Abouchami, W., Michard, A., Albarede, F., Arndt, N.T., 1992. Crustal Growth in West Africa at 2.1 Ga. J. Geophisical Res. 97, 345–369. doi:10.1029/91JB01640

Bouaouda, M.S., 2004. Le bassin atlantique marocain d'El Jadida-Agadir : Stratigraphie, paléogéographie, géodynamique et microbiostratigraphie de la série Lias-Kimméridgien. Université Mohammed V, Rabat.

Bouatmani, R., Ahmamou, M., El Ouarghioui, A., Medina, F., El Mourabit, A., Daoudi, L., 2004. Les environnements de dépôt des formation triasiques de la région de Meskala (bassin d'Essaouira, Maroc): apport de l'analyse des diagraphies et des carottes. Bull. l'Institut Sci. 26, 49–67.

Bradley, D.C., Motts, H.A., Horton, J.D., Giles, S., Taylor, C.D., 2015. Geologic map of Mauritania, in: Taylor, C.D. (Ed.), Second Project de Renforcement Institutionnel Du Secteur Minier de La République Islamique de Mauritanie (PRISM-II). U.S. Geological Survey.

Brown, R., 1980. Triassic rocks of Argana Valley, southern Morocco, and their regional structural implications. Am. Assoc. Pet. Geol. Bull. 64, 988–1003.

Charton, R., Bertotti, G., Arantegui, A., Bulot, L.G., 2018. The Sidi Ifni transect across the rifted margin of Morocco (Central Atlantic): Vertical movements constrained by low-temperature thermochronology. J. African Earth Sci.

Choubert, G., Faure-Muret, A., Hottinger, L., 1966. Aperçu géologique du bassin côtier de Tarfaya, in: Le Bassin Côtier de Tarfaya (Maroc Méridional). Notes et Mém. Serv. Géol. Maroc, 175.

Choubert, G., Marçais, J., 1956. Introduction géologique. Les grands traits de la Géologie du Maroc, in: Lexique Stratigraphique Du Maroc. Notes et Mém. Serv. Géol. Maroc.

Collignon, M., 1967. Les ammonites crétacées du bassin côtier de Tarfaya, Sud marocain. C. R. ACAD. Sc. PARIS 264, 1390–1392.

Collignon, M., 1966. Les céphalopodes crétacés du bassin côtier de Tarfaya: relations stratigraphiques et paléontologiques, in: Notes et Mém. Serv. Géol. Maroc, 175.

pp. 10–149.

Davies, J.H.F.L., Marzoli, A., Bertrand, H., Youbi, N., Ernesto, M., Schaltegger, U., 2017. End-Triassic mass extinction started by intrusive CAMP activity. Nat. Commun. 8, 15596. doi:10.1038/ncomms15596

Davison, I., 2005. Central Atlantic margin basins of North West Africa: geology and hydrocarbon potential (Morocco to Guinea). J. African Earth Sci. 43, 254–274. doi:10.1016/j.jafrearsci.2005.07.018

du Dresnay, R., 1988. Répartition des dépôts carbonatés du Lias inférieur et moyen le long dela côte atlantique du Maroc: conséquences sur la paléogéographie del'Atlantique naissant. J. African Earth Sci. 7, 385–396.

Einsele, G., von Rad, U., 1979. Facies and paleoenvironment of Lower Cretaceous sediments at DSDP Site 397 and in the Aaiun Basin (Northwest Africa), in: von Rad, U., Ryan, W.B.F. (Eds.), Init Repts Deep Sea Drilling Project, v 47, Part 1. Texas A & M University, Ocean Drilling Program, College Station, TX, United States, pp. 559–571. doi:10.2973/dsdp.proc.47-1.126.1979

El Albani, A., 1995. Les formations du Crétacé Supérieur du Bassin de Trafaya (Maroc Méridional): Sédimentologie et géochimie. Université des Sciences et Technologies de Lille.

El Albani, A., Kuhnt, W., Luderer, F., Herbin, J.P., Caron, M., 1999. Palaeoenvironmental evolution of the Late Cretaceous sequence in the Tarfaya Basin (southwest of Morocco), in: Cameron, N.R., Bate, R.H., Clure, V.S. (Eds.), The Oil and Gas Habitats of the South Atlantic. Geological Society, London, Special Publications, pp. 223–240. doi:10.1144/gsl.sp.1999.153.01.14

Ennih, N., Liégeois, J.-P. (Eds.), 2008. The Boundaries of the West African Craton, Geological Society, London, Special Publications. doi:10.1144/SP297.0

Freneix, S., 1972. Les mollusques bivalves crétacés du bassin côtier de Tarfaya (Maroc méridional). Notes Mémoires du Serv. géologique du Maroc 228, 49–255.

Frizon de Lamotte, D., Leturmy, P., Missenard, Y., Khomsi, S., Ruiz, G., Saddiqi, O., Guillocheau, F., Michard, A., 2009. Mesozoic and Cenozoic vertical movements in the Atlas system (Algeria, Morocco, Tunisia): An overview. Tectonophysics 475, 9–28. doi:10.1016/j.tecto.2008.10.024

Gouiza, M., Charton, R., Bertotti, G., Andriessen, P., Storms, J.E.A., 2017. Post-Variscan evolution of the Anti-Atlas belt of Morocco constrained from low-temperature geochronology. Int. J. Earth Sci. 106, 593–616. doi:10.1007/s00531-016-1325-0

Grosheny, D., Nourrisaid, I., Ferry, S., Bulot, L., Masrour, M., Bettar, I., Aoutem, M., Essafraoui, B., 2012. La série apto-albienne du bassin marginal de Tarfaya (Maroc méridional), in: Les Évènements de l'Aptien-Albien. pp. 23–27.

Haq, B.U., 2014. Cretaceous eustasy revisited. Glob. Planet. Change 113, 44–58. doi:10.1016/j.gloplacha.2013.12.007

Haq, B.U., Hardenbol, J., Vail, P.R., 1987. Chronology of fluctuating sea levels since the triassic. Science 235, 1156–1167. doi:10.1126/science.235.4793.1156

Heyman, M.A.W., 1989. Tectonic and depositional history of the Moroccan continental margin, in: Tankard, A.J., Balkwill, H.R. (Eds.), Extensional Tectonics and Stratigraphy of the North Atlantic Margins. AAPG Special Publications Memoir 46, pp. 323–340.

Hollard, H., Choubert, G., Bronner, G., Marchand, J., Sougy, J.M.A., 1985. Carte géologique du Maroc; Echelle: 1/1000 000. Notes Mém. Serv. Géol. Maroc 260.

Jansa, L.F., Wiedmann, J., 1982. Mesozoic-Cenozoic development of the Eastern North American and Northwest African continental margins: A comparison, in: von Rad, U., Hinz, K., Sarnthein, M., Seibold, E. (Eds.), Geology of the Northwest African Continental Margin. Springer Verlag Berlin Heidelberg New York, pp. 215–269.

Klitgord, K.D., Schouten, H., 1986. Plate kinematics of the central Atlantic, in: Vogt, P.R., Tucholke, B.E. (Eds.), The Geology of North America, Volume M, The Western North Atlantic Region. Geological Society of America, pp. 351–378.

Kuhnt, W., Holbourn, A., Gale, A., Chellai, E.H., Kennedy, W.J., 2009. Cenomanian sequence stratigraphy and sea-level fluctuations in the Tarfaya Basin (SW Morocco). Geol. Soc. Am. Bull. 121, 1695–1710. doi:10.1130/B26418.1

Labails, C., Olivet, J.-L., Aslanian, D., Roest, W.R., 2010. An alternative early opening scenario for the Central Atlantic Ocean. Earth Planet. Sci. Lett. 297, 355–368. doi:10.1016/j.epsl.2010.06.024

Lehner, P., De Ruiter, P.A.C., 1977. Structural history of Atlantic Margin of Africa.

Am. Assoc. Pet. Geol. Bull. 61, 961–981.

Leprêtre, R., Barbarand, J., Missenard, Y., Gautheron, C., Pinna-jamme, R., Saddiqi, O., 2017. Mesozoic evolution of NW Africa: implications for the Central Atlantic Ocean dynamics. J. Geol. Soc. London.

Leprêtre, R., Barbarand, J., Missenard, Y., Leparmentier, F., Frizon de Lamotte, D., 2013. Vertical movements along the northern border of the West African Craton: the Reguibat Shield and adjacent basins. Geol. Mag. 151, 885–898. doi:10.1017/S0016756813000939

Macgregor, D.S., Moody, R.T.J., 1998. Mesozoic and Cenozoic petroleum systems of North Africa, in: Macgregor, D.S., Moody, R.T.J., Clark-Lowes, D.D. (Eds.), Petroleum of North Africa. The Geological Society, London, Special Publications, pp. 201–216.

Martinis, B., Visintin, V., 1966. Données géologiques sur le bassin sédimentaire côtier de Tarfaya (Maroc méridional), in: Reyre, D. (Ed.), Bassin Sedimentaires Du Littoral Africain. Union Internationale des sciences géologiques, Paris, pp. 13–26.

Marzoli, A., Bertrand, H., Knight, K.B., Cirilli, S., Buratti, N., Vérati, C., Nomade, S., Renne, P.R., Youbi, N., Martini, R., Allenbach, K., Neuwerth, R., Rapaille, C., Zaninetti, L., Bellieni, G., 2004. Synchrony of the Central Atlantic magmatic province and the Triassic-Jurassic boundary climatic and biotic crisis. Geology 32, 973–976. doi:10.1130/G20652.1

Matte, P., 2001. The Variscan collage and orogeny (480-290 Ma) and the tectonic definition of the Armorica microplate: A review. Terra Nov. 13, 122–128. doi:10.1046/j.1365-3121.2001.00327.x

Meddah, A., Bertrand, H., Seddiki, A., Tabeliouna, M., 2017. The triassic-liassic volcanic sequence and rift evolution in the saharan atlas basins (Algeria). Eastward vanishing of the central Atlantic magmatic province. Geol. Acta 15, 11–23. doi:10.1344/GeologicaActa2017.15.1.2

Michard, A., Frizon de Lamotte, D., Liégeois, J.-P., Saddiqi, O., Chalouan, A., 2008a. Conclusion: Continental Evolution in Western Maghreb, in: Michard, A., Saddiqi, O., Chalouan, A., Frizon de Lamotte, D. (Eds.), Continental Evolution, The Geology of Morocco. pp. 395–404.

Michard, A., Saddiqi, O., Chalouan, A., Frizon de Lamotte, D., 2008b. Continental evolution: The geology of Morocco: Structure, stratigraphy, and tectonics of the Africa-Atlantic-Mediterranean triple junction.

Nomade, S., Knight, K.B., Beutel, E., Renne, P.R., Verati, C., Féraud, G., Marzoli, A., Youbi, N., Bertrand, H., 2007. Chronology of the Central Atlantic Magmatic Province: Implications for the Central Atlantic rifting processes and the Triassic-Jurassic biotic crisis. Palaeogeogr. Palaeoclimatol. Palaeoecol. 244, 326–344. doi:10.1016/j.palaeo.2006.06.034

Querol, R., 1966. Regional geology of the Spanish Sahara, in: Bassins Sédimentaires Du Littoral Africain. pp. 27–39.

Ranke, U., von Rad, U., Wissmann, G., 1982. Stratigraphy, facies and tectonic development of the On and offshore Aaiun-Tarfaya basin - a review, in: von Rad, U., Hinz, K., Sarnthein, M., Seibold, E. (Eds.), Geology of the Northwest African Continental Margin. Springer-Verlag, pp. 86–105.

Sahabi, M., Aslanian, D., Olivet, J.-L., 2004. Un nouveau point de départ pour l'histoire de l'Atlantique central. Comptes Rendus Geosci. 336, 1041–1052. doi:10.1016/j.crte.2004.03.017

Savostin, L.A., Sibuet, J.-C., Zonenshain, L.P., Le Pichon, X., Roulet, M.-J., 1986. Kinematic evolution of the Tethys belt from the Atlantic ocean to the pamirs since the Triassic. Tectonophysics 123, 1–35. doi:10.1016/0040-1951(86)90192-7

Schettino, A., Turco, E., 2011. Tectonic history of the western Tethys since the Late Triassic. Geol. Soc. Am. Bull. 123, 89–105. doi:10.1130/B30064.1

Schettino, A., Turco, E., 2009. Breakup of Pangaea and plate kinematics of the central Atlantic and Atlas regions. Geophys. J. Int. 178, 1078–1097. doi:10.1111/j.1365-246X.2009.04186.x

Schlüter, T., 2006. Geological Atlas of Africa: with Notes on Stratigraphy, Tectonics, Economic Geology, Geohazard and Geosites of Each Country, Geological Atlas of Africa. Springer Verlag Berlin Heidelberg. doi:10.2113/gsecongeo.103.6.1379

Scotese, C.R., 1991. Jurassic and cretaceous plate tectonic reconstructions. Palaeogeogr. Palaeoclimatol. Palaeoecol. 87, 493–501. doi:10.1016/0031-0182(91)90145-H

Snedden, J.W., Liu, C., 2010. A Compilation of Phanerozoic Sea-Level Change ,

Coastal Onlaps and Recommended Sequence Designations. Am. Assoc. Pet. Geol. Search Discov. Artic. 40594 40594, 2004–2006.

Steiner, C., Hobson, A., Favre, P., Stampfli, G.M., Hernandez, J., 1998. Mesozoic sequence of Fuerteventura (Canary Islands): Witness of Early Jurassic sea-floor spreading in the central Atlantic. Geol. Soc. Am. Bull. 110, 1304–1317. doi:10.1130/0016-7606(1998)110<1304

van Houten, F.B., 1977. Triassic-Liassic deposits of Morocco and Eastern North America: comparison. Am. Assoc. Pet. Geol. Bull. 61, 79–99.

Verati, C., Rapaille, C., Féraud, G., Marzoli, A., Bertrand, H., Youbi, N., 2007. 40Ar/39Ar ages and duration of the Central Atlantic Magmatic Province volcanism in Morocco and Portugal and its relation to the Triassic-Jurassic boundary. Palaeogeogr. Palaeoclimatol. Palaeoecol. 244, 308–325. doi:10.1016/j.palaeo.2006.06.033

Villeneuve, M., 2005. Paleozoic basins in West Africa and the Mauritanide thrust belt. J. African Earth Sci. 43, 166–195. doi:10.1016/j.jafrearsci.2005.07.012

Viotti, C., 1966. Resultats stratigraphiques du sondage Puerto Cansado 1 du bassin cotier de Tarfaya. Notes Mém. Serv. Géol. Maroc 175.

Viotti, C., 1965. Microfaunes et microfaciès du sondage Puerto Cansado 1 (Maroc méridional, province de Tarfaya), in: Mém. BRGM, 32, Colloque Intern. Micropaléontol. Dakar, pp. 29–40.

Westermann, G.E.G., 1993. Global bio-events in mid-Jurassic ammonites controlled by seaways, in: The Ammonoidea: Environment, Ecology and Evolutionary Change. pp. 187–226.

Wiedmann, J., Butt, A., Einsele, G., 1982. Cretaceous stratigraphy, environment, and subsidence history at the Moroccan continental margin, in: von Rad, U., Hinz, K., Sarnthein, M., Seibold, E. (Eds.), The Geology of the Northwest African Continental Margin. Springer Verlag Berlin Heidelberg, New York, pp. 366–395.

Wiedmann, J., Butt, A., Einsele, G., 1978. Vergleich von marokkanischen Kreide-Küstenaufschlüssen und Tiefseebohrungen (DSDP): Stratigraphie, Paläoenvironment und Subsidenz an einem passiven Kontinentalrand. Geol. Rundschau 67, 454–508. doi:10.1007/BF01802800

Wilson, M., Guiraud, R., 1998. Late Permian to Recent magmatic activity on the African-Arabian margin of Tethys, in: Macgregor, D.S., Moody, R.T.J., Clark-Lowes, D.D. (Eds.), Petroleum Geology of North Africa. Geological Society, London, Special Publications, pp. 231–263.

Zühlke, R., Bouaouda, M.S., Ouajhain, B., Bechstädt, T., Leinfelder, R., 2004. Quantitative Meso-/Cenozoic development of the eastern Central Atlantic continental shelf, western High Atlas, Morocco. Mar. Pet. Geol. 21, 225–276. doi:10.1016/j.marpetgeo.2003.11.014

Chapter 2

Constraining Mesozoic early post-rift evolution and depositional systems along the eastern Central Atlantic Margin

Constraining Mesozoic early post-rift evolution and depositional systems along the eastern Central Atlantic Margin

ANGEL ARANTEGUI[1], RHODRI JERRETT[1], STEFAN SCHRÖDER[1], LUC BULOT[1,2], STEFANO MONARI[3], ROBERTO GATTO[3] and JONATHAN REDFERN[1]

1 School of Earth and Environmental Sciences, University of Manchester, M13 9PL, Manchester, United Kingdom (E-email: angel.arantegui@manchester.ac.uk)

2 Aix-Marseille Université, CNRS, IRD, Coll France, CEREGE

3 Dipartimento di Geoscienze, Università di Padova

2.1 Abstract

Cretaceous to Cenozoic successions have been known onshore the Aaiun-Tarfaya Basin for decades. New age dating integrated with detailed sedimentology has identified for the first time a Middle Jurassic section along the eastern margin of the Central Atlantic in the Aaiun-Tarfaya Basin of Morocco that provides a valuable record of the syn- and early post-rift evolution of the basin.

Mesozoic exposures on the north-eastern margin of the Aaiun-Tarfaya Basin, on the coastal flank of the Ifni Inlier, expose a thick unit of red beds that, despite their sedimentological affinity to Triassic or Early Jurassic deposits regionally in Morocco, had previously been assigned an early Cretaceous age, based on limited or non-conclusive fauna. Detailed sedimentary facies analysis and new biostratigraphy has revised this interpretation, and gives a definitive Bathonian age for the conformable overlying mixed clastic carbonate succession. This suggests the section records the most southerly Triassic/Liassic to Middle Jurassic outcrop in NW Africa, and a valuable control point to understand the basin dynamics with implications for offshore exploration.

Three lithostratigraphic subdivisions have been informally proposed for this succession, comprising continental red beds at the base, overlain by intertidal clastics and microbial carbonates and capped by a mixed siliciclastic-carbonate shallow marine section. The overall transgressive trend, subdivided into three sequences, is opposed to the eustatic signal for the Bathonian. Enhanced subsidence in the basin is the main driver for sedimentation, modulated by local post-rift tectonic pulses of the exhuming Western Anti-Atlas and the eustatic sea-level drop.

Subsidence rate increases during the Middle Jurassic and more carbonates are deposited towards the south of the basin. Exhumation ceased by the early Callovian, reducing clastic input to the region and allowing the development of extensive carbonate platforms.

Comparison with other coastal basin fills along the Moroccan margin shows varying depositional fill, which is interpreted to record the impact of underlying pre-Mesozoic structural framework and local tectonic influence on sedimentation. This is important to recognise and has impact for offshore exploration for hydrocarbons and understanding of the development of passive margins through time.

Keywords:
Northwest Africa, Tarfaya Basin, Anti-Atlas, Jurassic, Bathonian

2.2 Introduction

In the Aaiun-Tarfaya Basin (ATB; Figure 2.1), previous outcrop studies are sparse and the stratigraphy and sedimentology of the Mesozoic successions poorly constrained. Syn- and early post-rift sediments were only recognised in well penetrations, frequently with poor biostratigraphic control. In this study we offer a significant additional contribution to the dating, stratigraphy and sedimentology of the Middle Jurassic part of the succession, re-interpreting outcrops exposed along the Atlantic margin of the Ifni inlier. The results allow improved understanding of the depositional system and evolution during this time interval, with new models presented. The data also indicate a link between the depositional history of the ATB and the tectonic history of the Anti-Atlas.

Mesozoic successions along the Atlantic margin of Morocco are an important target for hydrocarbon exploration in the offshore. Sedimentary basins still remain relatively underexplored and depositional systems through time are not sufficiently understood. These results offer an important contribution in characterising this poorly documented stratigraphic interval in the ATB. The proposed new litho- and sequence stratigraphic framework offers a valuable dataset that will aid regional correlation.

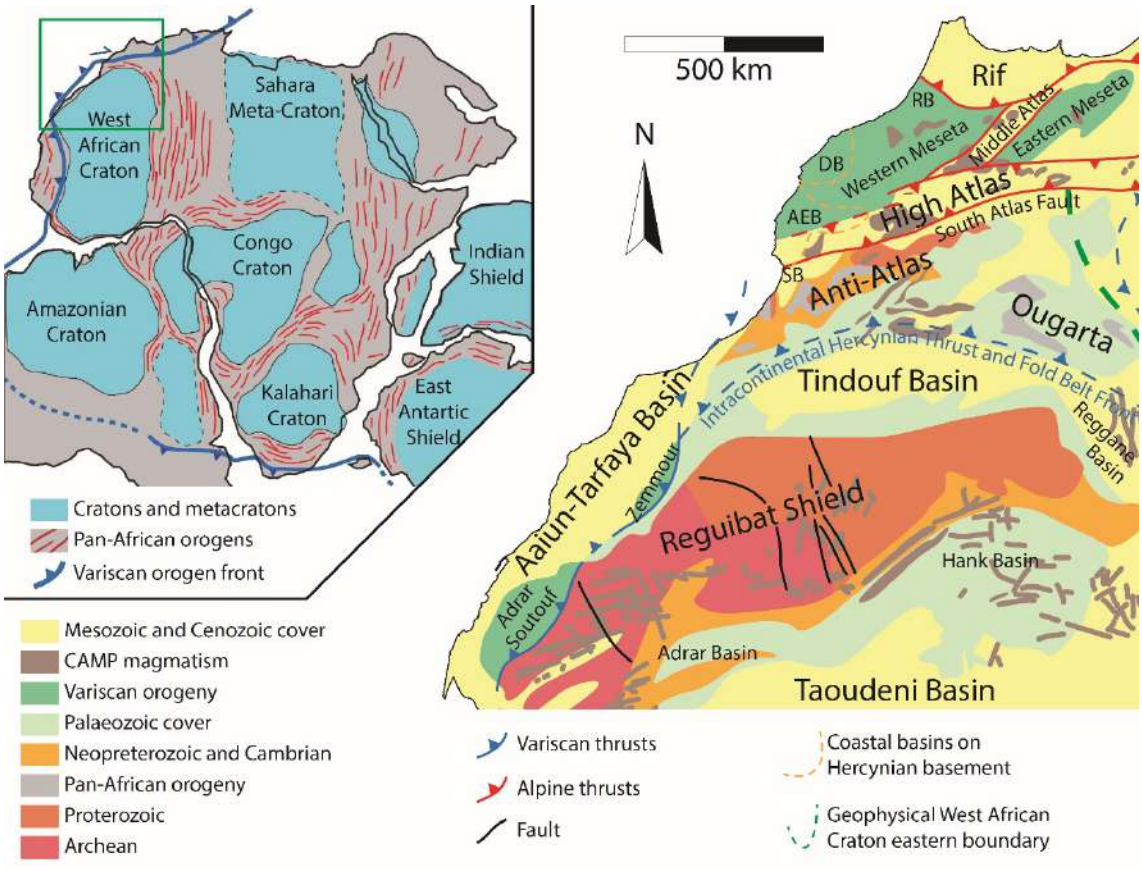

Figure 2.1. Main structural elements around the Aaiun-Tarfaya Basin. Inset: Area within the context of Gondwana. References as in Figure 1.2.

2.3 Geological setting

2.3.1 Central Atlantic

The breakup of Pangaea resulted in rifting and separation of Africa from North and South America, leading to the opening of the Atlantic Ocean and development of passive margins during the Mesozoic and Cenozoic (Jansa and Wiedmann, 1982; Lehner and De Ruiter, 1977). The Central Atlantic segment, between northwest Africa and North America, was the first to rift, starting in the Late Triassic with deposition of continental red beds (Brown, 1980; van Houten, 1977). Rifting along the northwest margin of Africa developed parallel to the old Variscan thrust and fold belt (Figure 2.1; Jansa and Wiedmann, 1982); generating grabens and half-grabens oriented approximately NE-SW belts (Bouatmani et al., 2004). These restricted basins were initially filled with coarse alluvial and fluvial syn-rift deposits and evaporites (Abou Ali et al., 2005, 2004; Brown, 1980; van Houten, 1977). From the very latest Triassic / beginning of the Jurassic (c. 201-190 Ma), extensive tholeiitic magmatic activity (Figure 2.1) occurred within the Central Atlantic Magmatic Province (Davies et al.,

2017; Marzoli et al., 2004; Nomade et al., 2007; Verati et al., 2007; Wilson and Guiraud, 1998). Extension was asymmetric, with eventual oceanic spreading starting earlier in the southern part of the Central Atlantic and progressing towards the north (Heyman, 1989). The first oceanic crust on the African side probably developed at some point before the oldest magnetic anomaly (M25) within the Jurassic Magnetic Quiet Zone. The timing of onset of the drift phase and creation of the first oceanic crust is still debated (e.g. (Biari et al., 2017; Davison, 2005; Klitgord and Schouten, 1986; Labails et al., 2010; Sahabi et al., 2004; Schettino and Turco, 2009; Scotese, 1991; Steiner et al., 1998). Depending on the dataset used, plate reconstruction model applied, input parameters, dating of the break-up unconformity, etc. an Early to Middle Jurassic age has been proposed, possibly as old as 190 Ma (Labails et al., 2010).

During late Early Jurassic open marine conditions were established (Jansa and Wiedmann, 1982) and a connection with the Pacific Ocean is postulated (Westermann, 1993), although restricted marine conditions still existed in some basins, like the Agadir-Essaouira Basin (AEB), with evaporites deposition in the Early Jurassic (Figure 2.2). Recent work examining the hinterland of northwest Africa suggests that rather than passive thermal subsidence at this time, the basin margin experienced significant syn- and post-rift km-scale vertical movements (Bertotti and Gouiza, 2012; Charton et al., 2018; Gouiza et al., 2017; Leprêtre et al., 2013, 2017; Sehrt et al., 2016).

The sedimentary record along the Moroccan Atlantic margin shows an increase in carbonate production throughout the Jurassic (Figure 2.2), which can reach thicknesses in-excess of 2 km along some segments of the margin (Figure 2.3). The carbonate platforms were widespread from the Middle to late Jurassic, forming a more or less continuous carbonate build-up extending along the northwest African margin, defining a Jurassic palaeoshelf (Jansa and Wiedmann, 1982). In the deep basins, time equivalent marls, fine clastics and calciturbidites were deposited (Figure 2.2). Carbonate production continued until the early Cretaceous, when increased terrigenous delivery to the basins, and establishment of a number of deltas along the margin, such as the Tan Tan and Boujdour systems in the ATB (Davison, 2005; Einsele and von Rad, 1979; Martinis and Visintin, 1966), eventually shut off carbonate production. In the AEB carbonate platform sedimentation ceased in the early Valanginian trough flooding (Ettachfini et al., 1998; Rey et al., 1988) and establishment of the “Atlas Gulf” (Behrens and Siehl, 1982).

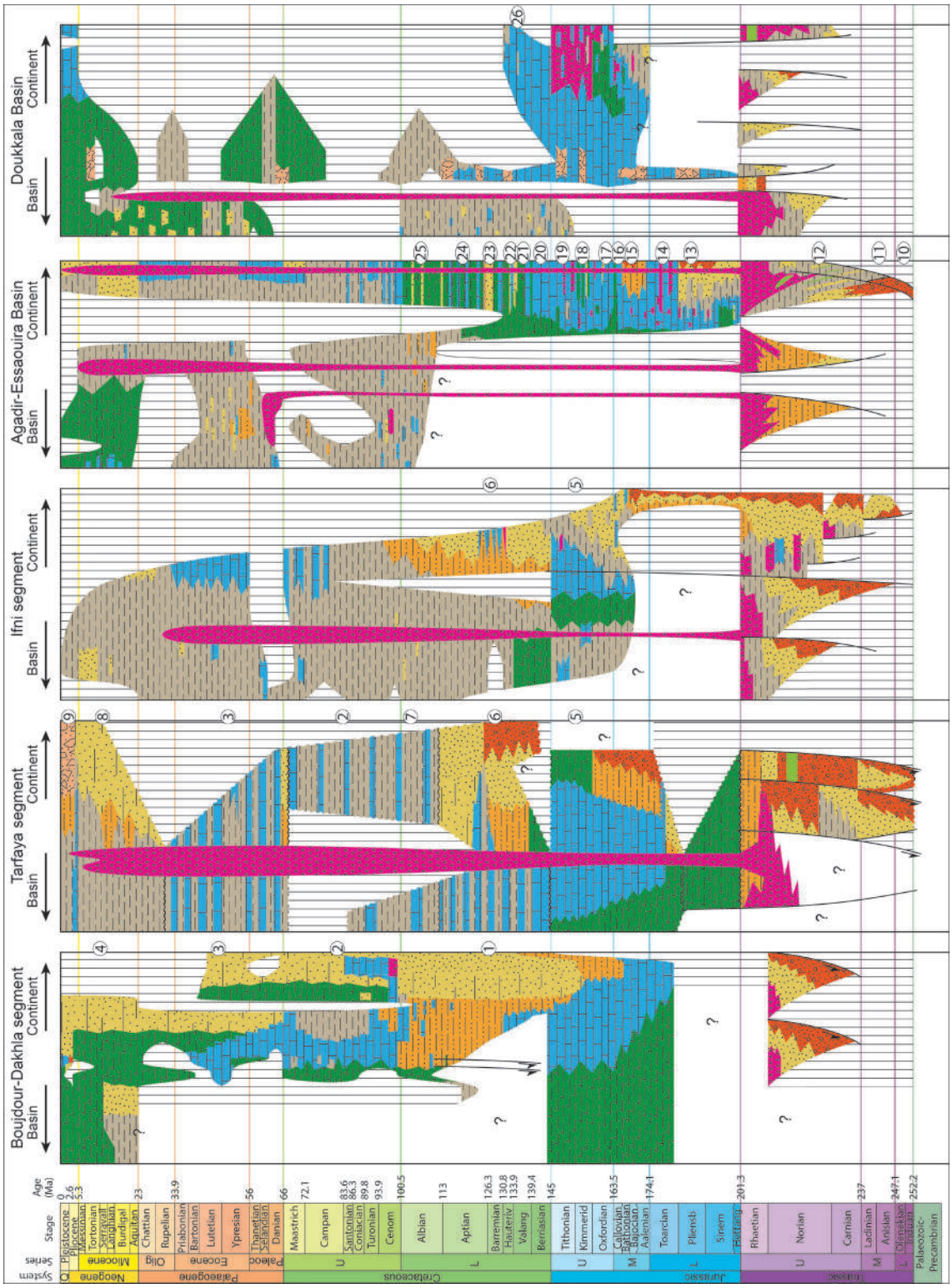

Figure 2.2. Generalized chronostratigraphy for different basins along the Atlantic Margin of Morocco. Basins as in Figure 2.3. From north to south: Doukkala basin; adapted after (Echarfaoui et al., 2002; Lancelot and Winterer, 1980; Meyer, 1978; Negroni et al., 1966; Price, 1980; Winterer and Hinz, 1984). Agadir-Essaouira Basin; offshore stratigraphy adapted after (Hafid et al., 2000; Tari et al., 2012) and unpublished well report; onshore stratigraphy modified after (Hafid, 2000) and Aude Duval-Arnould and Tim Luber, pers. comm. Aaiun-Tarfaya basin (Ifni segment); offshore stratigraphy adapted after (Abou Ali et al., 2005; Gouiza, 2011); onshore stratigraphy from this study. Aaiun-Tarfaya basin (Tarfaya segment); offshore stratigraphy adapted after (Wenke, 2015); onshore stratigraphy adapted after (Hollard et al., 1985) and field observations. Aaiun-Tarfaya basin (Boujdour-Dakhla segment); adapted after (von Rad and Einsele, 1980; von

Rad and Wissmann, 1982). Time scale after (Gradstein et al., 2012). Numbers to the right of each basin represent the most important formations as follows: 1) Jreibichat Fm., 2) Lebtaina Fm., 3) Samlat Fm., 4) Aaiun Fm., 5) Puerto Cansado Fm., 6) Tan Tan Fm., 7) Aguidir Fm., 8) Tah Fm., 9) Hammada Tellia Fm., 10) Ikakern Fm., 11) Timezgadiwine Fm., 12) Bigoudine Fm., 13) Amsittene Fm., 14) Id Ou Moulid Fm., 15) Ameskhoud Fm., 16) Ouanamane Fm., 17) Tidili Fm., 18) Imouzzer Fm., 19) Tismeroura Fm., 20) Cap Tafalney Fm., 21) Sidi Lhouseine Fm., 22) Tamanar Fm., 23) Bouzergoun Fm., 24) Tamzergout Fm., 25) Oued Tidzi Fm., 26) Calcaire de Dridat Fm. Lithology as in Figure 2.7.

2.3.2 Aaiun-Tarfaya Basin (ATB)

The opening of the Central Atlantic Ocean during the Mesozoic led to development of a series of coastal basins along the west coast of Morocco (Figure 2.1). Various names have been assigned historically to these basins. The nomenclature used in the present study follows the one used by (von Rad et al., 1982). The Aaiun-Tarfaya Basin **(**ATB) trends NE-SW (Figure 2.1) and extends along the Moroccan Atlantic margin for approximately 1100 km, with an onshore area of over 170000 km^2. It is bounded by the western termination of the Pan-African and Variscan Anti-Atlas mountain belt to the NE; the Palaeozoic Tindouf/Zag Basin to the E; and the Reguibat Shield and Mauritanides (Adrar Soutouf and Zemmour) to the SE (Figure 2.1).

Since the pioneering work in the 1940's to 1960's (Alia Medina, 1945, 1952; Choubert and Marçais, 1956; Martinis and Visintin, 1966; Querol, 1966) on the regional geology, few outcrop-based studies have been published on the Mesozoic of the ATB. Definition of the Triassic to upper Jurassic stratigraphy has been limited to data from on- and offshore exploration wells, drilled from the 1960´s onwards. Ages are mostly derived from the micropaleontological survey of the Puerto Cansado-1 well (Viotti, 1966) and subsequent reinterpretation by du Dresnay (1988) and Bouaouda (2004). The oldest unit drilled and formally defined is the upper Jurassic carbonates of the Puerto Cansado Fm. (Martinis and Visintin, 1966).

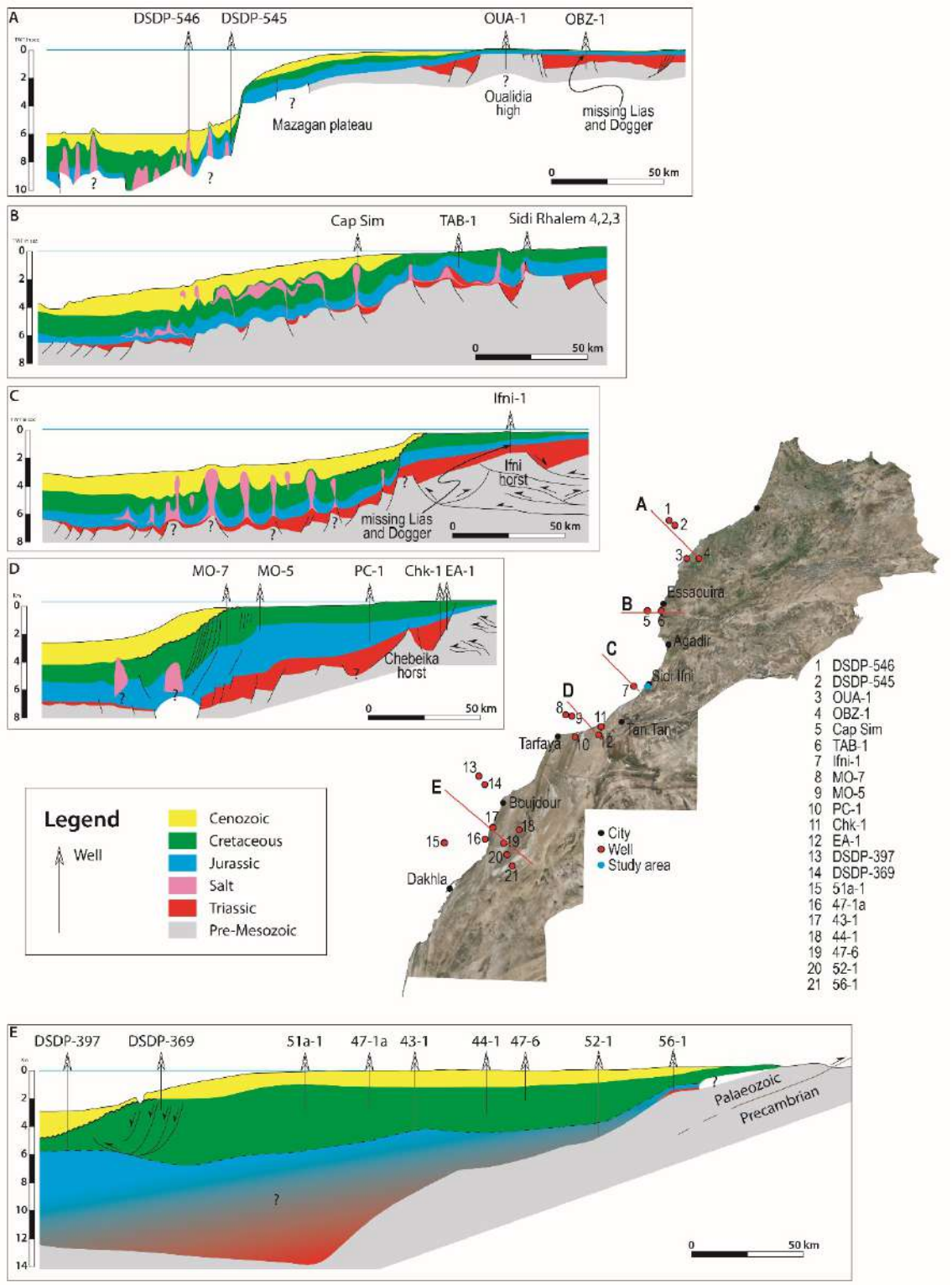

Figure 2.3. Schematic dip cross-sections showing the architecture of Moroccan coastal basins. From north to south: A) Doukkala basin, adapted after (Hinz et al., 1982; Hollard et al., 1985; Le Roy et al., 1997). B) Agadir-Essaouira basin, adapted after (Frizon De Lamotte et al., 2008; Hafid, 2000; Tari and Jabour, 2013). C) Aaiun-Tarfaya basin (Ifni segment), adapted after (Abou Ali et al., 2005; Hafid et al., 2008)**. D) Aaiun-Tarfaya basin (Tarfaya segment), adapted after** (Abou Ali et al., 2005; Hinz et al., 1982; Wenke et al., 2011)**. E) Aaiun-Tarfaya basin (Boujdour-Dakhla segment), adapted after (Hafid et al., 2008; Hollard et al., 1985; Piqué et al., 2006; von Rad et al., 1979; von Rad and Einsele, 1980).**

A general overview of the stratigraphy and evolution of the ATB follows, with differences from north to south (Figure 2.2) highlighted. Upper Triassic syn-rift clastics were deposited together with thick evaporite sequences offshore in the ATB during the early Norian. Open marine conditions were only established in the Sinemurian (Abou Ali et al., 2005; Davison, 2005; du Dresnay, 1988; Zühlke et al., 2004), followed in the Pliensbachian to Callovian by establishment of a carbonate platform. Later regressive marine sandstones were deposited, capped by a renewed transgression leading to deposition of open marine carbonates. Offshore, well and seismic data indicates the late Jurassic is represented by an extensive carbonate platform, the Puerto Cansado Fm. (Abou Ali et al., 2005; Michard, Saddiqi, et al., 2008) with reefal build-ups along the platform margin. Salt remobilisation started in the early Cretaceous representing the dominant structural driving force in this period (Michard et al., 2008; Zühlke et al., 2004). The platform margin slope collapsed during the Berriasian eustatic lowstand, and at this time some of the Jurassic succession was eroded.

The precise extent and subdivision of the lower Cretaceous section is poorly constrained due to the almost total lack of diagnostic fossils (Grosheny et al., 2012; Viotti, 1966). The overlying upper Aptian to upper Campanian interval is much better dated by the macro- and microfaunal succession from the onshore sections from Tan Tan to the south of Tarfaya (Collignon, 1967, 1966; El Albani, 1995; El Albani et al., 1999; Freneix, 1972; Grosheny et al., 2012; Kuhnt et al., 2009; Wiedmann et al., 1982, 1978).

Tertiary Atlasic compression in northwest Africa from Late Cretaceous onwards did not result in any significant deformation south of the South Atlas Fault (Figure 2.1), and as such the Mesozoic sedimentary fill of the ATB largely remains horizontal or only gently tilted.

2.4 Methods

The studied succession is exposed inland along outcrops cut by the Oued (Arabic for river) Craima and along coastal sections from Gueriza (Legzira) Beach to Foum Assaka (Figure 2.4 and Figure 2.5). The succession at Oued Craima and Sidi Ouarzik Beach was logged at a cm scale, identifying lithological changes, sedimentary structures, trace and body fossil content in order to undertake conventional facies analysis. A total of 53 samples from different sedimentary facies were collected for microfacies and petrographic characterisation. Additionally, 20 samples were also collected and

processed for macro-fauna analysis to aid in environmental interpretations and refine the dating of the succession.

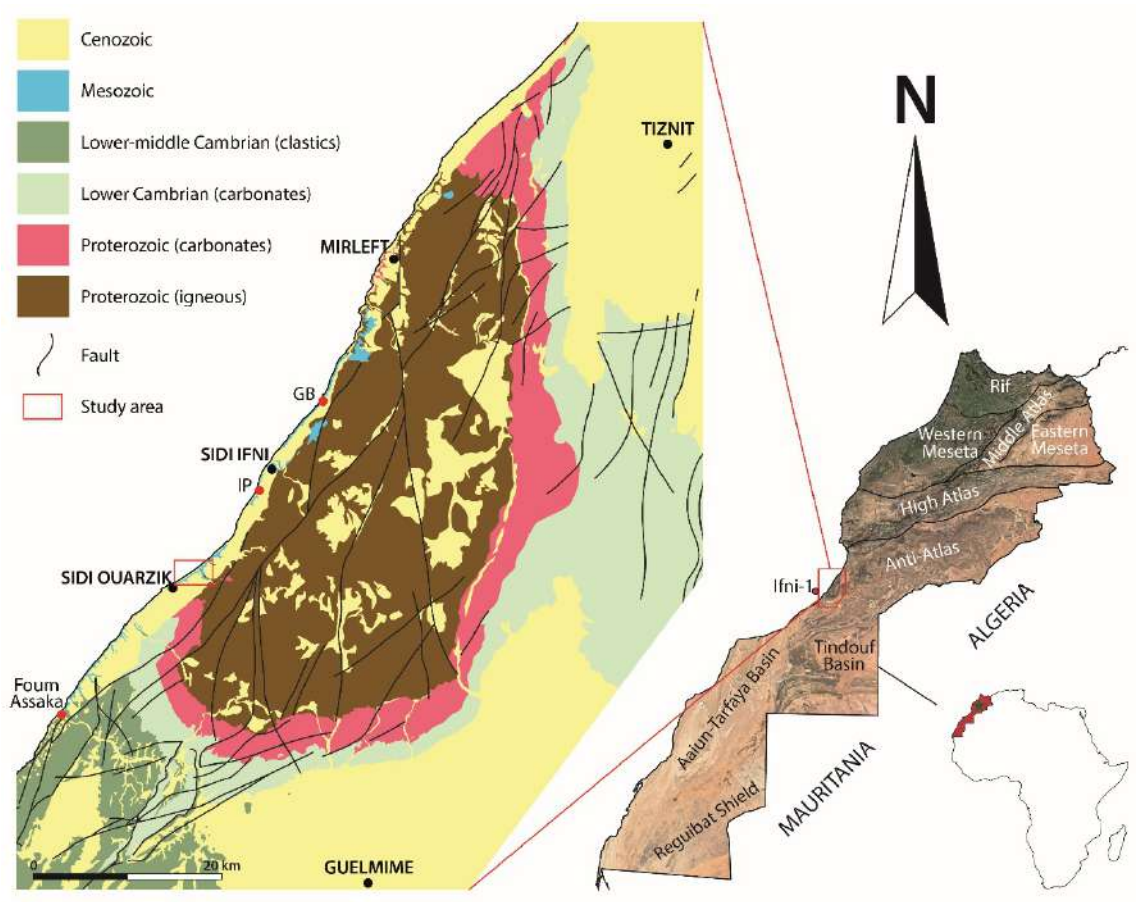

Figure 2.4. Main geological domains and study area. Geology of the Infi inlier and surroundings simplified after (Choubert, 1957; Destombes, 1991; Yazidi et al., 1986). A closer view of the study area is in Figure 2.5. GB: Guezira Beach outcrop. IP: Ifni Port outcrop.

2.5 Results

A composite sedimentary log of the studied succession is shown in Figure 2.6. The position of the samples collected for thin-section analysis and macro-fauna are shown on the log.

2.5.1 Facies analysis

Twenty five lithofacies have been defined (Table 2.1) and grouped into 7 Facies Associations (FA):

Figure 2.5. Satellite image from GoogleEarth™ southwest of Sidi Ifni showing exposures of formations proposed.

2.5.1.1 FA 1 (Alluvial fans)

This FA is composed predominantly of lithofacies A, with interbedded sparse lithofacies B and rare C. Cross-bedding and clasts imbrication are absent at Oued Craima section.

FA1 is exposed along the coast from Mirleft to Sidi Ouarzik (Figure 2.4). At Oued Craima, the lower 175 m of the succession are composed exclusively of this FA1 (Figure 2.6). From there, it punctuates the succession up to its last appearance at 347.5 m.

Interpretation:

The clast size and erosive sharp bases suggest high-energy flows. The absence of sedimentary structures and sheet-like nature of beds is indicative of ephemeral unconfined flows related to flash floods events in an alluvial fan environment.

Intervals which lack interbedded sandstones are interpreted to be deposited in a proximal setting, where avulsion and switching of active lobes is common. Units associated with channel forms containing very fine- to coarse-grained sandstones with pebble lags and crossbedding (lithofacies C) interbedded with the conglomerates are observed in the Ifni Port and Guezira Beach sections (Figure 2.4). The alternation of sandstones beds and conglomerates is interpreted to record a variation in flow regime, possibly indicating the lateral switching of lobes on the fan in a more medial location. The absence of palaeosols or rootlets in the finer sediments suggests high rates of sedimentation and short periods of time between flows.

Table 2.1. Lithofacies identified at Oued Craima and Sidi Ouarzik succession.

Code	Lithofacies	Description	Interpretation
A	*Normally-graded conglomerates*	Massive to normally graded clast-supported red conglomerates. Beds are 10 to 70 cm thick laterally continuous with erosive base, rarely channelized (up to 20 m wide) and lacking clast imbrication or cross-bedding. Clasts have heterogeneous composition (sedimentary, igneous and metamorphic) and size ranges from 2 mm to 60 cm (from angular to rounded depending on the location).	Migration of broad bars and dunes in unconfined gravel sheets
B	*Inversely graded conglomerates*	Inversely-graded, sometimes matrix-supported, red conglomerates. Beds are 10 to 50 cm thick, laterally discontinuous (up to 10-15 m) with erosional basal surfaces or draping previous topography. Clast composition is heterogeneous (sedimentary, igneous and metamorphic), sub-angular to rounded with a maximum grain size up to 15 cm.	Pseudoplastic debris flow in unconfined gravel sheets
J	*Matrix-supported granule-pebble conglomerate*	Structureless (to slightly normally graded) wavy to irregularly bedded matrix-supported brownish-grey pebble conglomerate. Top of individual beds can be wave- (and current-) rippled. Beds are from a few cm to 15 cm thick with sharp contacts and sometimes with pebbles accumulated in scoured bases. Occasional cm thick interbeds of muds. Floating granules and cm-scale pebbles are rounded to subrounded and pebbles may be absent. Matrix grain size ranges from fine-grained to very coarse-grained. Common bioturbation by vertical burrows (possible Dicplocraterion habichi, Arenicolites or Skolitos) up to 20 cm long.	Ripples and scattered pebble-size clasts indicate high energy oscillatory and unidirectional currents. Interbedded thin muds suggest periods dominated by suspension settling. Long vertical bioturbation suggests high sedimentation rates.
U	*Crossbedded fine- to very coarse-grained sandstones*	Fine- to very coarse-grained normally graded cross- and parallel-bedded sandstone. Beds up to 60 cm thick with cross sets 20-40 cm-thick, erosive sharp base or loadcasted. Sedimentary structures can also include current and wave ripples on the tops of some beds and possible herring-bone cross-stratification. Scattered granules and pebbles up to 2 cm may be present towards the top of some beds together with scattered shell fragments. Bioturbation and accumulation of bivalves and gastropods can be important at the base of some beds.	Migration of dunes under uniderectional flows puctuated by wave reworking. Rare storm- and bidirectional current-reworking.
V	*Ripple-laminated sandstone*	Fine-grained ripple cross-laminated sandstone with possible interlamination of silts. Beds are cm thick and the most striking sedimentary structure are climbing ripples. Clasts are mainly quartz, feldspar and opaques from subrounded to subangular.	Unidirectional current migration of ripples under conditions of high sediment supply

L	*Very fine- to medium-grained calcareous sandstone to packstone*	Yellow to withish very fine- to medium-grained calcareous sandstone with variable silt content. Structureless irregular, tabular to wavy cm thick beds up to 30 cm thick with sharp to gradual contacts commonly dewatered or loadcasted and locally erosive. Internally it may have basal parallel bedding, sometimes slumped or contorted internal bedding. Occasionally, beds are inverselly graded (bioclast content increase upwards). Rare ripple cross lamination. Clastics usually include subrrounded to angular quartz, feldspar, rock fragments and dolomite clasts in variable proportions. Bivalves, gastropods and ostracods can be from absent to abundant, including cm-scale gastropods. Other components may or may not include rip-up mud clasts, irregular ooids, scattered granules and pebbles, carbonaceous plant fragments and carbonate clasts (up to 15 cm). Rare wood fragments, galuconite, intraclasts and algal mat fragments. Usually rich in micritic matrix. Occassionally, bioturbation by Thalassinoides can be pervasive at the base of individual beds.	Dewatering structures and slumps suggest rapid deposition in a relatively steep marine environment. High content in subspheric and subrounded clastics, broken and abraded bioclasts and relatively small size of alloctonous microbial clots suggest agitated environment. Most of the bioclasts are probably alloctonous
C	*Massive sandstone*	Massive very fine to fine-grained red sandstone. Bed thickness ranges from a few cm to 25 cm. Lack of sedimentary or biogenic structures may be due to poor exposure and weathering.	Despite the lack of diagnostic structures association with surrounding lithofacies suggests overbank unconfined pulsatory (or wanning) flows.
D	*Normaly graded calcareous sandstone and silts*	Very fine-grained white calcareous wavy-, parallel- or ripple cross-laminated sandstones with rootlets grading into very fine-grained clay- to silt-rich red sandstones. Bed thickness ranges from 10 to 50 cm with shrap base (not erosive) and top. White basal sandstones are 5-10 cm thick. Main clasts are quartz, detrital dolomite clasts, and feldspars, calcite-cemented and patches rich in iron oxides. Sedimentary structures include wavy-, parallel- and ripple cross-lamination in the lower white part and wavy to discontinuous thin bedding to lamination in the upper red ("chippy" texture) with extremely rare cross-lamination and sparse rootlets.	Lamination and ripples suggest lower flow regime conditions of unidirectional unconfined wanning flows. Rootlets and precipitation of calcite and oxides indicate soil formation
W	*Wavy- to hummocky cross-laminated (bedded) sandstones*	Laminated/bedded to hummocky cross-stratified very fine- to coarse-grained, sometimes calcareous, sandstones and interlaminated muds. Beds are 15-50 cm thick with wavy contacts. Additional sedimentary structures include occasional planar cross-bedded sets up to 15 cm thick and wave ripples. Main clasts are quartz and feldspar. Gastropods, bivalves and scarce echinoderms may be present.	HCS generated by storm waves below the fair weather wave base combined with bars formed under unidirectional flows (planar cross-bedding) and wave reworking.

I	*Mottled to laminated palaeosols*	Massive to laminated micrite-rich and carbonate-cemented clay to fine-grained sandstones, usually mottled or with "chippy" texture in outcrop. Thickness ranges from a few cm up to 1.5 m. Contacts are diffuse to sharp and very irregular. Internal sedimentary structures are usually absent but occasional ripple cross-lamination is possible, but unfrequent. A wide range of detrital clasts includes angular to subrounded quartz, feldspars and opaques, minor reworked microbial lumps, peloids, intraclasts, filosilicates, microcodium fragments and heavy minerals, and traces of ostracods and unidentified bioclasts fragments.	Absence of sedimentary structures is probably due to intense bioturbation and cementation processes. Ripples suggest traction in unconfined flows. Micrite has mixed origin from suspension settling and chemical precipitation related with exposure and carbonate soil formation. Occasional restricted marine fauna is interpreted as occasional marine conection through bidirectional flows.
T	*Reworked mud to sandstone and carbonate clasts bed.*	Bed 35 cm thick made of mud, silt, sand and carbonate clats up to 6 cm in size. Usually clast-supported but clasts can be also floating in a sitly-sandy matrix. No apparent internal structure. Frequently irregular to wavy sharp erosional base and sometiems gradational top.	Plastic debris flow
G	*Clayey siltstones to very fine-grained sandstones*	Normally graded to massive yellow, red to grey clayey siltstones to very fine-grained sandstones with occasional cm thick interbeds of medium-grained sandstone. Bed thickness ranges from 5 cm to 1 m thick with flat to wavy basal and upper contacts, sometimes diffuse or interfingered with underlying and overlying beds. Internal irregular lamination may be present likely due to subtle changes in grain size. Occasional intense bioturbation may destroy any previous internal structure (massive appearance). Ripples may be relatively abundant in some parts of the succession usually related with the coarser spectrum of the grain size. Carbonaceous plant fragments and plant fragments are relatively abundant and sparse wood fragments. Fossils are rare but when present they can be very abundant and monospecific (cm-scale, thin-shelled *Falcimytilus* sp.). Frequent carbonate nodules following the bedding. Nodules can coalesce laterally and form continuous beds. Unidentified burrowing disturbing lamination can be intense but not common. Scarce horizontal burrows and possible rootlets.	Normal grading and ripples generated under lower flow regime conditions in unconfined wanning unidirectional flows combined with suspension settling. Abundant monospecific thin-shelled bivalves and/or intense bioturbation is interpreted as a quiet subaquatic setting with certain degree of stress.

K	*Laminated to thinly bedded dark clays to very fine-grained sandstones*	Alternating wavy laminated to thinly bedded black clays to red-yellow silts and very fine-grained sandstones. Thickness ranges from mm to cm scale. Erosional surfaces, small-scale slumps and dewatering structures can be abundant. Sub-mm carbonaceous plant fragments are very abundant together with sparse wood fragments. Bivalves and bioturbation are extremely rare.	Grain size variation, erosive surfaces, dewatering structures, absence of fauna and bioturbation together with abundance of carbonaceous plant fragments represent rapid deposition under unconfined fluctuating hyperpycnal flows with possible periodic suspension settling between events. Slumping suggest a steep setting.
H	*Algal laminated quartz-bearing packstone*	Interlaminated peloidal boundstones, microbial/algal stromatolite-like mats, peloidal packstones to wackestones. Beds range in thickness between 5 to 20 cm with wavy contacts and occasionaly can look slightly nodular. Dessication cracks are rare and only identified in thin section. Lamination at microscopic scale is determined by alternation of quartz- or reworked peloid-rich packstone (to wackestone) lamina with biologically induced/bound carbonates. Main components include clots of biologically-trapped silt-sized subspherical peloids and scattered fragments of reworked microbial/algal mats up to 2.5 mm in size. Resedimented peloids can be locally predominant, together with variable proportions of silt-sized angular to subangular clastic quartz, feldspars, rock fragments and opaques, scattered medium- to coarse-grained sand-sized subangular quartz, rock fragments and feldspars, ostracods, gastropods and bivalve bioclasts and scattered spherical to sub-spherical sand-sized multicoated radial ooids. Micritic matrix is not homogeneously distributed and may alternate with lamina richer in sparry cement filling fenestral porosities.	Alternation of lamina of reworked material with biologically induced carbonates suggests traction by unconfined pulsating flows and periods of no deposition with exposure (dessication cracks). Fauna assamblages indicate conextion with moderately restricted marine environmets probably transported by bidirectional flows. Micrite probably has two origins, from suspension settling and chemically precipitated during initial soil formation.

F	*Bioclastic-oolitic quartz-bearing grainstone (locally packstone)*	Normally graded coarse-grained to granule-sized, sometimes crossbedded and channelised, grainstone. Channel thickness can be up to 1.2 m and cross bedded sets up to 15 cm. Additional sedimentary structures may include lags of granules and shell fragments. Components include variable proprotions of bivalve and gastropod broken fragments up to 4 mm-long commonly displayed subparallel to bedding, microbial/algal fragments and intraclasts of a wide range of compositions and sizes (up to mm-scale), common sand-sized ooids, rock fragments of a wide range of compositions, spherity and roundness up to 2.5 mm, and silt- to coarse sand-sized quartz and feldspars, minor oolitic packstone/grainstone (up to 2.5 mm) and micrite intraclasts, echinoderm fragments, agglutinating benthic foraminifers (Reophax sp. probably), ostracods, filosilicates and other sedimentary minerals. Micritic matrix is mostly absent but can be present in layers parallel to bedding.	Channelised bases, crossbedding and broken bioclasts indicate high energy traction of confined flows. Alternation of a mixture of open and restricted marine fauna and continent-derived components, together with grainstone and packstone textures suggest tide-related bidirectional flows.
E	*Oncoid-bearing packstone*	Light grey oncoid-bearing (silty) packstone (occasionally wackestone). Wavy to planar beds 10 to 50 cm thick with sharp base and top. Main components include variable proportions of mm-scale oncoids, peloids, carbonaceous plant fragments, ostracods, microbial/algal lumps and intraclasts. Oncoids are mainly either porostromate-like with fenestral fabric or spongiostromate. Silt-sized terrigenous subangular quartz and feldspars can be relativelly abundant together with subordinate igneous and metamorphic rock fragments and detrital filosilicates. Usually, minor gastropods, bivalves, benthic foraminifers and ooids and traces of wood and echinoderm fragments and possible bryozoa.	Oncoids are typical in shallow subtidal to lower intertidal settings with moderate agitation. Fossil assamblages suggest moderately stressed marine environment with more or less connection with normal conditions. Relative abundance of errigenous clasts is related with proximity to the continent.
Y	*Calcareous siltstones-sandstones to silty packstones*	Massive to chaotic light grey siltstones to fine-grained sandstones. Bed thickness ranges from 5 to 15 cm, sharp irregular to erosive base and sharp top. Lithologies can range from clastic- to carbonate-dominated. Carbonaceous plant fragments are abundant. Occasionally, broken bivalves and gastropods are abundant. Reworked carbonate clasts up to 10 cm in size are possible.	Erosive bases and reworked clasts from continental and marine origin suggests high energy.
N	*Mudstone (to wackestone)*	Massive to thinly bedded light to dark grey micritic mudstones. Wavy to irregular beds, almost nodular sometimes, 5-30 cm thick, sometimes affected by soft sedimentary deformation. Bioclast-poor beds are usually intensely bioturbated at the base (Thalassinoides and possible Planolites). Components include different amounts of disarticulated bivalves, gastropods (up to several cm), silt-sized quartz clasts, carbonaceous plant fragments, ostracods, peloids, benthic foraminifers, dasycladaceas and ooids.	Mainly suspension settling and autochthonous fauna. Fine grained carbonate mud and absence of sedimentary structures is interpreted as indication of quiet and relatively deep conditions.

M	*Bioclast-bearing silty peloidal wackestone to packstone*	Massive to irregularly bedded grey bioclastic-bearing peloidal wackestone to packstone. Tabular bedding 5-40 cm thick with irregular to wavy sharp contacts, nodular and almost discontinuous sometimes, occasionally load casted and dewatered. Rare big-scale soft-sediment deformation and local erosive bases. Rare "lags of floating" bivalves and cm-scale gastropods. Grains include silt-sized peloids and quartz clasts, relatively abundant bivalves (sometimes thin-shelled), gatropods (nerinellids) and carbonaceous plant fragments. Dasycladacean and lumps of unidentified blue or green algae, can be locally the main allochem. Scattered intraclasts, ooids, wood fragments, scattered granules and pebbles and reworked carbonate clasts up to 7 cm in size may or may not be present. Scatered cm-scale gastropods may be present on top of individual carbonate beds. Ostracods may keep both valves preserved. Blue/green algae fragments or intraclasts up to 2 mm in size (most are silt- to very fine-graded). Traces of benthic foraminifers, wood fragments, fish remains and silt-sized quartz and feldspar. Some echinoderm fragments, unidentified blue/green algae may be present.	Combined episodes of rapid sedimentation (soft-sediment deformation and erosion) under moderate to high energy conditions and suspension settling. Fauna assemblage suggests shallow moderately restricted conditions with some open marine influence.
O	*Peloidal packstone*	Massive to faintly irregularly laminated peloidal packstones. Irregular to wavy bedding 10-15 cm thick. Sand-sized ovoid elongated to irregular peloids are the main allochem. Other grains include silt-sized quartz, ostracods, ooids, gastropods, bivalves, benthic foraminifers, carbonaceous plant fragments, microbial mats fragments and echinoderm fragments may or may not be present.	Lack of sedimentary strutures suggests micritic mud settled from suspension together with accumulation of authoctonous fauna. Admixtures of continent-derived clastics and bio-laminites and normal marine conditions bioclasts suggest weak currents and agitation.
P	*Silty (sandy) grainstone with blue/green algae*	Irregularly bedded silty/sandy grainstone to packstone with algae. Bed is 20 cm thick with irregular sharp surfaces, cross-bedding, shell lags and mud drapes (micritic)? Main allochems are sand-sized quartz, feldspar and rock fragments, intraclasts up to 3 mm and blue-green algae fragments up to several mm in size. Minor opaques, carbonaceous plant fragments. Scarce full and broken radial ooids. Bivalves in outcrop.	Sedimentary structures suggest traction and rapid deposition under energetic pulsating flows alternating with suspension settling.

Q	*Peloidal- and bioclastic-bearing grainstone*	Massive to laminated peloidal and bioclastic-bearing grainstones. Beds are tabular, 5-30 cm thick with irregular to wavy contacts, occasionally loadcasted. Occasionaly bioclast content increase slightly towards the top of individual beds. Main allochems include variable proportions of broken bivalves and gastropods, subspherical peloids silt- to fine sand-graded (possible fecal pellets), benthic foraminifers (agglutinating, miliolids and textularids mainly). Aggregates, intraclasts and composite ooids can be from common to traces. Subordinate components are wood and carbonaceous plant fragments, micrite concentric ooids (scarce with radial fabric), and broken echinoderm plates and spines. Minor dasyclads. None to very little silt-sized subangular to subrounded quartz and feldspar clasts. Possible bryozoa are extremely rare. Micritization rims can be thick and peloids are frequently allochem completely micritised.	Fauna assemblages are typical of normal to moderately restricted marine conditions. Broken bioclasts and absence of micrite suggest an agitated environment. Common micrite envelopes relates with deposition in a shallow marine setting.
R	*Oolitic grainstone*	Massive to normally graded grey oolitic grainstones. Beds are 15-25 cm thick with very sharp irregular erosive bases and occasionally loaded. Faint internal thin bedding (perhaps cross-bedding). Main grains are spherical to ovoid sand-sized concentrical micritic ooids, silt- to sand-sized spherical to ovoid peloids and intraclasts up to 3 mm in size. Minor broken bivalves and gastropods, dissarticulated ostracods and aggregates. Traces of benthic foraminifers, briozoa and likely fish scales. Possible microkarst developed on some beds. Rare bioturbation by Thalassinoides, but may be intense locally.	Abuntant ooids and sedimentary structures indicate shallow energetic waters with possible short-timed exposure (possible microkarst)
S	*Cross-bedded sandy grainstone (packstone)*	Normally graded cross-bedded quartz- and feldspar-rich oolitic grainstone. Beds are 15-60 cm thick with sigmoidal to tangential cross-bedding and sharp erosive bases. Foreset surfaces may be reworked subperpendicularly by waves (wavy ripples). Possible mud drapes on foresets. The majority of grains are sand-sized K-feldspar and quartz, many of them coated by one layer of micrite (incipient ooids) and far less abundant silt- to very fine sand-sized subspherical peloids. Minor subspherical sand-sized radial ooids cored by incipient ooids (first micritic layer). Traces of carbonaceous plant fragments, ostracods, gastropods and bivalves fragments. Minor ostracods and pebble-sized quartz up to 2 cm can be present. Occasional bioturbation. Micritization can be intense destroying the primary texture of some grains.	Migration of dunes under unidirectional currents modulated by wave reworking
X	*Coral-rich packstone*	Massive, chaotic to faintly laminated, wavy coral-bearing packstone. Beds are 10-50 cm thick and bases can be erosive and loadcasted. Usually, scattered coral fragments are present but individual beds can be packed with broken fragments of branchy corals and minor bulbous corals. Additional grains include silt-sized quartz and feldspar (some fd up to 400 microns), peloids, bivalves and gastropods up to several mm in size. Minor ostracods, intraclast/microbial clot fragments, echinoderm fragments and carbonaceous plant fragments.	Fragmented bioclasts and sedimentary structures suggest rapid deposition in a high energy waters. Branching coral usually develop in quiet water within the photic zone.

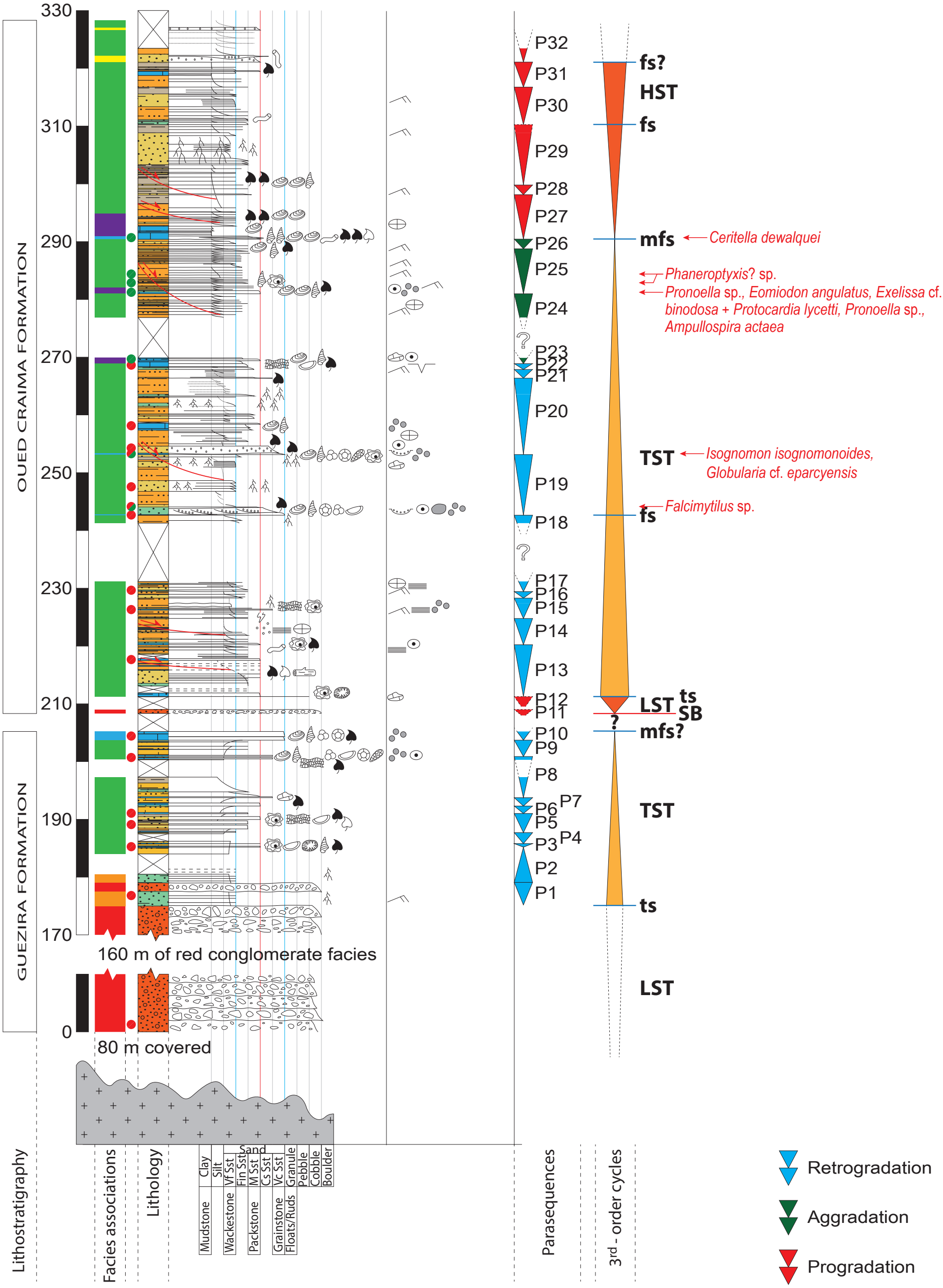
330
310
290
270
250
230
210
190
170
0
OUED CRAIMA FORMATION
GUEZIRA FORMATION
160 m of red conglomerate facies
80 m covered
P32
P31
P30
P29
P28
P27
P26
P25
P24
P23
P22
P21
P20
P19
P18
P17
P16
P15
P14
P13
P12
P11
P10
P9
P8
P7
P6
P5
P4
P3
P2
P1
fs?
HST
fs
mfs
Ceritella dewalquei
Phaneroptyxis? sp.
Pronoella sp., Eomiodon angulatus, Exelissa cf. binodosa + Protocardia lycetti, Pronoella sp., Ampullospira actaea
TST
Isognomon isognomonoides, Globularia cf. eparcyensis
Falcimytilus sp.
fs
ts
LST
SB
?
mfs?
TST
ts
LST
Lithostratigraphy
Facies associations
Lithology
Clay
Silt
Vf Sst
Fin Sst
M Sst
Cs Sst
Vc Sst
Granule
Pebble
Cobble
Boulder
Sand
Mudstone
Wackestone
Packstone
Grainstone
Floats/Ruds
Parasequences
3rd - order cycles
Retrogradation
Aggradation
Progradation

CRAIMA BEACH FORMATION

550
530
510
490
470
450
430
410
390
370
350
330

P84
P83
P82
P81
P80
P79
P78
P77
P76
P75
P74
P73
P72
P71
P70
P69
P68
P67
P66
P65
P64
P62
P63
P61
P60
P59
P58
P57
P56
P55
P54
P53
P52
P51
P50
P49
P48
P47
?
P46
P45
P44
P43
P42
P41
P40
P39
P38
P37
P36
P35
P34
P33

Nerinella elegantula
"Corbula" cf. islipensis
Ceritella dewalquei
Globularia cf. eparcyensis,
Globularia cf. tancredi, Ceritella dewalquei
fs
Costigervillia sp., *Trigonia pullus*, etc.
Eomiodon angulatus, Pseudomelania (Oonia) variata, Eligmoloxus limneiformis, etc.
Nerinella elegantula
fs
Placunopsis socialis, Pachyrisma grande, Nicaniella pulla, Nerinella elegantula
fs
TST
Dacryomya cf. *lacrima, Myophorella tuberculosa, Eocallista antiopa, Nerinella*? sp.
Exelissa cf. *binodosa, Ceritella dewalquei*
+
Nicaniella pulla, Eomiodon angulatus, Naricopsina matheroni
fs
ts
LST
SB

Figure 2.6 (Previous pages). Summarized stratigraphic log at Craima, including proposed formation names, individual parasequences, systems tracts and main macrofauna. Each vertical black and white bar represents 10 m. Legend in Figure 2.7.

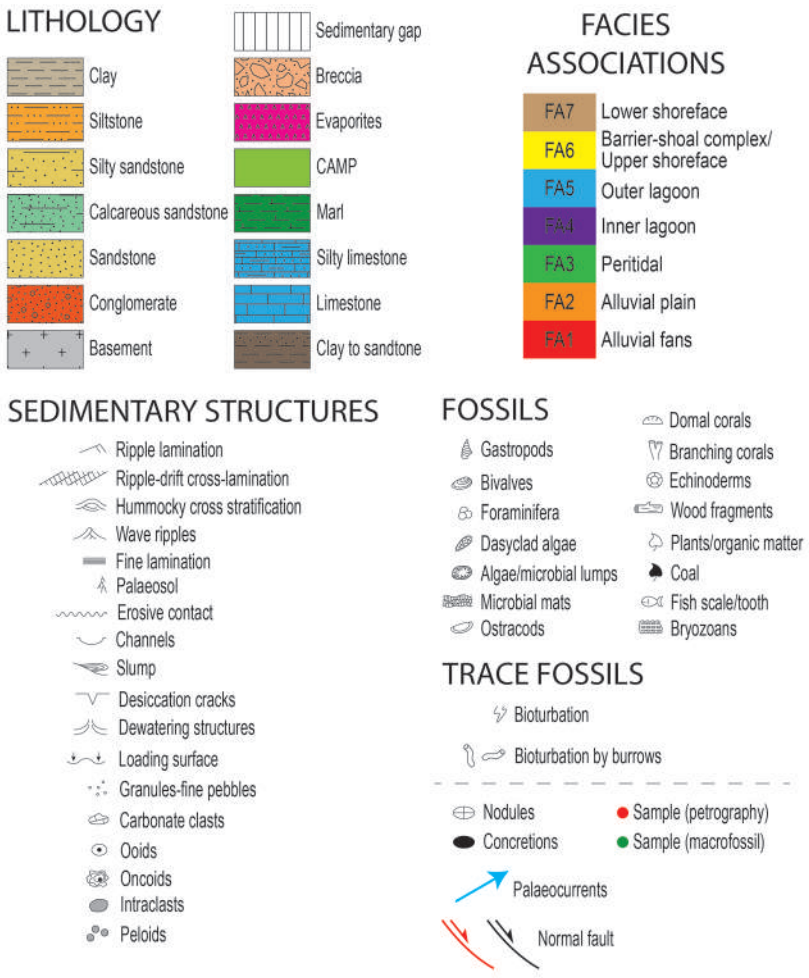

Figure 2.7. Legend for Figure 2.2, Figure 2.6, Figure 2.8, Figure 2.9 and Figure 2.10

2.5.1.2 FA 2 (Alluvial floodplain)

FA2 is composed of lithofacies D, interbedded with lithofacies A and rare lithofacies B. Basal contacts of white sandstones overlying red sandstones are sharp and not erosive. Basal contacts of conglomerates are erosive.

This FA is observed at Guezira Beach and Oued Craima (Figure 2.4 and Figure 2.6). At Oued Craima, it punctuates the succession, with a maximum thickness of 6 m located at a depth of 180 m (Figure 2.6).

Interpretation:

Rippled white sandstones grading into red sandstones with discontinuous lamination are indicative of lower flow regime unidirectional conditions evolving into periods of low

sedimentation rates, when plants can colonize the surface and develop palaesols (Figure 2.8; *2A*, *2B*) in an alluvial floodplain. Interbedded conglomerates are interpreted as distal fan lobe deposits.

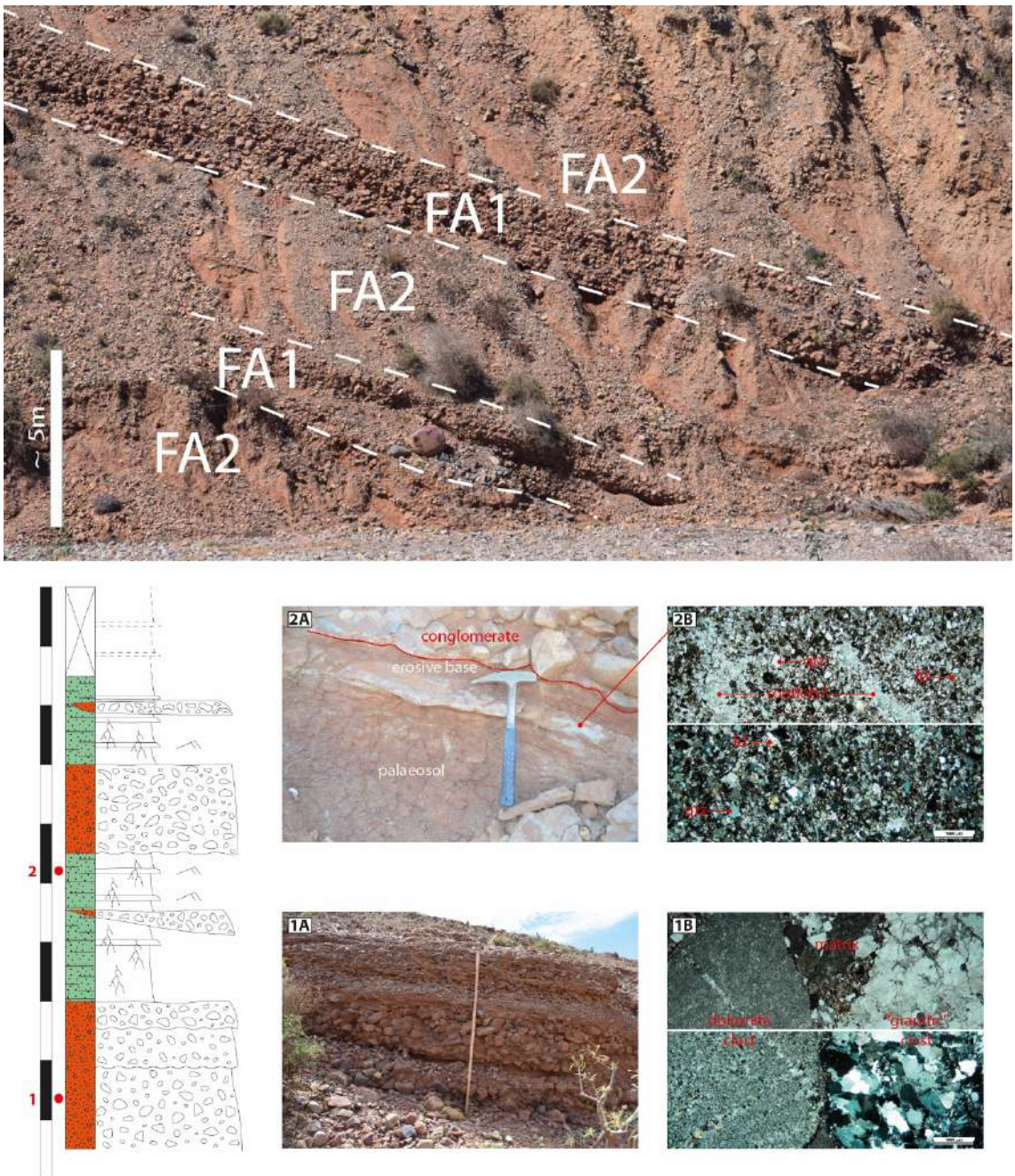

Figure 2.8. Examples from the field and microphotographs of alluvial fans and alluvial floodplain facies associations. Top) Field panorama showing alternating packages of red conglomerates and fine sandstones belonging to FA1 and FA2 (see text for details). Bottom left) Detail of sedimentary log collected in the field. Note the current-generated sedimentary structures are localized in the coarser sandstone levels. 1a, b) Field picture of conglomeratic beds, and microphotograph of the matrix (upper half in plane polarized light and lower half in cross polarized light). Stick for scale is 1.2 m long. 2a) Field picture of palaesols developed in fine-grained sandstones. Rootlet marks are visible. Hammer is 33 cm long. 2b) Microphotograph from the white sandstone level in 2a (upper half in plane polarized light and lower half in cross polarized light). Note the importance of carbonate clasts (dolomite) and cement in both microphotographs. Visual estimation in the field

yielded up to 60% of dolomite clasts in some conglomerate beds along Oued Craima. On the other hand, conglomerates from Guezira Beach overall present less dolomite and more igneous clasts which would be related with small catchment areas directly related with the composition of the Ifni Inlier (see Figure 2.4). Qtz: detrital quartz; fd: detrital feldspar.

2.5.1.3 FA 3 (Peritidal coastal plain)

This FA is exposed along Oued Craima and represented by fining upwards packages between 3 and 9 m thick (Figure 2.5 and Figure 2.6). The basal part of these packages is usually made of lithofacies E, Q and F, with sparse lithofacies Y, N and J. Dm-thick oncoidal packstones (lithofacies E) are the most abundant lithofacies at the base of these packages. Oncoids are the main allochem and show predominantly a fenestral fabric (porostromate oncoids). Cross-bedded, bioclast-ooid-bearing grainstones to calcareous sandstones with erosive and channelized-base (lithofacies F) overly peloidal and bioclastic grainstones (lithofacies Q). The latter can be defining the base of individual fining upwards packages of FA3. Lithofacies Y, N and J are underrepresented.

The middle part of the finning upwards packages is dominated by lithofacies G, punctuated by lithofacies H. Packstone interbeds, with microbial/algal mats (lithofacies H) are subordinated but can be stacked in limestone packages up to 1.2 m thick.

Packages of FA3 can be capped by lithofacies I, sometimes alternating with lithofacies G. The whole fining-upward sequence is rarely preserved and lithofacies I can be absent.

Carbonate nodules can be abundant in certain intervals, related with lithofacies G and developing along bedding planes. These nodules can grow laterally and coalesce to form laterally-continuous beds up to 20 cm thick.

Interpretation:

The typical fining-upward profile exhibited by individual packages of this facies association is interpreted as the record of progradation and shoaling of a tidal flat (e.g. Daidu et al., 2013; Flügel, 2010; Hardie, 1986; Wright, 1984). The lower, usually coarser, carbonates and/or clastics (lithofacies E, Q, F, J, Y and N) are interpreted as an initial subtidal unit overlain by the intertidal fine clastics (lithofacies G) with interbedded algal/microbial carbonates (lithofacies H) capped by supratidal palaeosoils (lithofacies I).

Oncoids in lithofacies E are typical of shallow subtidal to lower intertidal inner lagoons and shoals (Flügel, 2010) where a certain degree of agitation allows microorganisms to

develop a cortex around a nucleus and can mark the beginning of transgressive sequences (Wright, 1983). The combined presence of oncoids with terrigenous igneous and metamorphic rock fragments suggest a proximal setting within the subtidal zone, close to areas that source terrigenous clastics from the continent.

Channelised, cross-bedded grainstones (lithofacies F) contain a vast array of allochems with terrestrial, tidal and marine affinities. These include terrestrially-derived igneous and metamorphic rock fragments, tidal algal/bacterial mats fragments and marine broken echinoderm and mollusc bioclasts or oolitic grainstone intraclasts. The characteristic channelised geometry, sedimentary structures, coarse grain size, allochem of different origins and the lack of micritic or clastic mud is interpreted to record an energetic environment under the influence of tidal currents, such as migrating tidal creeks over sand/mud flats.

The coarse grain size of lithofacies J, together with long vertical burrowing (Table 2.1), indicates the coastal plain was subject to high-energy conditions and abundant sediment supply.

Lithofacies Y constitutes a minor component of the succession. The massive to chaotic fabric, erosive bases, sharp tops, reworked clasts and broken bioclasts indicate high energy and probably short-lived event beds. The high energy and the association with lithofacies G allows the interpretation as storm- or high tide-related beds.

Lithofacies E, Q, F, J, Y and N represent subtidal sedimentation. In this FA, they are at the base of individual peritidal cycles and they are overlain by alternating fine sandstones and muds (lithofacies G) characteristic of mud and sand flats that are exposed to the constant action of tides. In a “normal” prograding and shoaling cycle, ripples and wavy laminations are more abundant in the lower half whereas bioturbation, although not pervasive here, tends to be more abundant towards the finer-grained upper half. Horizontal burrowing, although scarce, suggests low sedimentation rates. Algal/bacterial-induced peloidal packstones and bindstones (lithofacies H) formed in intertidal algal marshes with initial carbonate soil development. At the microscopic scale, cyclic micrite- and siliciclastic-rich lamina, desiccation cracks and small amounts of marine bioclasts supports the intertidal interpretation with repeated periods of exposure and initial soil development.

The inward part of the tidal flat would be exposed most of the time and only reached by storms and extreme tides. Under these conditions of prolonged exposure carbonate-rich

palaeosols developed on fine-grained sandstones and muds (lithofacies I) and form the upper unit of the peritidal cycles.

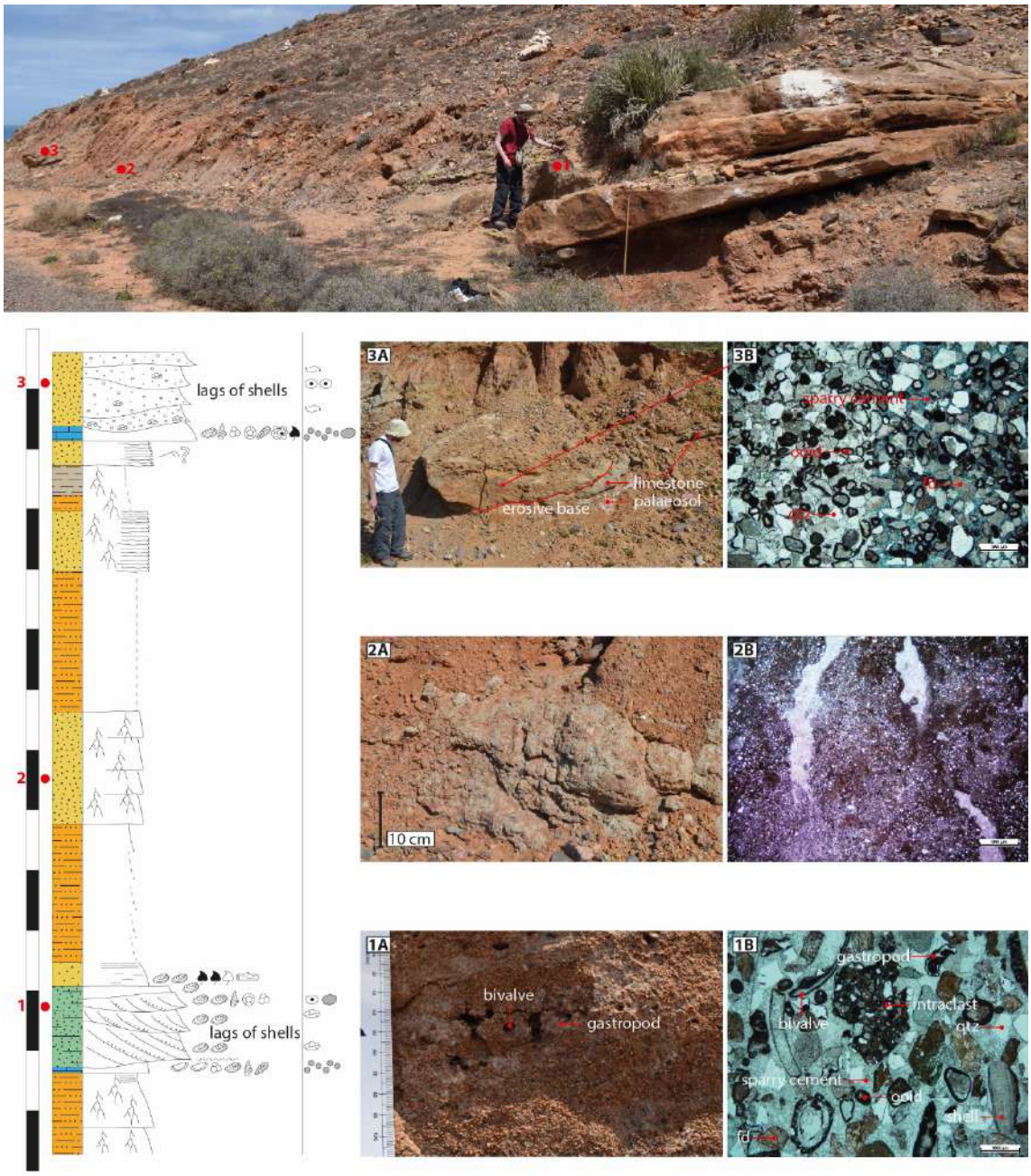

Figure 2.9. Example of a typical peritidal parasequence. Top image: field overview of a shallowing-upwards peritidal parasequence of cross-bedded grainstones overlain by silts and fine sandstones and capped by the next channelized coarse sandstone. Note the ostracods-rich limestone below the first cross-bedded grainstone/calcareous sandstone represents slightly deeper lagoonal facies and therefore the base of the overall fining upward profile typical of progradational parasequences in tidal flats. Lower images: detailed field pictures, microphotographs and annotated log from the field (each black/white bar represents 1 m). 1 (a, b) and 3 (a, b) are examples of lithofacies F and 2 (a, b) are mottled palaeosols developed on fine-grained sandstones. Qtz: detrital quartz; fd: detrital feldspar.

2.5.1.4 FA 4 (Inner lagoon)

This FA is exposed along Oued Craima and Sidi Ouarzik Beach. Most packages of this FA exhibit a coarsening upwards profile. It is composed of different lithologies ranging from pure carbonates, usually fossil-rich, to barren fine-grained clastics (Figure 2.10) and can be up to 6.5 m thick.

Most coarsening upwards cycles of FA4 start with lithofacies K grading into lithofacies L up to 2.7 m thick. These cycles can be punctuated by cm to dm thick interbeds of lithofacies M, T and E. Occasionally, lithofacies N can underlay lithofacies K.

Interpretation:

Absence of normal marine conditions fauna such as cephalopods and brachiopods can be interpreted as a relatively restricted environment with relatively stressed conditions. Slightly abnormal salinities in a lagoon or protected shelf could explain this absence (Aberhan et al., 2002). Green algae (*Holosporella siamensis*, possibly *Marinella* sp. and unidentified dasycladacea), possibly cyanobacterial lumps and benthic foraminifera (*Nautiloculina* spp.) also support a protected and shallow shelf/lagoon (Tasli, 2001). Sea urchins are very rare, but the fact that they are regular also supports the interpretation of a protected, relatively low-energy environment. Abundant micrite envelopes on most types of grains is indicative of a shallow marine setting (Flügel, 2010).

The clastic intervals alternating with silt-rich carbonate beds suggest an intermittent proximal source of clastics from the continent, interacting with the “carbonate factory” in the lagoon. The source of this clastic material is likely small-scale deltas prograding into the lagoon. Interlayered muds and very fine-grained sand (lithofacies K) with mm-scale erosive surfaces and the lack of burrowing and fauna is interpreted as the result of hyperpycnites (river-flood-generated turbidity currents) that would stress the environment damping colonization by organisms (Mulder et al., 2003). The characteristic dark colour of these units is due to very abundant sub-millimetre carbonaceous plant fragments delivered from a terrestrial source.

2.5.1.5 FA 5 (Outer lagoon)

FA5 is represented by limestone packages up to 3 m thick usually bounded by fine-grained clastics (lithofacies K). It is made of lithofacies M, O and Q (Figure 2.10) with

subordinated lithofacies R and P. This facies association is occasionally punctuated by thin cm- to dm-thick beds of lithofacies N and K.

Interpretation:

Common grainstone and packstone textures, absence of sedimentary structures, frequent load casting and sparse fine-grained facies suggest periods of rapid deposition in a relatively energetic environment punctuated by short-lived episodes of low energy conditions. The general paucity of green-blue algae and oncoids, together with a relative abundance in echinoderms and ooids over ostracods in some beds suggest some connection with open marine conditions in more energetic waters. Reworked carbonate clasts also support the interpretation of an agitated environment under the influence of waves, tides and storms probably.

Rare thin beds with highly irregular bedding and rich in green algae (lithofacies P) may be related with wash-over or back-shoal deposits reworking shallow marine fauna close to shoals.

2.5.1.6 FA 6 (Barrier-shoal complexes/Upper shoreface)

FA6 can be carbonate- or clastic-dominated. When FA6 is carbonate-dominated is usually found underlying FA4 and interstratified with FA5. When it is clastic-dominated it is usually found overlying FA7 and it is more frequent in the upper 70 m of the succession exposed at Sidi Ouarzik Beach.

Carbonate-dominated FA6 is composed of lithofacies Q, R and S, with minor interbeds of lithofacies M, stacked in packages up to 4 m thick. It is usually at the base of fining upwards packages that evolve into FA4. In lithofacies S, palaeocurrent direction inferred from foresets after bedding restoration is 269N (n=12) and foresets are reworked by wave ripples.

Clastic-dominated FA6 is made of lithofacies U, Q, L and J with minor intercalations of lithofacies M, V and K. Readings from crossbedded sandstones (lithofacies U) yielded a palaeocurrent towards 091N (n=5).

Interpretation:

Abundant grainstones and subordinated packstones together with frequent micritised grains in the carbonate-dominated lithofacies association suggest a high-energy environment and shallow water conditions. The dm thick oolitic grainstones, that can be

stacked in banks up to 3 m thick, are interpreted as oolitic shoals, also supporting an interpretation of shallow water conditions. Possible microkarst development on some beds (lithofacies R; Table 2.1) supports punctuated exposure of the shoals. Wave reworking on the cross-bedded grainstones (lithofacies S) represent subaqueous dunes formed under unidirectional currents in relatively shallow conditions above the fair weather wave base. Palaeoflow directions towards the west are subparallel to the palaeocoast line suggesting the presence of longshore currents. The association of these sediments and interpreted processes suggests a high-energy very shallow barrier complex setting associated with a lagoon.

The upper c. 70 m of the succession along Sidi Ouarzik Beach (Figure 2.6) becomes increasingly siliciclastic. Lithofacies L and J are frequently massive and affected by soft sediment-deformation, recording rapid sedimentation by unconfined flows due to a sudden deceleration of the original flow. These conditions are commonly observed in a setting where confined flows meet a standing body of water losing confinement and energy suddenly, therefore depositing the sediment they are transporting. Wave ripples on the top surfaces of individual beds suggest reworking by waves and the presence of occasional thin interbeds of muds can be interpreted to record a certain degree of tidal influence or suspension settling between higher discharge events. Due to the scale of these deposits (dm-scale to 1 m) they are interpreted as small-scale subaqueous bars. Occasional climbing ripples support the idea of periodic events of higher discharge and high sediment supply. Wave ripples on top surfaces of cross-bedded sand dunes suggest deposition above the fair weather wave base. Palaeoflow direction deduced from the subaqueous dunes is towards the north-east. Unlike the carbonate-dominated FA6, here the absence of oolitic grainstones and its association with FA7 (see below) is interpreted as slightly deeper water conditions. The depositional setting is interpreted as upper shoreface (inner ramp) above the fair weather wave base.

2.5.1.7 FA 7 (Lower shoreface/Middle ramp)

FA7 is mainly made of lithofacies K and W with subordinated lithofacies L, M, X and N. It usually coarsens upwards in packages up to 2.5 m, which can stack on top of each other up to 6.5 m thick.

Interpretation:

Frequent hummocky cross stratification preserved in sandstones and occasional abundant coral and shell debris evidence periodic rework by storms and big oceanic waves suggesting a lower shoreface setting for this facies association. The big majority of coral debris are branching and they are probably sourced from coral build-ups offshore, below the fair weather wave base, that were reworked by storm waves.

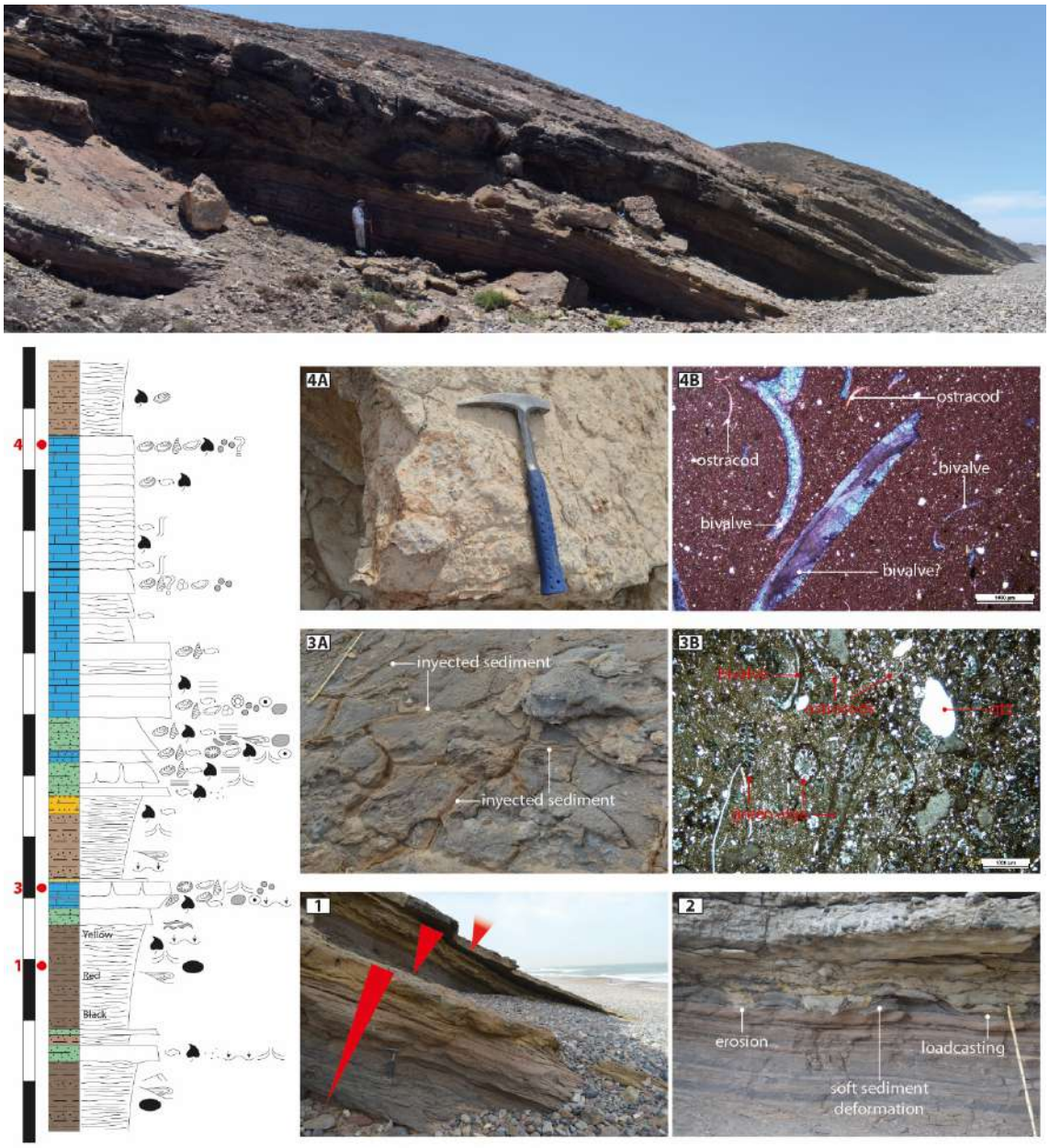

Figure 2.10. Examples of lagoonal facies (FA4 and FA5) along Craima Beach outcrop. Top) Field panorama showing several shoaling-upwards cycles. Prominent beds represent either the top of a progradational parasequence or more distal carbonates at the base of the next one (see sedimentary log to the left and text for explanation). 1) Closer view of coarsening- and shallowing-upwards parasequences of laminated to thinly bedded muds passing into fine sandstones (sometimes bioclastic) representing progradation of small-scale deltas that fill the proximal part of the lagoon. 2) Another example of muds overlain by sandstones. Sedimentation of these clastic-dominated bodies used to be quick as suggested by frequent soft sedimentary deformation and erosion. Stick in the field of view is 90 cm long, and each subdivision is 10 cm. 3A, B) Top surface completely

dissected by dewatering structures. Stick is 1.2 m long. Microphotograph to the right shows green algae fragments (*Holosporella siamensis*, Pia 1930) as main bioclast. Silt-graded detrital quartz (qtz) is abundant in this silty bioclastic packstone. 4A, B) Field view and microphotograph of silty bioclastic-bearing mudstones/wackestones. Main bioclasts are bivalves (*Dacryomya* cf. *lacrima*, *Myophorella tuberculosa*, *Eocallista antiopa*, *Nerinella*? sp.) and minor ostracods.

2.5.2 Biostratigraphy

Original dating of sedimentary successions along the margin of the Ifni inlier is unclear. Series of geological maps (e.g. Benziane and Yazidi, 1982; Choubert, 1957; Hollard et al., 1985) show sections cropping out along the coast from Mirleft to Foum Assaka (Figure 2.4) and are mapped as faciès détritique rouge (detritic red facies) from the early Cretaceous and undifferentiated "middle" Cretaceous. A later edition of the *Notes et Mémoires n^{o} 360* from the Moroccan Geological Service included more detailed geological maps at scale 1/100000 in which gastropod (*Natica*, *Ampulina, and* Nerineids) and bivalve (Trigonids and Alectryonids) faunas were reported and an early and "middle" Cretaceous age assigned (Destombes, 1991; Yazidi et al., 1986). In 2016 an explicative notice of the Sidi Ifni sheet at scale 1/50000 (Benziane et al., 2016) described the Craima succession and attributed the coarse clastics and the overlying fine clastics and carbonates to the Tan Tan Sand Fm. (Valanginian onwards) and Aguidir Limestone Fm. (upper Albian) respectively. The dating of the exposed sediments was based on not documented oysters, gastropods and arguably identified ostracods (*Brachycythere* sp., *Brachycythere beertheeaensis*, and *Paranotacythere* sp.) (Abou Ali et al., 2003; Choubert et al., 1966). The reported taxa are not restricted to the Cretaceous, and the previous dating is now revised (this study).

A new biostratigraphic framework is proposed for the studied succession based on identification of bivalves and gastropods and supported by foraminifera and algae. The macrofauna provides a Bathonian age for all the beds analysed, except the lowest one, in which abundant specimens of *Falcimytilus* sp. could not be identified to species level (Table 2.2; Figure 2.6, Figure 2.11 and Figure 2.12). The gastropods in particular belong to a stock of species characteristic of Bathonian sediments of the Paris Basin and southern England. A few bivalves show a wider stratigraphical and geographical distribution (Table 2.3).

Long ranging Jurassic groups of foraminifers identified in thin section (Mike Simmons pers. comm.) include *Nautiloculina oolithica* Mohler, 1938 and *Nautiloculina circularis* (Said & Barakat, 1959). A middle to late Jurassic age is generally accepted for those

foraminiferas (Kuznetsova et al., 1996; Tasli, 2001) and this age is supported by the co-occurrence of the green algae (Bruno Granier, pers. Comm.) *Holosporella siamensis* (Bassoulet, 1987; Elliott, 1983; Kuss, 1990; and references therein).

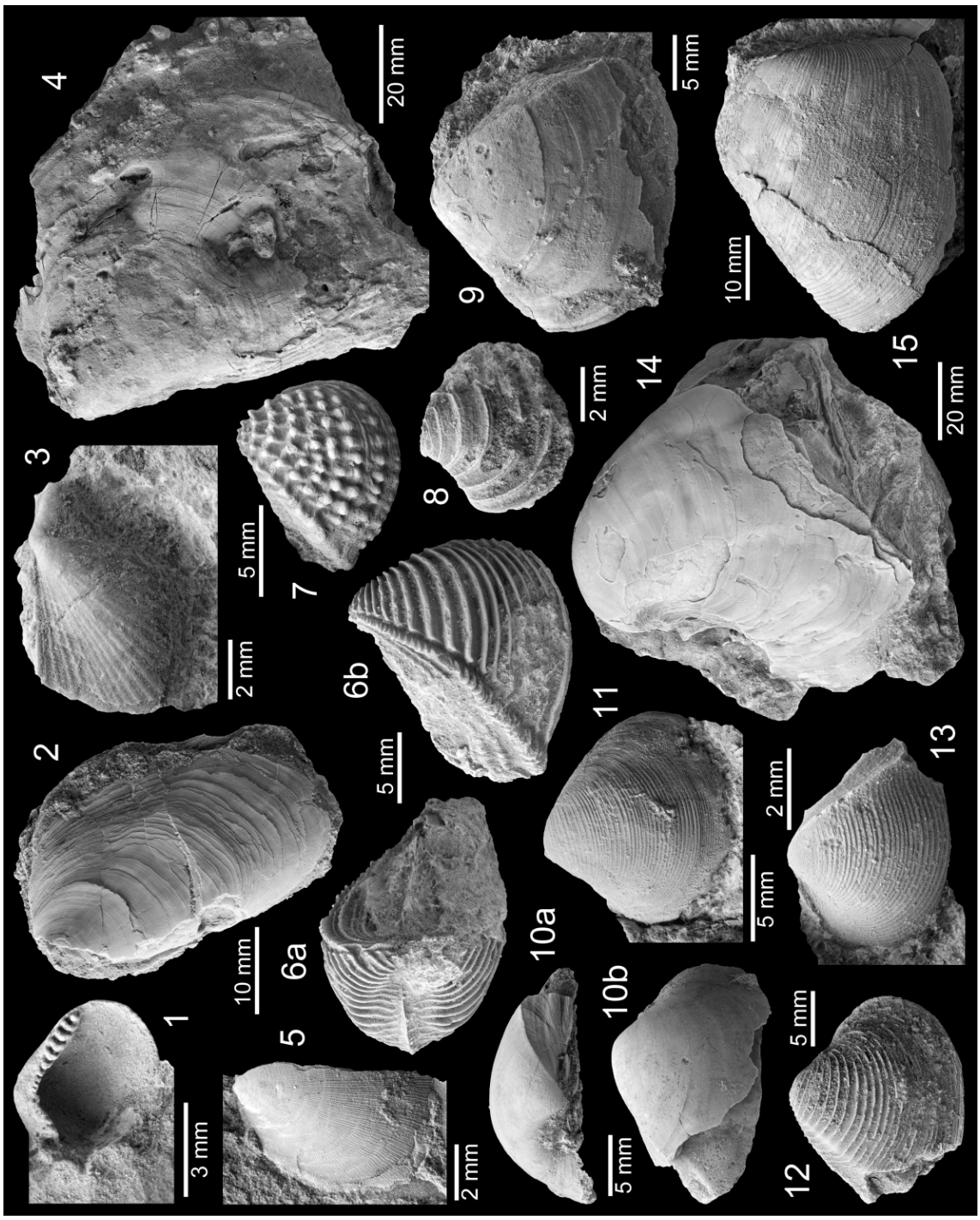

Figure 2.11. Bivalves identified in the succession. See Table 2.2 for additional information on stratigraphic and geographic distribution. 1 - Dacryomya cf. lacrima (J. de C. Sowerby, 1824), 2 - Falcimytilus sp., 3 - Costigervillia sp., 4 - Isognomon isognomonoides (Stahl, 1824), 5 - Placunopsis socialis Morris & Lycett, 1853, 6a, 6b - Trigonia pullus J. de C. Sowerby, 1826, 7 - Myophorella tuberculosa (Lycett, 1850), 8 - Nicaniella pulla (Roemer, 1836), 9 - Protocardia lycetti (Rollier, 1912), 10a, 10b - Pronoella sp., 11 - Eocallista antiopa (d'Orbigny, 1850), 12 - Eomiodon angulatus (Morris & Lycett, 1855), 13 - "Corbula" cf. involuta Münster in Goldfuss, 1837, 14 - Pachyrisma grande Morris & Lycett, 1850, 15 - Ceratomya concentrica (J. de C. Sowerby, 1825).

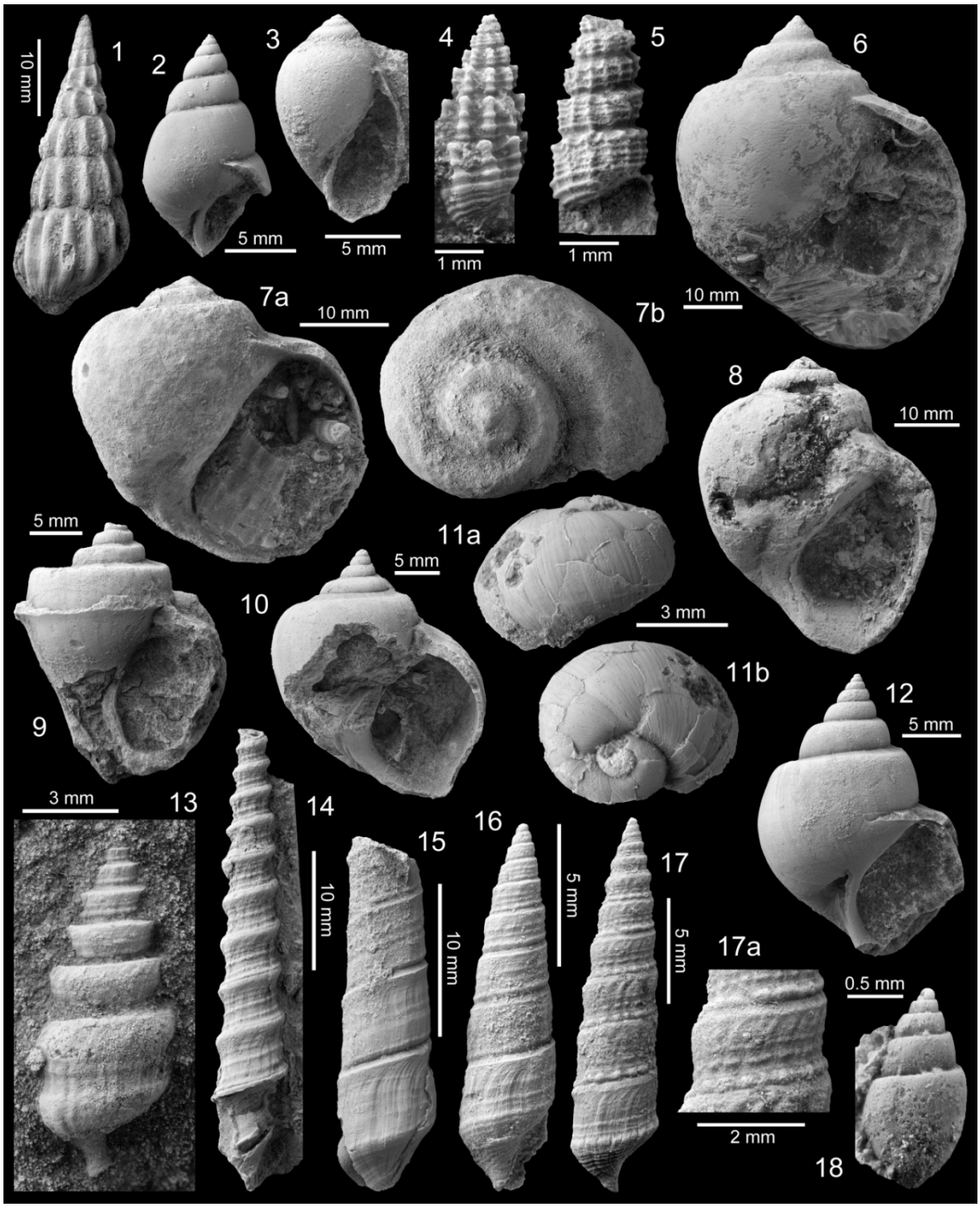

Figure 2.12. Gastropods identified in the succession. See Table 2.3 for additional information on stratigraphic and geographic distribution. 1 - Zygopleuridae indet., 2 - Pseudomelania (Oonia) variata (Lycett, 1863), 3 - Eligmoloxus limneiformis Cossmann, 1885, 4 - Exelissa cf. binodosa Grundel, 1990, 5 - Cryptaulax sp., 6, 7a, 7b - Globularia cf. eparcyensis (d'Archiac, 1843), 8 - Globularia cf. tancredi (Morris & Lycett, 1850), 9 - Ampullospira actaea (d'Orbigny, 1850), 10 - Globularia sp., 11a, 11b - Naricopsina matheroni (Gourret, 1884), 12 - Pictavia? cf. stricklandi (Morris & Lycett, 1850), 13 - Phaneroptyxis? sp., 14 - Nerinella elegantula (d'Orbigny, 1850), 15, 16, 17, 17a - Ceritella dewalquei (Piette, 1857), 18 - Sinuarbullina? Sp.

Table 2.2. Additional information about stratigraphic range and geographical distribution of bivalves from Oued Craima and Sidi Warzik

BIVALVIA			
Species	**Stratigraphic range**	**Geographic distribution**	**References**
***Dacryomya* cf. *lacrima* (J. de C. Sowerby, 1824)**	Bathonian-Lower Callovian	northern Germany, England, India	Stoll (1934), Cox (1940), Cox & Arkell (1948), Jaitly et alii (1995)
***Isognomon isognomonoides* (Stahl, 1824)**	Aalenian-Bajocian	England, Paris Basin	Cox & Arkell (1948), Benecke (1905)
	Bajocian	Romania	Lažar (2006)
	Bathonian	England, Paris Basin	Cox & Arkell (1948), Fischer (1969), Palmer (1979)
***Placunopsis socialis* Morris & Lycett, 1853**	Bathonian	Paris Basin, England	Cossmann (1907, Cox & Arkell (1948), Fischer (1969), Palmer (1979), Todd & Palmer (2002)
***Trigonia pullus* J. de C. Sowerby, 1826**	Bathonian	Egypt, England, Paris Basin, Tunisia	Douvillé (1916), Cox & Arkell (1948), Fischer (1969), Palmer (1979), Holzapfel (1998)
***Myophorella tuberculosa* (Lycett, 1850)**	Aalenian?-Bajocian	England	Lycett (1863)
	Bathonian	England	Lycett (1863)
***Nicaniella pulla* (Roemer, 1836)**	Uppermost Bajocian-Upper Bathonian	Poland	Pugaczewska (1986)
	Bathonian(?)	Germany	Roemer (1836)
	Lower Bathonian-Middle Callovian	Northern Germany	Stoll (1934)
***Protocardia lycetti* (Rollier, 1912)**	Bathonian	Paris Basin, England	Cossmann (1900), Arkell (1931), Cox & Arkell (1948), Palmer (1979)
***Eocallista antiopa* (d'Orbigny, 1850)**	Bathonian	England, Paris Basin	Cox & Arkell (1948), Fischer (1969), Palmer (1979)
***Eomiodon angulatus* (Morris & Lycett, 1855)**	Bathonian	England, southern France, China?	Arkell (1931), Cox & Arkell (1948), Fürsich et al. (1995), Yin & Fürsich (1991)
***"Corbula"* cf. *involuta* Münster in Goldfuss, 1837**	Bajocian?	Southern Germany	Goldfuss (1837)
	Bathonian	England, southern France	Lycett (1863), Cossmann (1905)
***"Corbula"* cf. *islipensis* Lycett, 1863**	Bathonian	England, Paris Basin	Lycett (1863), Fischer (1969)
***Pachyrisma grande* Morris & Lycett, 1850**	Bathonian	England	Cox & Arkell (1948)
***Ceratomya concentrica* (J. de C. Sowerby, 1825)**	Bajocian-Oxfordian	Europe, Africa, Middle East	de Loriol (1883), Douvillé (1916), Arkell (1934), Cox (1936), Cox & Arkell (1948), Cox (1965), Fischer (1969)

Table 2.3. Additional information about stratigraphic range and geographical distribution of gastropods from Oued Craima and Sidi Warzik

GASTROPODA			
Species	**Stratigraphic range**	**Geographic distribution**	**References**
***Pseudomelania* (*Oonia*) *variata* (Lycett, 1863)**	Upper Bathonian	north-eastern Paris Basin and south-western England	Lycett (1863), Cossmann (1885), Fischer (1969)
	Undiff. Bathonian	south-western England	Cox & Arkell (1950)
***Eligmoloxus limneiformis* Cossmann, 1885**	Lower Bathonian	north-eastern Paris Basin	Cossmann (1885)
***Exelissa* cf. *binodosa* Grundel, 1990**	Callovian	northern Germany	Gründel (1990, 1999)
***Globularia* cf. *eparcyensis* (d'Archiac, 1843)**	Middle and Upper Bathonian	north-eastern Paris Basin	d'Archiac (1843), d'Orbigny (1852), Cossmann (1885, 1895)Fischer (1969), Fischer & Weber (1997)
***Globularia* cf. *tancredi* (Morris & Lycett, 1850)**	(Upper?) Bathonian	south-western England	Lycett (1863), Cox & Arkell (1950)
***Ampullospira actaea* (d'Orbigny, 1850)**	Middle and Upper Bathonian	north-eastern Paris Basin	Fischer (1953, 1969), d'Orbigny (1850, 1852); Fischer & Weber (1997)
	Undiff. Bathonian	western England	Morris & Lycett (1851); Cox & Arkell (1950)
***Naricopsina matheroni* (Gourret, 1884)**	Undiff. Bathonian	southern France	Gourret (1884), Cox & Mouberge (1950)
***Pictavia*? cf. *stricklandi* (Morris & Lycett, 1850)**	Lower to Upper Bathonian	northern Paris Basin	Cossmann 1885);
	undiff. Bathonian	south-western England	Morris & Lycett (1851), Cox & Arkell (1950)
***Ceritella dewalquei* (Piette, 1857)**	Middle and Upper Bathonian	north-eastern Paris Basin	Piette (1857), Fischer (1969)
***Nerinella elegantula* (d'Orbigny, 1850)**	Lower Bathonian to Upper Bathonian	Paris Basin	d'Orbigny (1850, 1851), Cossmann (1885, 1898), Fischer 1953, 1969), Fischer & Weber (1997)

The resemblance in facies and fauna of our study with facies previously described in the area make us believe a probable generalized misdating of the Mesozoic outcrops in the Ifni area. A more likely Middle Jurassic age (probably Bathonian) is suggested for all the Mesozoic outcrops along the Atlantic margin of the Ifni inlier (Figure 2.4).

The lower ~250 m of the succession could not be confidently assigned to a specific age. At 205 m, foraminifer-rich grainstones yield specimens that are not age diagnostic but resemble Middle to late Jurassic taxa. Below this stratigraphic level, palynological analysis was attempted in the continental red beds of the Guezira Fm, but no ages could be assigned to the fine-grained sandstones (Figure 2.4). Nevertheless, superposition of the conformable sequence indicates a pre-Bathonian, Triassic to Bathonian, age.

The Bathonian age established in this study for the succession, is the oldest rocks Mesozoic sediments exposed in the ATB and the most southerly Jurassic outcrops in NW Africa south of the Atlas mountain range.

2.5.3 Sequence Stratigraphy

A sequence stratigraphic framework is proposed based on the combination of facies analysis, base-level change inferred from sequence-bounding surfaces and eustatic sea-level. In order for this framework to have regional significance, different stratal units and bounding surfaces have been defined attending to their physical relationships of the strata, facies and environmental interpretations. Parasequences, parasequence set and systems tracts have been constructed and used as the building blocks for the sequence stratigraphic framework. To establish true parasequences with a regional-scale significance a group of beds, or bedsets, genetically related must be bounded at base and top by small-scale flooding surfaces or their correlative surface (Mitchum and Van Wagoner, 1991; van Wagoner et al., 1990, 1988). Genetically related successions of parasequences, bounded by higher order marine flooding surfaces can be grouped in parasequence sets exhibiting a distinctive stacking pattern (van Wagoner et al., 1988).

Three 3rd order depositional sequences have been interpreted along the succession exposed at Oued Craima and Craima Beach (Figure 2.6). Tens of m-scale thinning and coarsening upwards packages, representing mainly progradation (see section 2.5.1) have been identified (Figure 2.6). These packages may represent the response of the system to allocyclic or autocyclic controls. The succession described along Oued Craima and Craima Beach is the only Jurassic section exposed in DLT Basin known to date. The

lack of time-equivalent successions make impossible to establish regional-scale parasequences that can be correlated from outcrop to outcrop and it poses a limitation to any sequence stratigraphic framework derived. Without this correlation, individual coarsening and fining upwards packages have been assumed to be parasequences bounded by marine flooding surfaces. A sequence stratigraphic framework is proposed for the late Middle Jurassic based on parasequence stacking patterns (Figure 2.6).

Despite the 1D nature of the succession, parasequences, bounded by flooding surfaces, together with parasequence stacking patterns are tentatively identified (Figure 2.6). The lower c. 175 m of the studied section consists of alluvial fan conglomerates (FA1). Due to the difficulty of identifying parasequences in fluvial sections with absent marginal marine or marine sediments (van Wagoner et al., 1990) parasequences have not been studied in the lower part of the section. The first transgressive surface (ts) has been placed at the base of parasequence P1 where the first sharp change in depositional environment is recorded (FA2 overlain FA1). The transition from continental alluvial plain to peritidal and marine lagoon facies is interpreted as a retrogradational parasequence set (P1-P10). The package is capped by limestones that record the deepest facies of this interval. In the absence of clearer palaeodepth indicators a maximum flooding surface (mfs) has been placed tentatively coinciding with the top of the bioclastic-rich grainstone at 205 m. Poor exposure between 205-211 m does not allow clear identification of parasequences. The sharp change in lithology and return to a proximal continental setting suggest the presence of a sequence boundary (SB), which has been placed at the base of the first appearance of conglomerates. Progradational parasequence set (P11-P12) has been identified and interpreted as the lowstand systems tract (LST).

P13-P26 mainly represent peritidal facies punctuated by short marine transgressions. They display an overall trangressive trend and therefore interpreted as a transgressive systems tract (TST). The mfs is placed at 290 m within outer lagoon bioclastic packstones. One flooding surface (fs) is interpreted at 243 m. Parasequences P27-P31 are stacked in a progradational fashion. The section contains facies that suggest upward shallowing conditions and it has been interpreted as the highstand systems tract (HST). Two fs, at 310 m and at 321 m, have been recognized. The latter is at the base of P32, which due to poor exposure could not be confidently interpreted.

An abrupt change in sedimentary facies, from c. 327 m to 340 m suggests another SB, which has been placed at the base of the first conglomerate bed. P33-P38 display a progradation stacking pattern with one flooding event (fs) at 347 m. These correspond to the TST. The ts has been placed above a thin conglomerate bed overlain by oncoidal limestones at 359 m. From this point, the rest of the succession is a thick TST, with at least, four fs identified. Parasequence sets in the lower ~105 m show a retrogradational to aggradational stacking pattern. This changes around 455 m, where individual parasequence sets start to exhibit progradation, although the overall stacking is still retrogradational.

The succession has been subdivided in three 3rd order sedimentary sequences, marked at the base by the presence of red conglomerates. The overall shallowing trend from entirely continental facies to marine, punctuated throughout by pulses of coarse continental clastics probably is part of a 2nd order transgressive systems tract. The absence of equivalent outcrops in the basin prevents verification of this hypothesis.

2.6 Discussion

2.6.1 New lithostratigraphy

A probable misdating of the Mesozoic sections exposed in the area next to the Ifni Inlier has been proposed already (see section 2.5.2). For the purpose of future mapping in the area and for comparison with other time equivalent units in Morocco, we informally propose the subdivision of the succession into three lithostratigraphic subdivisions with rank of formations (Figure 2.6). Definition of the formations has been performed following the recommendations given by Whittaker et al., (1991). The main criteria used to define the formations have been the presence of a sharp lithologic contrast at the base, which in turn make them easily recognizable in the field. Upper limits are usually poorly exposed but they are perfectly defined by the base of the overlying formation.

2.6.1.1 Guezira Formation

This formation is exposed along the Oued Craima (Figure 2.5). The total thickness of the unit is c. 205 m (Figure 2.6). Its lower part is made of 175 m of red conglomerates and minor red sandstones unconformably overlying the Precambrian ignimbrites and andesites of the Ouarzazate Group of the Ifni inlier (Yazidi et al., 1986). They evolve into c. 8 m of inter stratified dm- to m-scale fining upwards packages of red/white fine

sandstones with evidence of palaeosol development and red conglomerates. The upper c. 22 m consists of dm thick interbedded muds, fine-grained sandstones and limestones capped by a final limestone unit 1.5 m thick with abundant bioclasts, ooids and peloids. This lithostratigraphic unit is continuously exposed along Oued Craima, but lateral exposures are relatively limited due to tectonic tilting. Stratigraphically-equivalent coarse-grained red beds have excellent lateral exposures and abundance of sedimentary structures at Guezira Beach (Figure 2.4) but the upper interbedded fine-grained clastics and carbonates are not exposed. The most striking feature of this unit is the thick package of reddish coloured coarse clastics. These are superbly exposed along Guezira Beach and hence Gueriza Fm. is used as the name for this lower unit.

2.6.1.2 Oued Craima Formation

This interval comprises ~120 m of exposed section along Oued Craima (Figure 2.5). The lower and upper contacts of this lithostratigraphic unit are not exposed. The unit starts with c. 5 m of poorly exposed red conglomerates that rapidly transition into c. 110 m of relatively monotonous, thinly interbeded red to grey muds and fine-grained sandstones punctuated by dm- to m-thick grey oncoidal packstones, algal laminites and bioclastic- and/or peloidal-bearing mudstones/wackestones to packstones. Carbonate nodules parallel to bedding are abundant; sometimes they coalesce and form continuous beds. Occasional m-scale channelized cross-bedded bioclastic grainstones and carbonate-rich mottled palaeosols may be present. The last c. 7 m are poorly exposed coarse-grained sandstones to matrix-supported conglomerates interbedded with mud and silt, and bioturbated by dm-long vertical burrows. The unit is overlain by a 12 m gap.

2.6.1.3 Sidi Ouarzik Formation

This formation is exposed along the right bank of Oued Craima, close to the river mouth opening out into the Atlantic, and southwest of the river mouth along the beach (Figure 2.5). It is c. 217 m thick and starts with a basal c. 8 m thick unit of red conglomerates overlain by c.16 m of interbedded fine clastics and limestones similar to the Oued Craima Fm. The succession becomes increasingly carbonate rich, with numerous dm- to m-thick interstratified units of laminated muds (and fine-grained sandstones), calcareous sandstones and bioclastic-, peloid- and ooid-bearing limestones. The upper 60-70 m of

the formation show interstratified beds of hummocky cross-laminated fine-grained sandstones to silts in addition to the previous lithologies.

2.6.2 Sediment provenance

The main candidate provenance area is the Ifni inlier, a domal structure cored by Proterozoic igneous rocks overlain by Proterozoic and Palaeozoic carbonates located to the immediate east of the coastal outcrops (Figure 2.4). Post-rift uplift is postulated for the western Anti-Atlas until the Middle Jurassic (Charton et al., 2018). Due to its domal geometry, during uplift, preferential erosion of the central areas of the Ifni inlier would expose Proterozoic igneous lithologies, while the Palaeozoic carbonate-dominated sedimentary cover would be exposed and eroded towards the margins of the dome (Figure 2.4). Qualitative field observations of roundness, sphericity and clast composition on the Guezira Fm. show variations along the coasts. Conglomerates at Guezira Beach (Figure 2.4) tend to be more angular and some are dominated by clasts of igneous origin (up to dm-scale basalts with hexagonal habit). At Oued Craima, the conglomerate beds of the same formation tend to exhibit more rounded clasts and lithologies can be dominated up to 60% (visual estimation) by recrystallized limestones and dolomites with basalt clasts being minor components. We interpret the difference in the overall clast lithology as the result of small-scale catchment areas (~ 100's km^2) draining preferentially igneous rocks or carbonates within, and in the proximity, of the Ifni inlier. The different roundness of the clasts is, in our interpretation, probably related to the mechanical stability of the main lithologies involved and not to longer transport distances/larger catchments.

In the overlying marine sandstones, clasts are dominated by quartz, although individual beds can have a significant proportion of feldspars and igneous rock fragments. Well-rounded dolomite clasts can be also present, but not common. Quartz angulosity, concentrations of igneous rock fragments and feldspars and occasional dolomite clasts also points towards locally-derived sediment with relative short transport.

2.6.3 Tectonics *vs* eustacy and timing of Western Anti-Atlas exhumation

The exhumation and subsidence history of the western Anti-Atlas can be summarized as syn- and post-rift exhumation until the Middle Jurassic, subsidence during late Jurassic and early Cretaceous and resumed exhumation from Late Cretaceous onwards (Charton et al., 2018).

In the Ifni-1 well (Figure 2.3 and Figure 2.4), drilled offshore on the Ifni horst, an unconformity between late Callovian sediments resting on Permo-Triassic (Evans et al., 1976) suggests the presence of a palaeohigh starved of sediments or eventually exposed and eroded during the Early and most of the Middle Jurassic.

The succession presented here was deposited during the Bathonian eustatic sea-level drop (Haq et al., 1987; Snedden and Liu, 2010). Sedimentological interpretation has resulted in a model of continental to peritidal to shallow-marine deposition in a series of palaeoenvironments under overall transgressive conditions. The overall deepening upwards trend is the opposite that could be expected under this scenario and a strong subsidence at this point of the basin is needed.

2.6.3.1 Subsidence rates

An attempt to estimate subsidence rates for this segment of the basin has been made. Post-sedimentary compaction of the sediments has not been taken into account. The duration of the Bathonian, the estimated sea-level fall and the thickness of sediments confidently dated have been combined in order to produce estimated ranges of subsidence. One of the main limitations of this approach has been the lack of lower and upper limits of the Bathonian in the studied outcrops. To overcome that limitation the succession logged and dated has been assumed to represent the entire Bathonian.

Acceptable duration for the Bathonian ranges approximately between 2.2 Ma (e.g. Gradstein et al., 2012) to 3 Ma (e.g. Snedden and Liu, 2010). Eustatic curves predict a sea-level fall ranging between ca. 10-20 m (Haq et al., 1987; Snedden and Liu, 2010) during the Bathonian. Due to the small difference in comparison with the total thickness of sediments an average sea-level fall of 15 m has been assumed for simplicity. Approximately 300 m of succession has been dated confidently as Bathonian (see section 2.5.2 and Figure 2.6).

Calculated subsidence rates range between 105 and 143 m/Ma, considering the maximum and minimum duration of the Bathonian in this study. Although this numbers are high, comparable subsidence rates (80-120 m/Ma) have been reported in the southern segment of the DLT Basin for the Jurassic by von Rad and Einsele (1980). Furthermore, comparable high subsidence rates on the conjugate margin at the Baltimore Canyon Trough have been estimated around 130 m/Ma during the Jurassic (Scholle, 1977).

A considerable thickness of sediments is recorded in the proximity of an overall exhuming domain during this period of time. A strong subsidence in the basin was needed to accommodate that thickness of sediment and overcome the coupled drop in sea-level. The Callovian unconformity in Ifni-1 well, the highly subsiding domain at Craima next to a mainly exhuming Western Anti-Atlas suggest a strong structural control on deposition, probably related with inherited Triassic syn-rift structures.

2.6.4 Comparison of Jurassic stratigraphy along the Moroccan coastal basins

The stratigraphy of the passive margin coastal basins along the Atlantic margin of Morocco may be expected to be very similar, but important differences can be highlighted (Figure 2.2, Figure 2.3 and Figure 2.13). These differences are related to the complex inherited structure of the basement from northeast to southwest, including terrains that have undergone several orogenic episodes since the Proterozoic (Figure 2.1), and subsequent tectonics that played an important part in sediment delivery to the basins.

Salt deposition is another key factor. Upper Triassic - Lower Jurassic syn-rift salt basins are unevenly distributed along the Moroccan margin. The salt became diapiric during the post-rift phase (Figure 2.3) and affected subsequent sediment distribution.

In basins to the north (i.e. Doukkala and Agadir-Essaouira) Lower and Middle Jurassic carbonates coexist with clastics and evaporates, while towards the south, in the Aaiun-Tarfaya basin (ATB) clastic input is higher and evaporites are absent (Figure 2.2). Terrigenous sedimentation during the Jurassic is not homogeneous and the northern half of the ATB seems to contain higher clastic sediment (Figure 2.2).

Doukkala Basin (DB): This basin developed during the Mesozoic resting with an unconformity on deformed Palaeozoic rocks of the Western Meseta (Figure 2.1), which exerted a strong structural control on sedimentation (Figure 2.2). The Mesozoic post-rift sedimentary cover on the offshore Mazagan Plateau (Figure 2.2) is much thinner than in other basins (von Rad et al., 1985) such as the Agadir-Essaouira Basin (AEB) or the ATB. Middle Jurassic sediments are not exposed, but they have been penetrated by exploration wells onshore and DSDP wells offshore. Sedimentary facies record an overall vertical transgression and exhibit, more proximal continental-marginal marine clastic-dominated to the east and distal micritic limestones and breccias to the west

(Figure 2.3). The Middle Jurassic is thin in the DB and both the Lower and Middle Jurassic are missing towards the northeast, (Figure 2.2 and Figure 2.3).

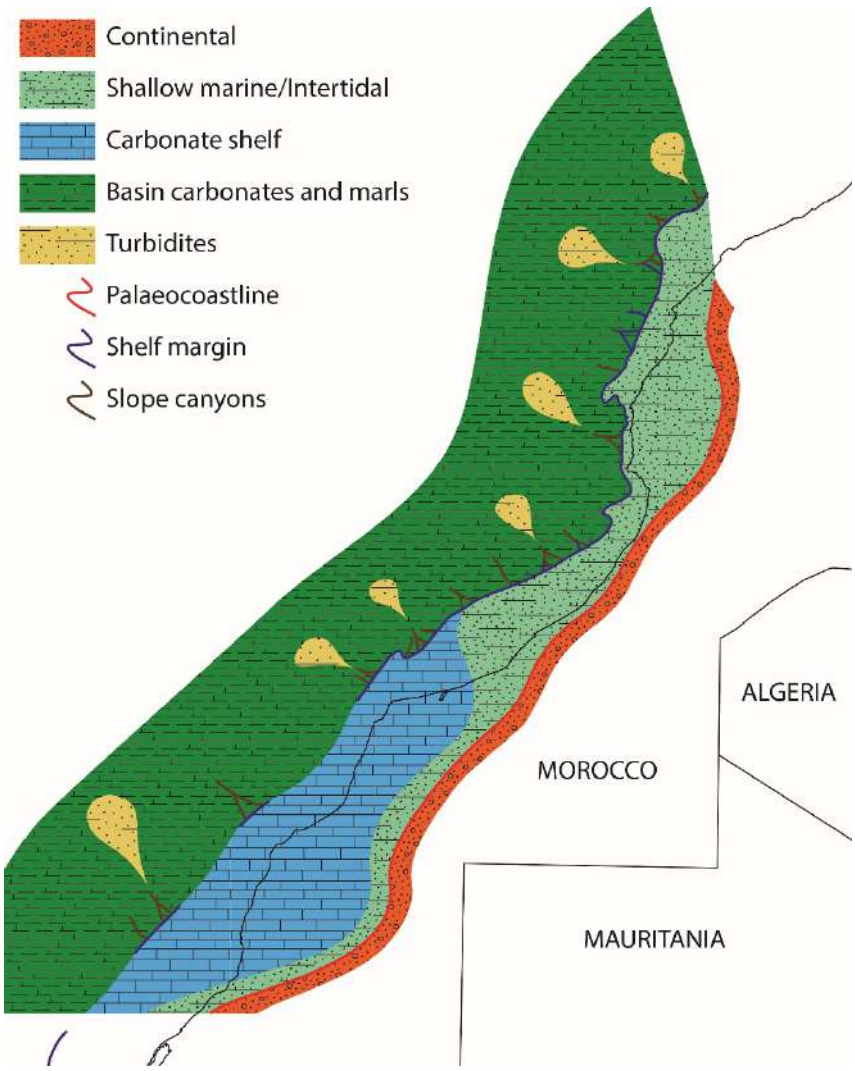

Figure 2.13. Palaeoenvironmental reconstruction along the Moroccan Atlantic margin for the Bathonian. Jurassic shelf after (Hafid et al., 2006; Hinz et al., 1982; Seibold, 1982). Shoreline in the Doukkala and Agadir-Essaouira basins after (Medina, 1995).

Agadir-Essaouira Basin (AEB): The Bathonian in the southern AEB is represented by the upper part of the Ameskhoud Fm. and the lower part of the Ouanamane Fm. (Adams, 1979; Bouaouda, 2004). The latter are made of continental red clastics with minor carbonates and fossiliferous marine carbonates respectively, showing an overall transgressive trend comparable to the one observed in the DB and the ATB, logged in this study at Oued Craima and Sidi Ouarzik Beach. In the middle part of the AEB, along the Amsittene anticline, the Bathonian is characterized by subtidal carbonates of the "Dolomies de l'Amsittene" (Duffaud, 1960). In the northern part of the AEB, where the Middle Jurassic is mainly known from on- and offshore exploratory wells,

biostratigraphic resolution is not good enough, so this time period is broadly referred to as Dogger in the well reports. The Dogger is represented by microconglomerates, sandstones, clays, dolomites and anhydrite of the Ameskhoud Fm. deposited in a continental to proximal marine environment.

The facies show an overall decrease in grain size towards the northwest together with a relative increase in proportion of dolomites and anhydrites, indicative of more distal settings. In wells drilled on the present day shelf, the Middle Jurassic is carbonate-rich, with occasional fine clastics and minor anhydrite. Limestones range from micrite to oolitic grainstones denoting a shallow carbonate shelf to tidal flats with occasional periods of exposure. The great areal extension of these shallow marginal marine to distal continental facies over virtually the entire basin suggests a stable, wide, low relief basin extending over the present day shelf, covered by a shallow epicontinental sea, periodically exposed due to small eustatic or tectonic variations. Halokinesis also plays an important role in local differences in sedimentation, as Triassic salt diapirs were probably already active during the Middle Jurassic. The uplift of Palaeozoic terrains of the "Massif Central du Haut Atlas" to the SE during Middle Jurassic provided the sediment delivered to the basin (Ambroggi, 1963).

Aaiun-Tarfaya Basin (ATB): The ATB can be divided into three segments (or sub-basins). A comparison from north to south among the three segments reveals some striking variations in facies and sediment thickness (Figure 2.2 and Figure 2.3). The Jurassic succession exhibits a clear overall increase in thickness towards the south, especially under the present day shelf and slope (Figure 2.3). The thickness of Jurassic decreases in the Ifni segment ranges up to 500 m (364 m in the Ifni-1 well, although the presence of a late Callovian unconformably overlying the Permo-Triassic in the Ifni-1 well (Evans et al., 1976) results in missing section. In the central Tarfaya segment, the Puerto Cansado-1 well encountered a 2126 m thick Jurassic section (Martinis and Visintin, 1966; Viotti, 1966), and the Middle Jurassic recorded in the TanTan-1 well is c. 950 m thick. In the most southerly Dakhla-Boujdour segment, the thickness of the pre-Cretaceous succession has been estimated up to 8 km (von Rad and Einsele, 1980). Subsidence rates for the Dakhla-Boujdour segment were high, between 80-120 m/Ma (von Rad and Einsele, 1980).

In the Ifni segments, some c. 35 km to the east of the offshore Ifni-1 well, 250-300 m of the succession is exposed at Oued Craima and Sidi Ouarzik Beach, confidently assigned

to the Bathonian. Further c. 250 m of underlying red beds of the Guezira Fm are age indeterminate, but probably range from Triassic to Bathonian age. This, contrasts with the 236 m of undifferentiated Upper Lias and Dogger fine clastics and carbonates in the Puerto Cansado-1 well (Viotti, 1966).

Thickness variations and unconformities indicate a complicated tectonic history triggered by the Middle Jurassic exhumation of the Anti-Atlas and Reguibat Shield (Leprêtre, 2015; Gouiza *et al.*, 2017) and subsidence in the basin. This complex interplay triggered a variable response in the three segments of the ATB, especially the Ifni segment. The Dakhla-Boujdour segment represents a stable, steadily subsiding distal part of the basin progressively thinning towards the hinterland (von Rad and Einsele, 1980). This produces a tapered Jurassic sedimentary wedge opening towards the deep offshore basin (Figure 2.3). The Tarfaya segment seems to have a similar evolution, with a wedge of Jurassic, although thinner and developing over a much shorter distance. This indicates less subsidence in this segment of the basin, especially during the Middle Jurassic as the Upper Lias and Dogger is only 236 m thick in the Puerto Cansado-1 well (Viotti, 1966). In the Ifni segment, the Middle Jurassic is represented only by the Bathonian succession onshore and the late Callovian in the Ifni-1 well. The missing part of the succession and the documented exhumation of the Anti-Atlas, suggest increased tectonic activity related to faulting and periodic uplift of this segment in the Middle Jurassic. Sedimentation occurred where accommodation developed in structural lows adjacent to the Ifni inlier and faulted highs. The upper Jurassic seismic sequences are continuous and thicken towards the west (Abou Ali et al., 2005), leaving a Jurassic wedge equivalent to the other segments of the ATB, although much thinner. The Jurassic thickness increase, from NE to SW (Figure 2.3), seems to be closely related with the Anti-Atlas tectonics during the Mesozoic combined with an enhanced subsidence in the basin.

2.6.5 Palaeoenvironmental implications and depositional model

Seven FA have been described, grouped into continental (FA1 and FA2), peritidal (FA3) and marine (FA4-FA7) broad depositional environments. The evolution of the Bathonian section in the studied outcrop shows an overall transgression, punctuated by continental clastics eroded from the Anti-Atlas. Conglomerate interbeds are interpreted to record pulses of uplift within the Western Anti-Atlas. After each tectonic pulse, the system stabilised and continuous basin subsidence resulted in transgression of the

peritidal to marine facies deposition, until the next tectonic pulse and renewed progradation. The Bathonian is a period of time characterized by eustatic sea-level fall (Haq et al., 1987; Snedden and Liu, 2010). The succession at Oued Craima and Sidi Ouarzik Beach is interpreted to reflect the opposite depositional response to the global eustatic signal. Individual periods of coarse clastic progradation are recording the combined effect of local tectonic activity in the Anti-Atlas and the superposed sea-level fall.

Figure 2.14 summarizes a depositional model for the succession at Oued Craima and Sidi Ouarzik Beach. The model depicts four stages in the evolution of the coastal section on the flank of the Ifni inlier. A lower part of the succession (c. 180 m) comprises coarse alluvial fans deposited next to the prominent topography of the Ifni inlier (Figure 2.6 and Figure 2.14A). Intense subsidence in the basin extended to the coastal margin of the Ifni Inlier that combined with progressive erosion and loss in topography allowed transgression and development of a thick peritidal succession (Figure 2.6; from ~185-325 m). The significant amount of fine-grained clastics, together with carbonate palaeosols, microbial mats and periodic marine-influenced beds suggests a remaining topography in the hinterland of the Anti-Atlas and the development of a tidal flat in front of it (Figure 2.14B). The tidal flat was wide enough to allow the development of tidal creeks and marshes that supplied abundant carbonaceous plant material to the succession. A shallow lagoon is postulated along the shoreline, supplying oncoids, ostracods and other bioclasts inland, transported by tidal currents or storms. The upper c. 190 m of the succession is represented exclusively by marine sedimentation (Figure 2.6) recording an overall deepening; lagoonal muds and bioclastic limestones overlain by a mixed siliciclastic/carbonate shoreface succession (inner to middle ramp; Figure 2.14C and Figure 2.14D). The abundant carbonaceous plant fragments in these sediments suggest adjacent tidal flats inland, over what previously was positive topography on the flanks of the Western Anti-Atlas.

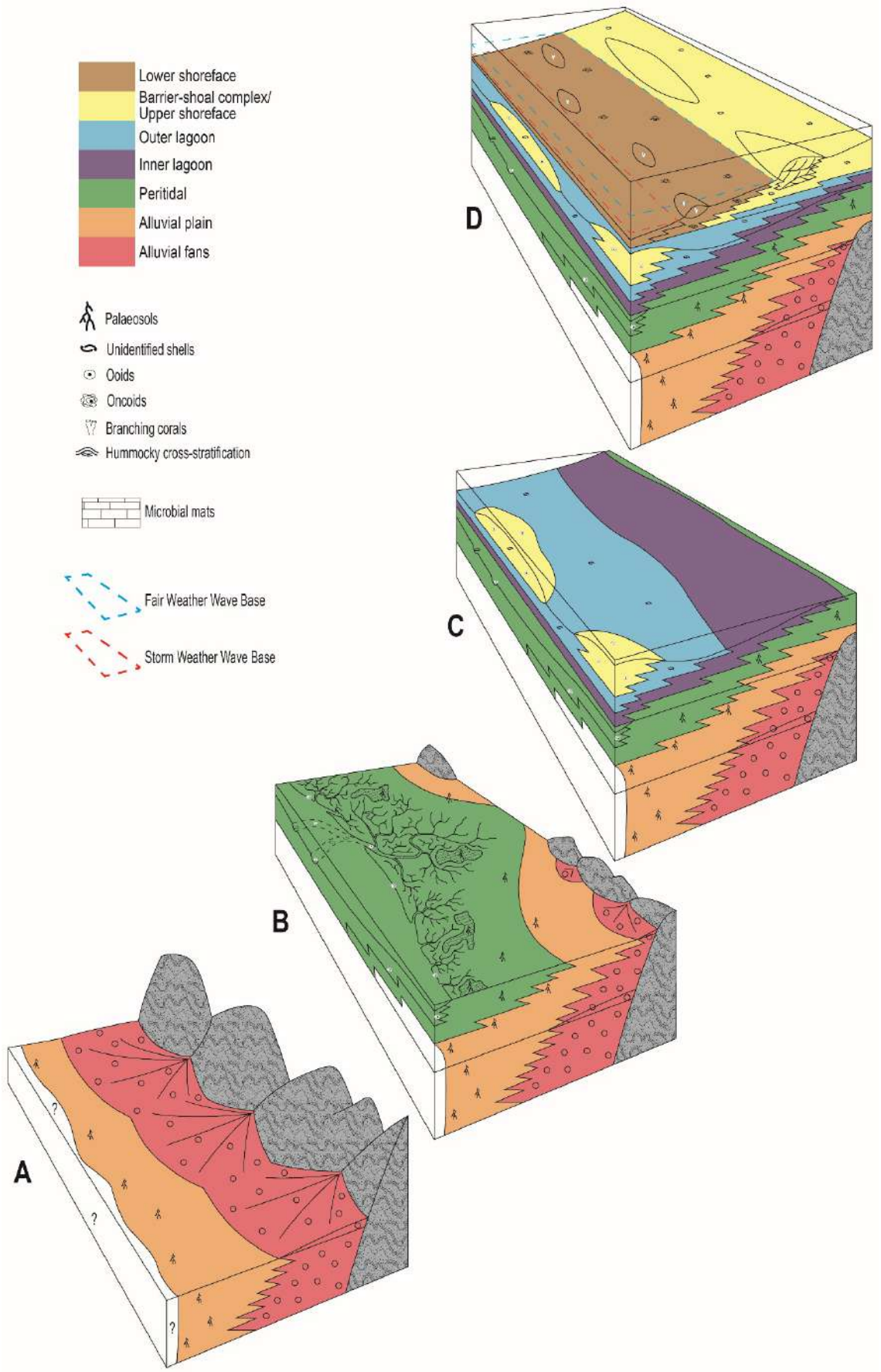
Lower shoreface
Barrier-shoal complex/
Upper shoreface
Outer lagoon
Inner lagoon
Peritidal
Alluvial plain
Alluvial fans
Palaeosols
Unidentified shells
Ooids
Oncoids
Branching corals
Hummocky cross-stratification
Microbial mats
Fair Weather Wave Base
Storm Weather Wave Base
A
B
C
D

Figure 2.14. Depositional model illustrating the main four stages in the evolution of the system during the Bathonian.

2.7 Conclusions

In this study we present for the first time a lithostratigraphic and sequence stratigraphic model for the Mesozoic sediments deposited on the flanks of the Ifni inlier, with a revised biostratigraphic framework. This provides the first recorded interpretation of outcrops of Middle Jurassic sediments along this part of the NW African Central Atlantic Margin. The main findings of this study are:

Biostratigraphy

- The section exposed at Oued Craima and Sidi Ouarzik Beach has been reassigned to a Middle Jurassic, Bathonian age, based on newly recovered gastropod and bivalve assemblages.

Lithotratigraphy and Depositional Environments

- Three lithostratigraphic formations are proposed: Guezira Fm., Oued Craima Fm. and Sidi Ouarzik Fm.
- The Guezira Fm. unconformably overlies basement, and is made of ~180 m of mainly continental red conglomerates and minor sandstones, capped by ~20 m of peritidal and shallow marine fine clastics and carbonates. Red conglomerates and sandstones belonging to this formation are exposed along the coast from Mirleft to Foum Assaka.
- The Oued Craima Fm. is ~115 m thick and mainly composed of peritidal fine sandstones, silts and microbial limestones punctuated by shallow marine lagoonal carbonates and silts.
- The ~190 m thick Sidi Ouarzik Fm. evolves from a thin unit of continental red conglomerates and mixed siliciclastic-carbonate tidal flats into marine mixed siliciclastic-carbonate lagoon and upper-middle ramp.

Sequence Stratigraphy

- The Bathonian succession is overall transgresssive, anti-correlated to the global eustatic signal and tectonic-crontrolled. Periods of coarse clastic progradation

are interpreted to record short-lived local tectonics related to post-rift Anti-Atlas exhumation.

- The three formations are defined as depositional sequences, bounded by sequence boundaries. Maximum flooding surfaces (mfs) and transgressive surfaces (ts) have been also identified.
- The Guezira Fm. is interpreted to be a LST and overlying TST. The ts has been confidently placed, but the mfs is speculative due to poor exposure.
- The Oued Craima Fm comprises a thin basal LST, followed by a well-developed TST and HST.
- The Sidi Ouarzik Fm. is composed of a basal LST and a thick overlying TST.

Regional palaeogeography

- The results suggest that far from being a simple passive margin sag, inherited basement structure has controlled the distribution and type of syn-rift sedimentation, and post-rift tectonics and exhumation of Precambrian and Variscan domains play a key role in the early post-rift sedimentation along the Atlantic margin of Morocco.
- Clastic input vs. carbonate production and thickness of sequences along the Aaiun-Tarfaya Basin (ATB) are directly influenced by the exhumation / subsidence history of the Western Anti-Atlas.
- The evidence for tectonic activity ended by the early Callovian, and following this time the stratigraphy of the ATB is comparable along its length.
- Mixed siliciclastic-carbonate continental to shallow marine sedimentation dominate all the sub-basins along the Moroccan passive margin, including the Doukkala, Agadir-Essaouira and the northern half of the Aaiun-Tarfaya Basins.
- Carbonate platforms are better developed and much thicker in the southern half of the ATB.

Along the Atlantic margin of Morocco early post-rift sedimentary sequences are tectonically-controlled. Inherited structures, differential subsidence rates and vertical uplift and exhumation phases in the basement terranes are the main factors controlling sediment distribution in the basins with eustacy playing a subordinated role. Sea-level gains importance by the late Jurassic when sedimentation along the Atlantic margin becomes more homogeneous.

2.8 References

Aberhan, M., Bussert, R., Heinrich, W.-D., Schrank, E., Schultkal, S., Sames, B., Kriwet, J., Kapilima, S., 2002. Palaeoecology and depositional environments of the Tendaguru Beds (Late Jurassic to Early Cretaceous, Tanzania). Mitt. Mus. Nat.kd. Berl., Geowiss. R. 5, 19–44.

Abou Ali, N., Chellaie, E.H., Nahim, M., 2004. Anatomie d'une marge passive hybride. Marge Ifni/Tan-Tan (sud du Maroc) au Mesozoique: apports des donnees geophysiques. Estud. Geológicos 60, 111–121. doi:10.3989/egeol.04603-683

Abou Ali, N., Hafid, M., Chellaï, E.H., Nahim, M., Zizi, M., 2005. Structure de socle, sismostratigraphie et héritage structural au cours du rifting au niveau de la marge d'Ifni/Tan-Tan (Maroc sud-occidental). Comptes Rendus Geosci. 337, 1267–1276. doi:10.1016/j.crte.2005.07.003

Adams, A.E., 1979. Sedimentary environments and palaeogeography of the western High Atlas, Morocco, during the Middle and late jurassic. Palaeogeogr. Palaeoclimatol. Palaeoecol. 28, 185–196. doi:10.1016/0031-0182(79)90118-4

Alia Medina, M., 1952. Bosquejo geológico del Sahara Español. Mapa. Consejo Superior de Investigaciones Cientificas, Madrid.

Alia Medina, M., 1945. Características morfográficas y geológicas de la zona septentrional del Sahara español. Consejo Superior de Investigaciones Cientificas, Madrid.

Ambroggi, R., 1963. Étude géologique du versant méridional du Haut Atlas occidental et de la Plaine du Souss. Notes Mém. Serv. Géol. Maroc 157, 1–321.

Bassoulet, J.-P., 1987. Sarfatiella dubari Conrad & Peybernès 1973: a junior synonym of Holosporella siamensis Pia 1930, in: 4th International Symposium on Fossil Algae (Cardiff 6-11, July 1987), Abstracts, Friends of the Algae Newsletter. pp. 20–21.

Behrens, M., Siehl, A., 1982. Sedimentation in the Atlas Gulf: I. Lower cretaceous clastics, in: von Rad, U., Hinz, K., Sarnthein, M., Seibold, E. (Eds.), The Geology of the Northwest African Continental Margin. Springer Verlag Berlin Heidelberg New York, pp. 427–438.

Benziane, F., Yazidi, A., 1982. Géologie de la Boutonnière précambrienne d'Ifni (Anti-

Atlas occidental). Notes Mém. Serv. Géol. Maroc 312.

Benziane, F., Yazidi, A., Schulte, B., Boger, S., Stockhammer, S., Lehmann, A., Saadane, A., Yazidi, M., 2016. Explicative notice of the Geological map of Morocco at 1/50000, Sidi Ifni sheet. Geol. Surv. Morocco n° 542 bis.

Bertotti, G., Gouiza, M., 2012. Post-rift vertical movements and horizontal deformations in the eastern margin of the Central Atlantic: Middle Jurassic to Early Cretaceous evolution of Morocco. Int. J. Earth Sci. 101, 2151–2165. doi:10.1007/s00531-012-0773-4

Biari, Y., Klingelhoefer, F., Sahabi, M., Funck, T., Benabdellouahed, M., Schnabel, M., Reichert, C., Gutscher, M.-A., Bronner, A., Austin, J.A., 2017. Opening of the Central Atlantic Ocean: implications for geometric rifting and asymmetric initial seafloor spreading after continental breakup. Tectonics 1–22. doi:10.1002/2017TC004596

Bouaouda, M.S., 2004. Le bassin atlantique marocain d'El Jadida-Agadir : Stratigraphie, paléogéographie, géodynamique et microbiostratigraphie de la série Lias-Kimméridgien. Université Mohammed V, Rabat.

Bouatmani, R., Medina, F., Ait Salem, A., Hoepffner, C., 2004. Le bassin d ' Essaouira (Maroc) : géometrie et style des structures liées au rifting de l ' Atlantique central. Africa Geosci. Rev. 11, 107–123.

Brown, R., 1980. Triassic rocks of Argana Valley, southern Morocco, and their regional structural implications. Am. Assoc. Pet. Geol. Bull. 64, 988–1003.

Charton, R., Bertotti, G., Arantegui, A., Bulot, L.G., 2018. The Sidi Ifni transect across the rifted margin of Morocco (Central Atlantic): Vertical movements constrained by low-temperature thermochronology. J. African Earth Sci. 141, 22–32.

Choubert, G., 1957. Carte géologique du Maroc; Feuille Marrakech; Echelle: 1/500 000. Notes Mém. Serv. Géol. Maroc 70.

Choubert, G., Faure-Muret, A., Hottinger, L., 1966. Aperçu géologique du bassin côtier de Tarfaya, in: Le Bassin Côtier de Tarfaya (Maroc Méridional). Notes et Mém. Serv. Géol. Maroc, 175.

Choubert, G., Marçais, J., 1956. Introduction géologique. Les grands traits de la Géologie du Maroc, in: Lexique Stratigraphique Du Maroc. Notes et Mém. Serv.

Géol. Maroc.

Collignon, M., 1967. Les ammonites crétacées du bassin côtier de Tarfaya, Sud marocain. C. R. ACAD. Sc. PARIS 264, 1390–1392.

Collignon, M., 1966. Les céphalopodes crétacés du bassin côtier de Tarfaya: relations stratigraphiques et paléontologiques, in: Notes et Mém. Serv. Géol. Maroc, 175. pp. 10–149.

Daidu, F., Yuan, W., Min, L., 2013. Classifications, sedimentary features and facies associations of tidal flats. J. Palaeogeogr. 2, 66–80. doi:10.3724/SP.J.1261.2013.00018

Davies, J.H.F.L., Marzoli, A., Bertrand, H., Youbi, N., Ernesto, M., Schaltegger, U., 2017. End-Triassic mass extinction started by intrusive CAMP activity. Nat. Commun. 8, 15596. doi:10.1038/ncomms15596

Davison, I., 2005. Central Atlantic margin basins of North West Africa: geology and hydrocarbon potential (Morocco to Guinea). J. African Earth Sci. 43, 254–274. doi:10.1016/j.jafrearsci.2005.07.018

Destombes, J., 1991. Carte géologique du Maroc, feuille au 1/100000, Tiznit. Notes Mém. Serv. Géol. Maroc 360.

du Dresnay, R., 1988. Répartition des dépôts carbonatés du Lias inférieur et moyen le long dela côte atlantique du Maroc: conséquences sur la paléogéographie del'Atlantique naissant. J. African Earth Sci. 7, 385–396.

Duffaud, F., 1960. Contribution a l'étude stratigraphique du Bassin Secondaire des Haut Atlas occidental (Sud-ouest Marocain). Bull. Soc. geol. Fr. 7, 728–734.

Echarfaoui, H., Hafid, M., Aït Salem, A., Abderrahmane, A.F., 2002. Analyse sismo-stratigraphique du bassin d'Abda (Maroc occidental), exemple de structures inverses pendant le rifting atlantique. Comptes Rendus Geosci. 334, 371–377. doi:10.1016/S1631-0713(02)01768-6

Einsele, G., von Rad, U., 1979. Facies and paleoenvironment of Lower Cretaceous sediments at DSDP Site 397 and in the Aaiun Basin (Northwest Africa), in: von Rad, U., Ryan, W.B.F. (Eds.), Init Repts Deep Sea Drilling Project, v 47, Part 1. Texas A & M University, Ocean Drilling Program, College Station, TX, United States, pp. 559–571. doi:10.2973/dsdp.proc.47-1.126.1979

El Albani, A., 1995. Les formations du Crétacé Supérieur du Bassin de Trafaya (Maroc Méridional): Sédimentologie et géochimie. Université des Sciences et Technologies de Lille.

El Albani, A., Kuhnt, W., Luderer, F., Herbin, J.P., Caron, M., 1999. Palaeoenvironmental evolution of the Late Cretaceous sequence in the Tarfaya Basin (southwest of Morocco), in: Cameron, N.R., Bate, R.H., Clure, V.S. (Eds.), The Oil and Gas Habitats of the South Atlantic. Geological Society, London, Special Publications, pp. 223–240. doi:10.1144/gsl.sp.1999.153.01.14

Elliott, G.F., 1983. Distribution and affinities of the Jurassic dasycladalean alga Sarfatiella. Palaeontology 26, 671–675.

Ettachfini, M., Company, M., Rey, J., Taj-Eddine, K., Tavera, J.M., 1998. Le Valanginien du bassin de Safi (Maroc atlantique) et sa faune d'ammonites. Implications paleobiogeographiques. Comptes Rendus l'Académie Sci. - Ser. IIa Sci. la Terre des Planètes 327, 319–325. doi:10.1016/S1251-8050(98)80050-5

Evans, D.J., Fisher, M.J., Haskins, C.W., Laing, J.F., 1976. Biostratigraphy and depositional environments of the interval 729' to 6560' TD in the Sun Oil Company Ifni No. 1 well offshore South-West Morocco.

Flügel, E., 2010. Microfacies of carbonate rocks: analysis, interpretation and application, 2nd ed. Springer Berlin Heidelberg.

Freneix, S., 1972. Les mollusques bivalves crétacés du bassin côtier de Tarfaya (Maroc méridional). Notes Mémoires du Serv. géologique du Maroc 228, 49–255.

Frizon De Lamotte, D., Zizi, M., Missenard, Y., Hafid, M., El Azzouzi, M., Maury, R.C., Charrière, A., Taki, Z., Benammi, M., Michard, A., 2008. The Atlas System, in: Michard, A., Saddiqi, O., Chalouan, A., Frizon De Lamotte, D. (Eds.), Continental Evolution, The Geology of Morocco. Springer Verlag Berlin Heidelberg, pp. 133–202.

Gouiza, M., 2011. Mesozoic Source-to-Sink Systems in NW Africa: Geology of vertical movements during the birth and growth of the Moroccan rifted margin. VU University Amsterdam.

Gouiza, M., Charton, R., Bertotti, G., Andriessen, P., Storms, J.E.A., 2017. Post-Variscan evolution of the Anti-Atlas belt of Morocco constrained from low-

temperature geochronology. Int. J. Earth Sci. 106, 593–616. doi:10.1007/s00531-016-1325-0

Gradstein, F.M., Ogg, J.G., Hilgen, F.J., 2012. On The Geologic Time Scale. Newsletters Stratigr. 45, 171–188. doi:10.1127/0078-0421/2012/0020

Grosheny, D., Nourrisaid, I., Ferry, S., Bulot, L., Masrour, M., Bettar, I., Aoutem, M., Essafraoui, B., 2012. La série apto-albienne du bassin marginal de Tarfaya (Maroc méridional), in: Les Évènements de l'Aptien-Albien. pp. 23–27.

Hafid, M., 2000. Triassic-early Liassic extensional systems and their Tertiary inversion, Essaouira Basin (Morocco). Mar. Pet. Geol. 17, 409–429. doi:10.1016/S0264-8172(98)00081-6

Hafid, M., Salem, A.A., Bally, A.W., 2000. The western termination of the Jebilet High- Atlas system (Offshore Essaouiara Basin, Morocco). Mar. Pet. Geol. 17, 431–443.

Hafid, M., Tari, G., Bouhadioui, D., El Moussaid, I., Echarfaoui, H., Aït Salem, A., Nahim, M., Dakki, M., 2008. Atlantic Basins, in: Michard, A. (Ed.), Continental Evolution, The Geology of Morocco. Springer Berlin Heidelberg, pp. 303–329.

Hafid, M., Zizi, M., Bally, A.W., Ait Salem, A., 2006. Structural styles of the western onshore and offshore termination of the High Atlas, Morocco. Comptes Rendus Geosci. 338, 50–64. doi:10.1016/j.crte.2005.10.007

Haq, B.U., Hardenbol, J., Vail, P.R., 1987. Chronology of fluctuating sea levels since the triassic. Science 235, 1156–1167. doi:10.1126/science.235.4793.1156

Hardie, L.A., 1986. Stratigraphic models for tidal deposition, in: Hardie, L.A., Shinn, E.A. (Eds.), Carbonate Depositional Environments, Modern and Ancient. Colorado School of Mines, pp. 59–74.

Heyman, M.A.W., 1989. Tectonic and depositional history of the Moroccan continental margin, in: Tankard, A.J., Balkwill, H.R. (Eds.), Extensional Tectonics and Stratigraphy of the North Atlantic Margins. AAPG Special Publications Memoir 46, pp. 323–340.

Hinz, K., Dostmann, H., Fritsch, J., 1982. The continental margin of Morocco: seismic sequences, structural elements and geological development, in: von Rad, U., Hinz, K., Sarnthein, M., Seibold, E. (Eds.), Geology of the Northwest African

Continental Margin. Springer Berlin Heidelberg, Berlin, Heidelberg, pp. 34–60. doi:10.1007/978-3-642-68409-8

Hollard, H., Choubert, G., Bronner, G., Marchand, J., Sougy, J.M.A., 1985. Carte géologique du Maroc; Echelle: 1/1000 000. Notes Mém. Serv. Géol. Maroc 260.

Jansa, L.F., Wiedmann, J., 1982. Mesozoic-Cenozoic development of the Eastern North American and Northwest African continental margins: A comparison, in: von Rad, U., Hinz, K., Sarnthein, M., Seibold, E. (Eds.), Geology of the Northwest African Continental Margin. Springer Verlag Berlin Heidelberg New York, pp. 215–269.

Klitgord, K.D., Schouten, H., 1986. Plate kinematics of the central Atlantic, in: Vogt, P.R., Tucholke, B.E. (Eds.), The Geology of North America, Volume M, The Western North Atlantic Region. Geological Society of America, pp. 351–378.

Kuhnt, W., Holbourn, A., Gale, A., Chellai, E.H., Kennedy, W.J., 2009. Cenomanian sequence stratigraphy and sea-level fluctuations in the Tarfaya Basin (SW Morocco). Geol. Soc. Am. Bull. 121, 1695–1710. doi:10.1130/B26418.1

Kuss, J., 1990. Middle Jurassic Calcareous Algae from the Circum-Arabian Area. Facies 22, 59–85.

Kuznetsova, K.K., Grigelis, A., Adjamian, J., Hallaq, L., 1996. Zonal stratigraphy and foraminifera of the Tethyan Jurassic (Eastern Mediterranean). Gordon & Breach Science, Amsterdam.

Labails, C., Olivet, J.-L., Aslanian, D., Roest, W.R., 2010. An alternative early opening scenario for the Central Atlantic Ocean. Earth Planet. Sci. Lett. 297, 355–368. doi:10.1016/j.epsl.2010.06.024

Lancelot, Y., Winterer, E.L., 1980. Evolution of the Moroccan oceanic basin and adjacent continental margin—a synthesis. Init Rep Deep Sea Drill. Proj. 801–821.

Le Roy, P., Piqué, A., Le Gall, B., Ait Brahim, L., Morabet, A.M., Demnati, A., 1997. Les bassins cotiers triasico-liasiques du Maroc occidental et la diachronie du rifting intra-continental de l'Atlantique central. Bull. la Société Géologique Fr. 168, 637–648.

Lehner, P., De Ruiter, P.A.C., 1977. Structural history of Atlantic Margin of Africa. Am. Assoc. Pet. Geol. Bull. 61, 961–981.

Leprêtre, R., 2015. Evolution phanérozoïque du Craton Ouest Africain et de ses

bordures Nord et Ouest.

Leprêtre, R., Barbarand, J., Missenard, Y., Gautheron, C., Pinna-jamme, R., Saddiqi, O., 2017. Mesozoic evolution of NW Africa: implications for the Central Atlantic Ocean dynamics. J. Geol. Soc. London.

Leprêtre, R., Barbarand, J., Missenard, Y., Leparmentier, F., Frizon de Lamotte, D., 2013. Vertical movements along the northern border of the West African Craton: the Reguibat Shield and adjacent basins. Geol. Mag. 151, 885–898. doi:10.1017/S0016756813000939

Martinis, B., Visintin, V., 1966. Données géologiques sur le bassin sédimentaire côtier de Tarfaya (Maroc méridional), in: Reyre, D. (Ed.), Bassin Sedimentaires Du Littoral Africain. Union Internationale des sciences géologiques, Paris, pp. 13–26.

Marzoli, A., Bertrand, H., Knight, K.B., Cirilli, S., Buratti, N., Vérati, C., Nomade, S., Renne, P.R., Youbi, N., Martini, R., Allenbach, K., Neuwerth, R., Rapaille, C., Zaninetti, L., Bellieni, G., 2004. Synchrony of the Central Atlantic magmatic province and the Triassic-Jurassic boundary climatic and biotic crisis. Geology 32, 973–976. doi:10.1130/G20652.1

Medina, F., 1995. Syn- and postrift evolution of the El Jadida-Agadir basin (Morocco): constraints for the rifting model of the Central Atlantic. Can. J. Earth Sci. 32, 1273–1291.

Meyer, D.E., 1978. Microfacies and microfabrics of early Middle Cretaceous sediments selected from Site 370, DSDP Leg 41 (deep basin off Morocco), in: Initial Reports of the Deep Sea Drilling Project; Supplement to Volumes XXXVIII, XXXIX, XL, and XLI. pp. 961–981. doi:-

Michard, A., Saddiqi, O., Chalouan, A., Frizon de Lamotte, D., 2008. Continental evolution: The geology of Morocco: Structure, stratigraphy, and tectonics of the Africa-Atlantic-Mediterranean triple junction.

Mitchum, R.M.J., Van Wagoner, J.C., 1991. High-frequency sequences and their stacking patterns: sequence stratigraphic evidence of high frequency eustatic cycles. Sediment. Geol. 10, 131–160. doi:Doi: 10.1016/0037-0738(91)90139-5

Mulder, T., Syvitski, J.P.M., Migeon, S., Faugères, J.C., Savoye, B., 2003. Marine hyperpycnal flows: Initiation, behaviorand related deposits. A review. Mar. Pet.

Geol. 20, 861–882. doi:10.1016/j.marpetgeo.2003.01.003

Negroni, P., Gendrot, C., Jahn, Skwirblies, 1966. Forage de reconnaissance OLD 1 A (Oualidia 1 A). Rapport geologique et technique.

Nomade, S., Knight, K.B., Beutel, E., Renne, P.R., Verati, C., Féraud, G., Marzoli, A., Youbi, N., Bertrand, H., 2007. Chronology of the Central Atlantic Magmatic Province: Implications for the Central Atlantic rifting processes and the Triassic-Jurassic biotic crisis. Palaeogeogr. Palaeoclimatol. Palaeoecol. 244, 326–344. doi:10.1016/j.palaeo.2006.06.034

Piqué, A., Soulaimani, A., Laville, E., Amrhar, M., Bouabdelli, M., Hoepffner, C., Chalouan, A., 2006. Géologie du Maroc.

Price, I., 1980. Provenance of the Jurassic-Cretaceous flysch, deep sea drilling project sites 370 and 416. Init Reps Deep Sea Drill. Proj. 50, 751–757.

Querol, R., 1966. Regional geology of the Spanish Sahara, in: Bassins Sédimentaires Du Littoral Africain. pp. 27–39.

Rey, J., Canérot, J., Peybernès, B., Taj-Eddine, K., Thieuloy, J.P., 1988. Lithostratigraphy, biostratigraphy and sedimentary dynamics of the Lower Cretaceous deposits on the northern side of the western High Atlas (Morocco). Cretac. Res. 9, 141–158. doi:10.1016/0195-6671(88)90014-6

Sahabi, M., Aslanian, D., Olivet, J.-L., 2004. Un nouveau point de départ pour l'histoire de l'Atlantique central. Comptes Rendus Geosci. 336, 1041–1052. doi:10.1016/j.crte.2004.03.017

Schettino, A., Turco, E., 2009. Breakup of Pangaea and plate kinematics of the central Atlantic and Atlas regions. Geophys. J. Int. 178, 1078–1097. doi:10.1111/j.1365-246X.2009.04186.x

Scholle, P.A., 1977. Geological studies on the COST No. B-2 Well, U.S. Mid- Atlantic Outer Continental Shelf Area, U. S. Geological Survey Circular. U.S. Geological Survey.

Scotese, C.R., 1991. Jurassic and cretaceous plate tectonic reconstructions. Palaeogeogr. Palaeoclimatol. Palaeoecol. 87, 493–501. doi:10.1016/0031-0182(91)90145-H

Sehrt, M., Glasmacher, U.A., Stockli, D.F., Jabour, H., Kluth, O., 2016. The southern Moroccan passive continental margin: An example of differentiated long-term

landscape evolution in Gondwana. Gondwana Res. in press. doi:10.1016/j.gr.2017.03.013

Seibold, E., 1982. The northwest African Continental Margin, in: von Rad, U., Hinz, K., Sarnthein, M., Seibold, E. (Eds.), Geology of the Northwest African Continental Margin. Springer Verlag Berlin Heidelberg New York, New York, pp. 3–20.

Snedden, J.W., Liu, C., 2010. A Compilation of Phanerozoic Sea-Level Change , Coastal Onlaps and Recommended Sequence Designations. Am. Assoc. Pet. Geol. Search Discov. Artic. 40594 40594, 2004–2006.

Steiner, C., Hobson, A., Favre, P., Stampfli, G.M., Hernandez, J., 1998. Mesozoic sequence of Fuerteventura (Canary Islands): Witness of Early Jurassic sea-floor spreading in the central Atlantic. Geol. Soc. Am. Bull. 110, 1304–1317. doi:10.1130/0016-7606(1998)110<1304

Tari, G., Jabour, H., 2013. Salt tectonics along the Atlantic margin of Morocco. Geol. Soc. London, Spec. Publ. 369, 337–353. doi:10.1144/SP369.23

Tari, G., Jabour, H., Molnar, J., Valasek, D., Zizi, M., 2012. Deep-Water Exploration In Atlantic Morocco, in: Gao, D. (Ed.), Tectonics and Sedimentation: Implications for Petroleum Systems. AAPG Special Publications Memoir 100, pp. 337–355. doi:10.1306/13351560M1003141

Tasli, K., 2001. Benthic Foraminifera of the Upper Jurassic Platform Carbonate Sequence in the Aydincik (Içel) Area, Central Taurides, S Turkey. Geol. Croat. 54, 1–13.

van Houten, F.B., 1977. Triassic-Liassic deposits of Morocco and Eastern North America: comparison. Am. Assoc. Pet. Geol. Bull. 61, 79–99.

van Wagoner, J.C., Mitchum, R.M., Campion, K.M., Rahmanian, V.D., 1990. Siliciclastic Sequence Stratigraphy in Well Logs, Cores, and Outcrops: Concepts for High-Resolution Correlation of Time and Facies. AAPG Methods Explor. Ser. 7 1–55. doi:0-89181-657-7

van Wagoner, J.C., Posamentier, H.W., Mitchum, R.M., Vail, P.R., Sarg, J.F., Loutit, T.S., Hardenbol, J., 1988. An overview of the fundamentals of sequence stratigraphy and key definitions, in: Wilgus, C.K., Posamentier, H.W., Ross, C.K.,

Kendall, C.G.S.C. (Eds.), Sea-Level Changes: An Integrated Approach. SEPM Society for Sedimentary Geology, Tulsa, pp. 39–45. doi:10.2110/pec.88.01.0039

Verati, C., Rapaille, C., Féraud, G., Marzoli, A., Bertrand, H., Youbi, N., 2007. 40Ar/39Ar ages and duration of the Central Atlantic Magmatic Province volcanism in Morocco and Portugal and its relation to the Triassic-Jurassic boundary. Palaeogeogr. Palaeoclimatol. Palaeoecol. 244, 308–325. doi:10.1016/j.palaeo.2006.06.033

Viotti, C., 1966. Resultats stratigraphiques du sondage Puerto Cansado 1 du bassin cotier de Tarfaya. Notes Mém. Serv. Géol. Maroc 175.

von Rad, U., Auzende, J.-M., Ruellan, É., 1985. Stratigraphy, structure, paleoenvironment and subsidence history of the Mazagan Escarpment off central Morocco: a CYAMAZ synthesis, in: Oceanologica Acta, Special Volume. pp. 161–182.

von Rad, U., Čepek, P., von Stackelberg, U., Wissmann, G., Zobel, B., 1979. Cretaceous and Tertiary sediments from the Northwest African slope (dredges and cores supplementing DSDP results). Mar. Geol. 29, 273–312.

von Rad, U., Einsele, G., 1980. Mesozoic-Cainozoic Subsidence History and Palaeobathymetry of the Northwest African Continental Margin (Aaiun Basin to D. S. D. P. Site 397). Philos. Trans. R. Soc. A Math. Phys. Eng. Sci. 294, 37–50. doi:10.1098/rsta.1980.0010

von Rad, U., Hinz, K., Sarnthein, M., Seibold, E. (Eds.), 1982. Geology of the Northwest African continental margin, 1st ed. Springer Verlag Berlin Heidelberg, New York.

von Rad, U., Wissmann, G., 1982. Cretaceous-Cenozoic history of the West Saharan continental margin (NW Africa): development, destruction and gravitational sedimentation, in: von Rad, U., Hinz, K., Sarnthein, M., Seibold, E. (Eds.), Geology of the Northwest African Continental Margin. Springer Berlin Heidelberg, Berlin, Heidelberg, pp. 106–131.

Wenke, A.A.O., 2015. Sequence stratigraphy and basin analysis of the Meso- to Cenozoic Tarfaya- Laâyoune Basins, on- and offshore Morocco. Ruprecht-Karls-Universität Heidelberg.

Wenke, A.A.O., Zühlke, R., Jabour, H., Kluth, O., 2011. High-resolution sequence stratigraphy in basin reconnaissance: example from the Tarfaya Basin, Morocco. first Break 29, 85–96.

Westermann, G.E.G., 1993. Global bio-events in mid-Jurassic ammonites controlled by seaways, in: The Ammonoidea: Environment, Ecology and Evolutionary Change. pp. 187–226.

Whittaker, A., Cope, J.C.W., Cowie, J.W., Gibbons, W., Hailwood, E.A., House, M.R., Jenkins, D.G., Rawson, P.F., Rushton, A.W.A., Smith, D.G., Thomas, A.T., Wimbledon, W.A., 1991. A guide to stratigraphical procedure. J. Geol. Soc. London. 148, 813–824. doi:10.1144/gsjgs.148.5.0813

Wiedmann, J., Butt, A., Einsele, G., 1982. Cretaceous stratigraphy, environment, and subsidence history at the Moroccan continental margin, in: von Rad, U., Hinz, K., Sarnthein, M., Seibold, E. (Eds.), The Geology of the Northwest African Continental Margin. Springer Verlag Berlin Heidelberg, New York, pp. 366–395.

Wiedmann, J., Butt, A., Einsele, G., 1978. Vergleich von marokkanischen Kreide-Küstenaufschlüssen und Tiefseebohrungen (DSDP): Stratigraphie, Paläoenvironment und Subsidenz an einem passiven Kontinentalrand. Geol. Rundschau 67, 454–508. doi:10.1007/BF01802800

Wilson, M., Guiraud, R., 1998. Late Permian to Recent magmatic activity on the African-Arabian margin of Tethys, in: Macgregor, D.S., Moody, R.T.J., Clark-Lowes, D.D. (Eds.), Petroleum Geology of North Africa. Geological Society, London, Special Publications, pp. 231–263.

Winterer, E.L., Hinz, K., 1984. The evolution of the Mazagan Continental Margin: a synthesis of geophysical and geological data with results of drilling during DSDP leg. 79, in: DSDP Initial Reports, Vol. 79. pp. 893–919. doi:10.2973/dsdp.proc.79.138.1984

Wright, V.P., 1984. Peritidal carbonate facies models: A review. Geol. J. 19, 309–325. doi:10.1002/gj.3350190402

Wright, V.P., 1983. Morphogenesis of Oncoids in the Lower Carboniferous Llanelly Formation of South Wales, in: Coated Grains. Springer Berlin Heidelberg, Berlin, Heidelberg, pp. 424–434. doi:10.1007/978-3-642-68869-0_37

Yazidi, A., Benziane, F., Hollard, H., Destombes, J., Oliva, P., 1986. Carte géologique

du Maroc, feuille au 1/100000, Sidi Ifni. Notes Mém. Serv. Géol. Maroc n° 310.

Zühlke, R., Bouaouda, M.S., Ouajhain, B., Bechstädt, T., Leinfelder, R., 2004. Quantitative Meso-/Cenozoic development of the eastern Central Atlantic continental shelf, western High Atlas, Morocco. Mar. Pet. Geol. 21, 225–276. doi:10.1016/j.marpetgeo.2003.11.014

Chapter 3

Sedimentology of Lower Cretaceous fluvial to shallow marine deposits on the Central Atlantic passive margin; a case study in the Aaiun-Tarfaya Basin, Morocco

Sedimentology of Lower Cretaceous fluvial to shallow marine deposits on the Central Atlantic passive margin; a case study in the Aaiun-Tarfaya Basin, Morocco

A. Arantegui, R. Jerrett, L. Bulot, J. Redfern

Keywords:

3.1 Abstract

Decades of hydrocarbon exploration in the Aaiun-Tarfaya Basin have yielded several shows and three non-commercial discoveries in Jurassic carbonates and Cretaceous clastics, proving the existence of a working petroleum system. Lower Cretaceous clastic reservoirs, associated with the Tantan delta, have been one of the main targets. The Tantan Fm. described onshore, has previously been reported as a thick clastic-dominated succession and as such a reservoir target offshore, in its deepwater equivalent. However, unsuccessful offshore drilling to date has been missing the reservoir clastics facies suggesting an insufficient understanding of the evolution of the Tantan system, and a motivation for study.

This paper presents the first integrated regional outcrop-based sedimentological study of the northern Aaiun-Tarfaya Basin. The Tantan Fm. has been subdivided into six new members and placed within a sequence stratigraphic framework. Four incomplete depositional sequences have been interpreted, bounded by amalgamated sequence boundaries and transgressive surfaces. Strong thickness variations of individual lithostratigraphic units from north to south suggest differential subsidence and tectonic control on sedimentation.

The results provide valuable insights into the timing of local tectonics in the Western Anti-Atlas and the control on the evolution of the sedimentary system. Deposition of each of these six units is interpreted to be the result of a complex interplay between an overall sea-level rise during the early Cretaceous, sediment delivery controlled by tectonic movements in the Western Anti-Atlas and Reguibat Shield and periods of differential subsidence in the basin.

The results document the style of evolution of a large deltaic system feeding into the Central Atlantic during the passive margin phase. The improved facies and depositional

models together with improved understanding of the evolution of the delta have significant implication for exploring the deep-water equivalents offshore.

3.2 Introduction

Hydrocarbon exploration in the Aaiun-Tarfaya Basin (ATB) started in the late 1950's and early 1960's (Choubert et al., 1966; El Mostaine, 1991) with the acquisition of the first seismic lines and drilling of the first onshore wells. Km-scale thickness of Mesozoic sediments have been drilled offshore and sequences more than 10 km thick have been postulated in the deep offshore (von Rad and Einsele, 1980). A focus was placed on the lower Cretaceous wedge that was interpreted to be fed by a large fluvio-deltaic system (Tantan delta). In parallel with subsurface exploration, fieldwork on the Mesozoic and Cenozoic units onshore the northern part of the ATB started in 1959 by SOMIP (Société Maroco-Italienne de Pétrole). The Mesozoic and Cenozoic stratigraphy was first defined by Martinis and Visintin (1966) who named the Tantan Fm. This formation was described as a 785 m thick interval of continental sandstones and subordinated muds, with minor marine incursions that become more frequent towards the top. Precise dating of the Tantan Fm. was challenging due to the lack of age-diagnostic fossils in the continental sections and the limitation of long-ranging groups found in the marine intervals, although a pre-Albian age was widely-accepted.

The Tantan Fm. has been the most important reservoir target in the northern ATB. Sixteen offshore wells have been drilled to-date in the outer shelf and deep offshore, several with oil shows. Two further non-commercial discoveries have been made in Jurassic carbonates and one more in lower Cretaceous clastics (Figure 3.1), all of which proves the existence of a working petroleum system, but the basin still remains greatly underexplored compared with its conjugate counterpart in Nova Scotia. The expected deep water clastic reservoir outboard of the Tantan delta has proven elusive and a better understanding of this system is needed.

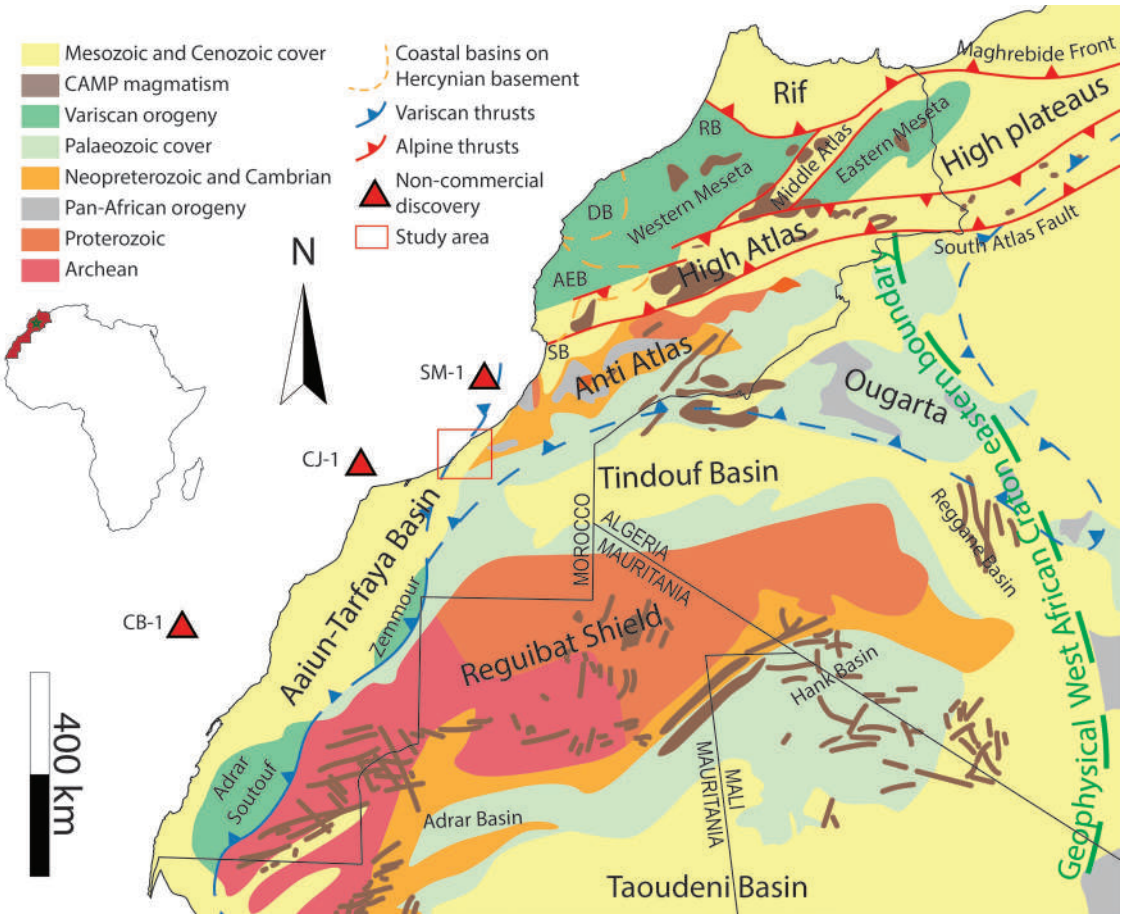

Figure 3.1. Schematic map of structural elements of Morocco and northern West African Craton. References as in Figure 1.2.

For the last few decades most exploration efforts have been focused on acquisition and interpretation of on- and offshore subsurface data. Little work has been published on the lower Cretaceous exposures. This new contribution establish an updated outcrop-based litho-, bio- and sequence stratigraphic framework that can improve the existing knowledge of the evolution of the Tantan delta, and ultimately develop a depositional model that can help in reducing reservoir risk.

3.3 Geological setting

The origin of the ATB (Figure 3.1) is linked with the opening and evolution of the Central Atlantic during the Mesozoic. The break up between Africa and North America along the Central Atlantic segment started during the Triassic. Rifting developed restricted basins that were filled with continental red clastics and later salt deposits on both sides of the nascent Atlantic. The first oceanic crust was formed in the Early Jurassic, marking the beginning of the drift stage. Favourable conditions during the Jurassic triggered carbonate production and the development of extensive carbonate

platforms along both conjugate margins. The Cretaceous is characterized by the shut-off of carbonate production, with development of large clastics systems during the early Cretaceous followed by an overall transgressive system associated with rising sea-level, resulting in deposition of thick marine shales during the Late Cretaceous.

The current distribution of Cretaceous outcrops is the result of the Atlasian Orogeny, that whilst only having a mild effect south of the South Atlas Fault (Figure 3.1), uplifted and exposed the basin margin. All Mesozoic outcrops along the Atlantic margin in the ATB were previously tentatively assigned to the Cretaceous. A re-interpretation of a number of outcrops along the Atlantic side of the Ifni inlier has yielded an updated Bathonian or older age (see Chapter 2).

Older sediments have also been recorded by commercial wells onshore and offshore and by the DSDP drilling program.

3.3.1 Lower Cretaceous stratigraphy in the Aaiun-Tarfaya Basin

The Cretaceous interval is very well exposed in the onshore ATB. Regional tilting to the west and lack of significant tectonism have resulted in gently dipping lower Cretaceous exposures along a NE-SW strip of the eastern part of the onshore ATB, along the western limit of the Anti-Atlas, Tindouf Basin and Reguibat Shield.

The Lower Cretaceous exposed in the ATB comprises the sandstone dominated Tantan Fm. and the lower part of limestones and muds of the Aguidir Fm. (Figure 3.2; Martinis and Visintin, 1966).

Tantan Fm. This interval was described north of the locality of Tantan, along the Oued Draa (Figure 3.3), extending to the Atlantic river mouth, and following the coast SW up to Oued Chebeika. It was reported to attain a thickness of 785 m.

The formation starts with a basal unit of red conglomerates approximately 50 m thick unconformably overlying the Palaezoic of the Anti-Atlas (Figure 3.2). The majority of the Fm. is made of monotonous unit of cross-bedded sands with intercalations of clays and sandy marls. A unit, 65 m thick, of marls and limestones with bioclasts has been further subdivided as the *Marnes du Draa membre* (Dra Marls Member).

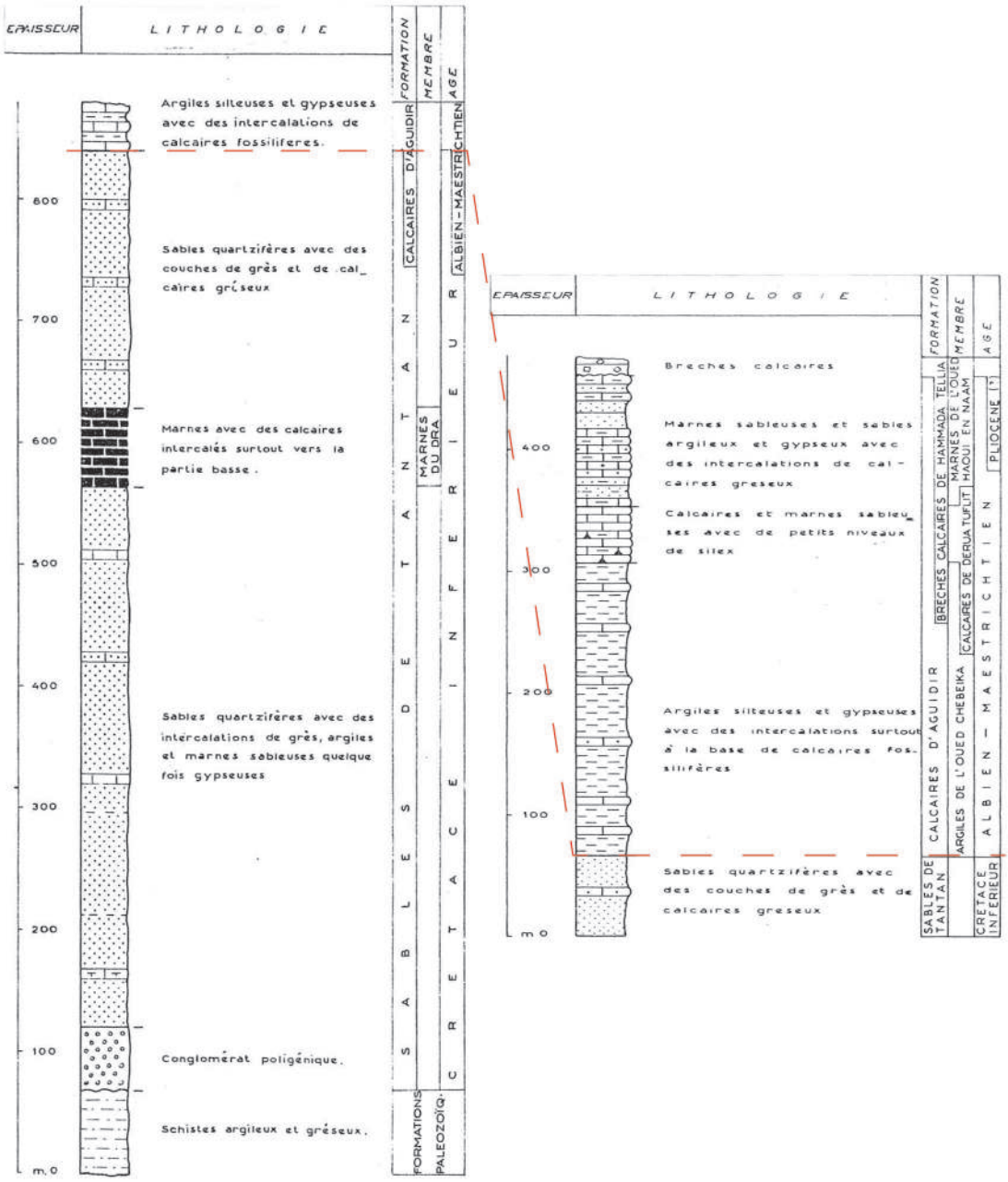

Figure 3.2. Type sections of the Tantan Sands Fm. and Aguidir Limestones Fm. as defined by (Martinis and Visintin, 1966).

Most of the Fm. has been interpreted as deposited in a continental environment, with episodes of marine sedimentation, mainly related with the Marls of Dra Member. The fossil record is restricted to the marine units, where ammonites, bivalves and gastropods were recovered. The base of the Tantan Fm. is undated and rests unconformably on Paleozoic basement of the Anti-Atlas. Age for the top of this formation is constrained by Upper Aptian ammonites from the upper Tantan Fm. (Collignon 1966, 1967) and by the overlying Albian-Maastrichtian Aguidir Fm. (Martinis and Visintin 1966).

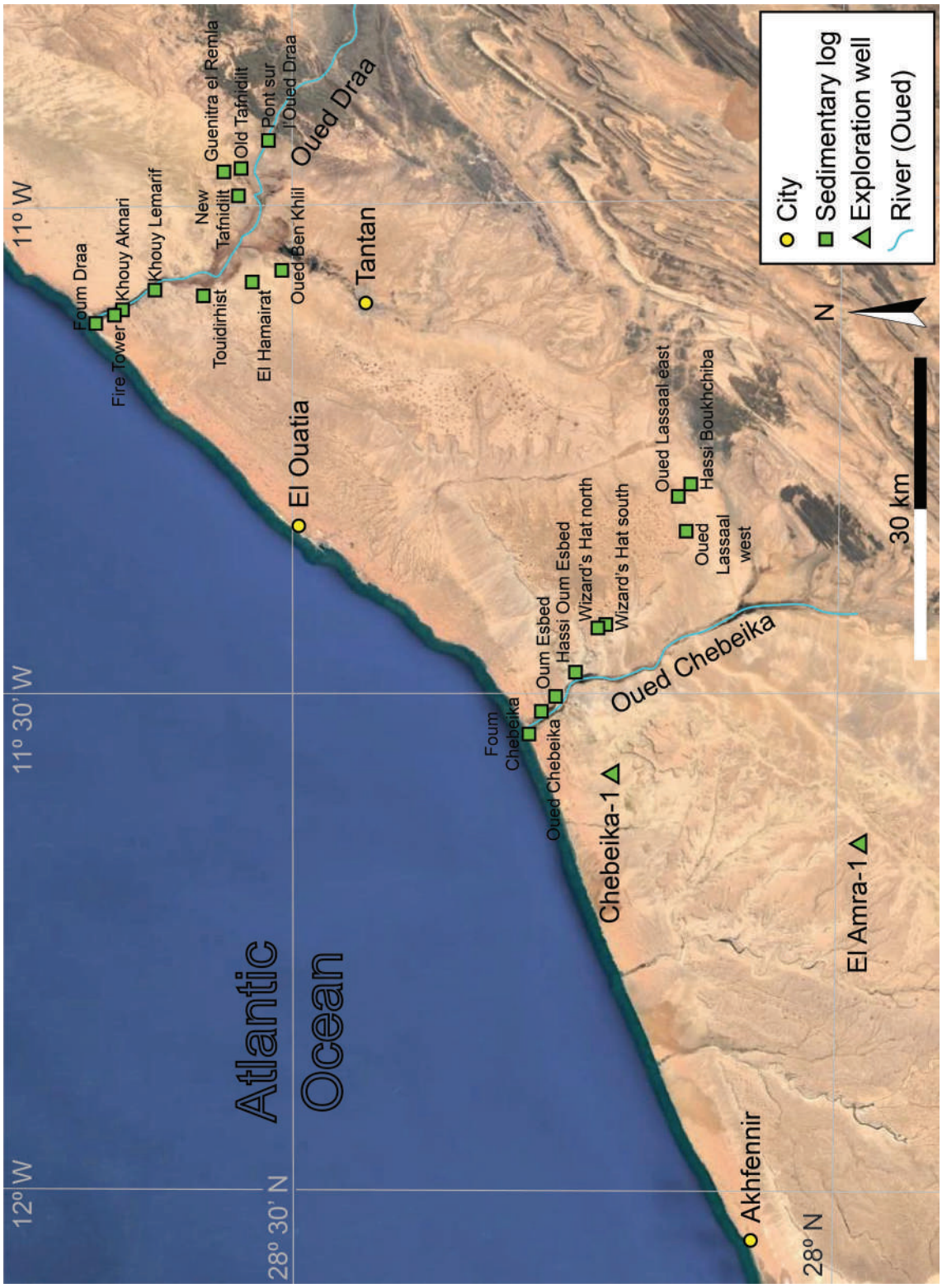

Figure 3.3. Location map of the outcrops along the two transects presented in this work. More detailed satellite images and location of outcrops is in Figure 3.4. Satellite image taken from GoogleEarth™.

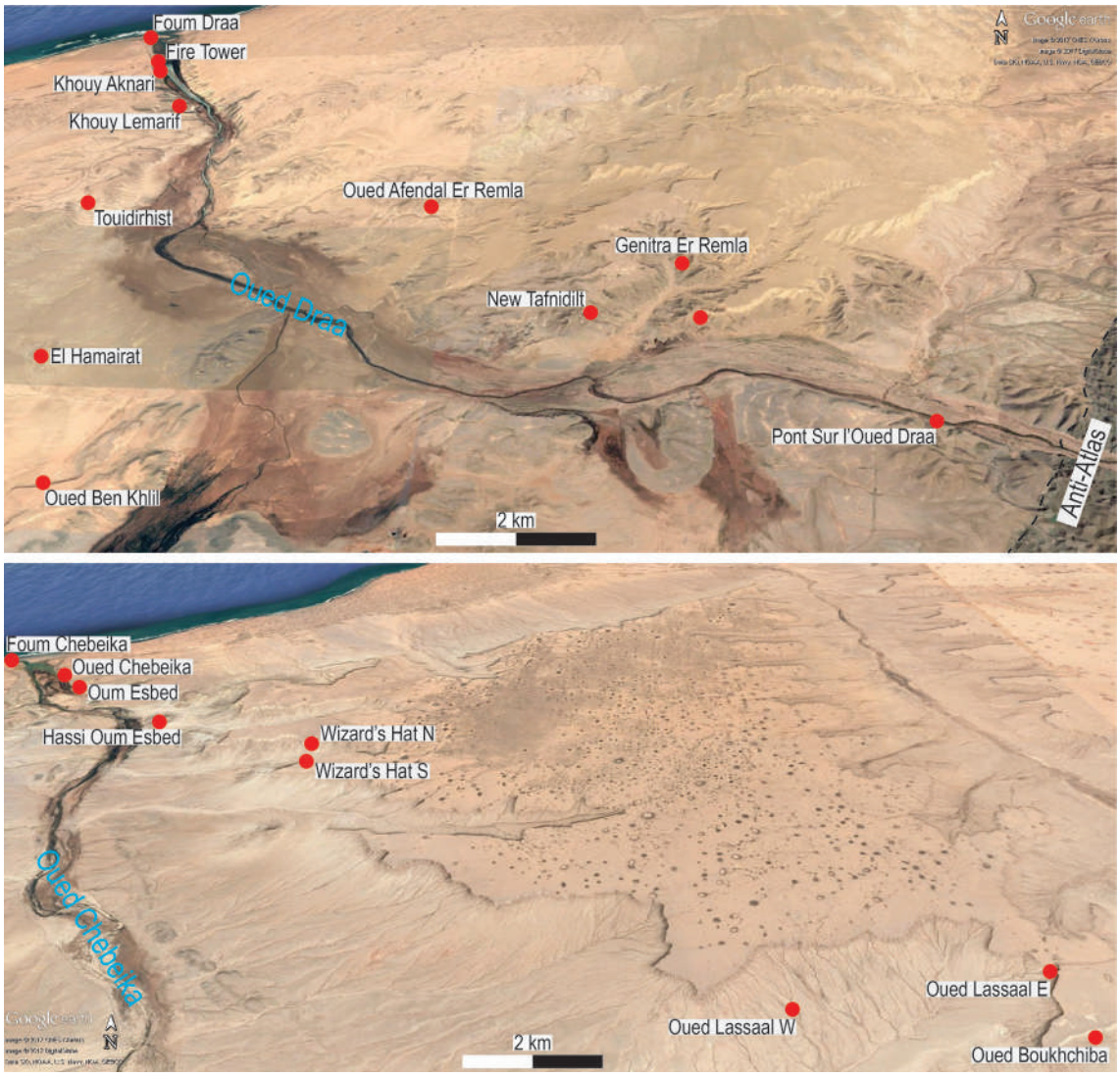

Figure 3.4. Sections logged along Oued Draa transect (top) and Oued Chebeika transect (bottom). 3D images taken from GoogleEarth™.

Aguidir Fm. This formation is exposed along the coastal basin from the river mouth of Oued Chebeika to the west (Figure 3.2), with a total reported thickness of 395 m. The age of the Fm. ranges from Albian to Maastrichtian. Although the Fm. is usually referred to as Aguidir Limestone Fm. (Martinis and Visintin, 1966) the unit is mainly made of clays and marls. The limestone beds constitute the prominent units sticking out from the cliffs and hence the name. The unit has been interpreted to be deposited in a shallow marine environment with poor water circulation.

This Fm. has been subdivided in three members, Oued Chebeika Clays (*Argiles de l'Oued Chebeika*), Derua Tuflit Limestones (*Calcaires de Derua Tuflit*) and Oued Haoui En Naam Marls (*Marnes de l'Oued Haoui En Naam*). The top of the Oued

Chebeika Member has a reported age of Cenomanian-Turonian. The Oued Chebeika Member thickens westwards.

3.4 Methodology

The successions studied crop out along the Oued Draa and Oued Chebeika (Figure 3.3 and Figure 3.4), running approximately SE-NW, north and south of the city of Tantan. The study involved extensive regional mapping to describe facies / facies associations in order to define the lithostratigraphic units. Petrography was undertaken to aid in the facies descriptions and interpretation of depositional environments and sampling for biostratigraphic dating, based on ammonites and palynomorphs, and superposition related to newly dated underlying units.

3.5 Results

3.5.1 Sedimentary facies

Sixteen lithofacies (Table 3.1) and 9 facies associations (Table 3.2) have been defined. Each facies association represents a distinct depositional environment. Example of detailed sedimentary logs covering the main sedimentary features and depositional environments interpreted can be found in Figure 3.5.

3.5.1.1 Alluvial fan FA

This FA is present only at the lowermost part of the Oued Draa transect, preserved within a number of discontinuous exposures. It consists of fining upwards packages, up to 6 m thick, of red polygenic conglomerates (lithofacies A1 and A2) with thin interbeds of coarse sandstones (lithofacies C; Figure 3.6A). Sedimentary structures are absent both in the conglomerates and the sandstones. The basal contacts of individual beds are sharp and erosive.

Interpretation. The coarse grain size, erosive bases and absence of sedimentary structures suggest high-energy unconfined flows deposited quickly as gravel sheets within an alluvial fan (Miall, 2006).

3.5.1.2 Fluvial bar and channel fill

This FA is represented by finning-upward packages up to 6 m thick of mainly cross-bedded sandstones (lithofacies B; Figure 3.6B). Subordinated lithofacies include matrix-supported conglomerates (lithofacies A2), interbedded structureless sandstones

(lithofacies C), and occasional beds with ripples at the top (lithofacies H). Bases of the packages are very erosive and sometimes channel-shaped. Lags of granules and pebbles are common either at the base of beds or cross-sets. Fossils and bioturbation are absent, except for occasional root traces. Palaeosols may develop in the coarse-grained sandstones as iron hardgrounds (lithofacies K).

Occasional m-scale inclined bedding (accretion) surfaces of medium to fine-grained sandstones are present. Bioturbation and palaesols developed at the top of the beds are common in fine-grained sediment. Relatively common gypsum veins at the bedding contacts and filling desiccation cracks.

Interpretation. Cross-bedding, coarse-grain size, fining-upwards trends and erosive surfaces, together with the absence of bioturbation and occasional palaesols and root traces are typical of deposition in a continental setting. Sedimentary structures are generated by intermittent waning flows representing subaqueous dunes stacked forming bars (Miall, 2006). Occasional channelized basal surfaces indicate channel fills.

The inclined bedding represents lateral accretion surfaces in a point bar environment or the filling of small ephemeral channels.

Table 3.1. Lithofacies recognized in the Tantan Fm. in the north Aaiun-Tarfaya Basin.

Name	Description	Interpretation
Conglomerate (A1)	10-110 cm-thick red conglomerates. Normally graded to massive with no sedimentary structures. Bases are sharp undulating and erosive. Clast size ranges from pebble to cobble, poorly sorted, angular to subrrounded and heterogeneous lithology.	Pseudoplastic debris flow froming sheets
Matrix-supported conglomerate (A2)	60 cm-thick matrix-supported conglomerates. Matrix is very coarse-grained sand. Clasts are pebble to cobble size, poorly sorted, subangular to subrrounded and heterogeneous lithology.	Viscous plastic to pseudoplastic debris flow froming sheets
Cross-bedded sandstones (B)	15-210 cm-thick, normally graded, cross-bedded gravelly to fine-grained sandstone. Rare packstone to grainstone. Bases are sharp and usually erosive and can cut down the stratigraphy up to 200 cm, occasionally resembling channels. Sedimentary structures include planar, tangential and trough cross-bedding in sets from a few cm up to 2 m thick. Rare cross-sets can be over steepened and deformed. Soft sediment deformation can be locally intense represented by load-casts, injected sands and contorted internal bedding. Pebble and granule lags are common, either at the base of beds and of individual foresets. Rip up mudclasts up to 15 cm may be present at the base of the bed. Rare horizontal bedding in very coarse-grained sandstones. Usually poorly sorted and relatively rounded. Clast mineralogy is mainly mono and policrystalline quartz and subordinated feldspars. Feldspar clasts can be locally common, euhedral and cm-scale. Check thin sections. Locally, bivalves can be from present to common. Occasionally, horizontal burrows can be abundant on the top surface and vertical burrows throughout. Unidentified bioturbation can be intense locally. Possible vertical root traces. Rare mottling and soil development.	Migration of 2D and 3D dunes by traction under unidirectional (wanning) flows Occasional plane-bed flow under super-critical flow
Parallel-bedded sandstones (C)	10-40 cm-thick massive to normally graded very coarse- to very fine-grained sandstones to calcareous sandstones. Beds are tabular with sharp undulating contacts, locally, erosive and load-casted. Occasional soft sedimentary deformation. Crude lamination is rare. Absence of sedimentary structures is likely due to weathering? Floating scattered quartz pebbles or mudclasts may be locally common. Sandstone clasts are rare but can reach 20 cm. Common bivalves and minor gastropods are possible (either body fossils or dissolved moulds), sometimes accumulated at the base of individual beds. Red mottling is possible. Red cementation. Rare iron "hardgrounds" developed on top of beds. Occasional green beds.	Sediment-gravity flow deposits. Suspension fall-out. Destratification by intense bioturbation.
Laterally accreting Sandstones (D)	10-20 cm-thick normally graded very coarse- to very fine-grained grey/green to red sandstones displaying inclined bedding surfaces. Grey/green usually is at the bottom of beds. Pebbles and reworked clasts may be common at the base of beds. Desiccation cracks and probable rootlets may be present. Gypsum veins fill the desiccation cracks and sometimes follow bedding planes. Bioturbation can be intense in the upper part of beds. Current ripples may be present in the finer spectrum of grain size.	Lateral Accretion surfaces Grey/red colour related with reduction/oxidation of periodic exposure

Hummocky cross-stratified sandstones/limestones (E)	20-100 cm-thick coarse- to very fine-grained sandstones and calcareous sandstones. Main lithology can range up to recrystallized sandy packstone. Sedimentary structures include hummocky and low-angle cross-bedding/lamination. Infrequent sole marks at the base of beds. Symmetrical or combined-flow ripples capping beds are common. Scarce to abundant broken bivalves and unidentified bioclast fragments. Occasionally, floating quartz pebbles may be abundant. Bioturbation (*Diplocraterion paralellum*) can be locally intense.	High-energy oscillatory and combined flows during waning storm events
Intensily bioturbated sandstones/calcareous sandstones (F)	10-110 cm-thick massive to normally graded medium- to very fine-grained sandstone to calcareous sandstone. Massive appearance and absence of sedimentary structures is likely due to intense bioturbation and weathering. Rare relicts of horizontal and ripple lamination. Occasional load casts. Minor floating granules/pebbles. Rarely, pebbles can be concentrated at the base of beds but do not form lags. Occasional lenses of slightly coarser sand. Some beds may have abundant bivalves and gastropods. Bioclast can be dissolved and recrystallized. Rare sideritised plant material, pyrite pseudomorphs and iron nodules. When fossils are absent the sand tends to be very clean? Individual beds can be better cemented and pervasive bioturbation by vertical burrows or Thalassinoides ichnofacies are indentified.	Complete destratification by intense bioturbation. Possible sediment fall-out, migration of 2D/3D ripples and/or reworking by oscillatory currents.
Wave-rippled sandstones (G)	5-10 cm-thick fine-grained to very fine-grained sandstones with interlayered thin silt laminae. The main sedimentary structure is symmetrical ripple-lamination, with occasional flaser and lenticular bedding. Bioturbation can be moderate. Ichnofacies may include Thalassinoides.	Migration of ripples by oscillatory flows and periods of suspension settling
Current-rippled laminated sandstones (H)	5-30 cm-thick asymmetrical ripple-laminated medium- to very fine-grained sandstones. Interbedded muds within the sands and scattered "isolated" ripple sets (lenticular and flaser bedding). Contorted discontinuous sandstone clasts might be possible. Plant fragments and bioturbation (Thalassinoides and Diplocraterion paralellum) may be locally common.	Migration of ripples by unidirectional currents under loweer flow regime alternating with periods of suspension settling
Inversely-graded siltstones/sandstones (I)	20-40 cm-thick inversely graded siltstone to very fine-grained sandstone. Floating quartz granules and pebbles may range from abundant to absent. Mudclasts, cm-scale broken bivalves and bioturbation are possible. Thalassinoides possible. Mottling and/or palaeosol development may be possible.	Debris flow
Pebble-bearing structureless siltstones/sandstones (J)	10-50 cm-thick structureless to normally graded, fine-grained sandstone to siltstone with floating quartz granules and pebbles and occasional reworked mud-clasts and sandstone-clasts up to 10 cm. Common bivalves and scarce gastropods and plant fragments may be present. Moderate bioturbation and/or palaeosol development may be possible.	Sediment-gravity flow deposits.

Mottled palaeosol (K)	20-120 cm-thick, usually red, mottled silt to very fine-grained sandstone. Colours may range from red/purple/mustard/green/grey. Red cementation may be possible, likely iron-related. Carbonate-cemented calcrete soils are frequent. Mottling and root traces occasionally developed in coarse sandstones. Occasional iron hardgrounds and gypsum concretions.	Soil formation with root development and chemical precipitation
Muds/calcareous muds (L)	Laminated to thinly bedded silts to clays with organic remains. Can be calcareous (marls). Minor small-scale shells (bivalves, gastropods, ammonites). Plant fragments can be abundant locally, including cm-scale leaves. Bioturbation can be intense locally.	Suspension settling
Mudstone-Wackestone (M)	10-40 cm-thick massive bioclastic-bearing micritic mudstone to wackestone. Rare faint undulating layering resembles HCS. Silt/sand content can range from absent to moderate. Bioclasts are mainly bivalves, and occasionally the content can increase upwards. Some bivalves are articulated. Oysters and other cm-scale bivalves can be locally abundant. Rare belemnites. Bioturbation can be intense.	Autoctonous fauna or short transport. Absence of sedimentary structures suggest quiet environment
Wackestone-packstone (N)	15-40 cm-thick beds of bioclastic-rich wackestones to packstones. Sharp undulating surfaces. Rare wave ripples on top surface. Bioclasts are mainly disarticulated bivalves and sometimes they can form lags. Gastropods can be locally common. Occasional nodules. Locally, abundant bivalves and intense bioturbation by Thalassinoides. Rare belemnites and serpulids.	Autoctonous fauna combined with current traction, migration of ripples and suspension settling
Grainstone (O)	10-65 cm-thick bioclastic-rich grainstones. Bivalves are the main bioclasts but gastropods (nerinellids and scalarids) can be locally abundant. Sometimes coquinas. Shells can be completely recrystallized. Rare small-scale bulbous corals in the coquinas.	Reworking of bioclasts and washing out of fine-grained components by waves

Table 3.2. Summary of the interpreted facies associations in the Tantan Fm. in the north Aaiun-Tarfaya Basin. In brackets subordinated lithofacies.

	Main depositional environment	**Sub-environment**	**Lithofacies**	**Main features**
FA1	Alluvial fans		A1, A2, (C)	Fining-upwards packages up to 6 m (not clear due to poor exposure)
FA2.1	Fluvial	Channel fills Bars	B, (C, H, K)	Cross-bedded fining-upwards packages up to 6 m Possible meter-scale inclined surfaces (HIS) Frequent lags of granules/pebbles Occasional roots and palaeosols developed in medium- to coarse-grained sandstones Rare desiccation cracks Occasional normally-graded beds are capped by ripples
FA2.2	Fluvial	Flood plain	K, (B, C, H)	Frequent palaeosol developed in silts to very fine-grained sandstones Interbedded sandstones (massive to small-scale cross-bedded to rippled) Thickness up to 2.5 m
FA3.1	Estuarine/peritidal	Channel fills Bars	B, C, (H, K, G, F)	Cross-bedded fining-upwards packages up to 7 m (overlying and underlying mud successions) Sedimentary structures suggest bidirectional flows with one predominant Frequent reworked mud clasts in the lower sandstone beds Common soft sediment deformation Occasional thin interbeds of mottled silt to very fine-grained sandstone Occasional vertical bioturbation by burrows Rare coarsening-upwards packages up to 2.5 m thick of very fine- to coarse-grained sandstones Occasional bivalves Characteristic white to light grey colour

FA3.2	Estuarine/peritidal	Peritidal flats	K, F, (C, B, H, G)	Packages of mottled red and green (sometimes grey) muds up to 7 m interbedded with tabular fine-grained sand bodies up to 1 m thick without a clear grain size trend Frequent palaeosols developed in muds with interbedded thin fine-grained sandstones Sandstones may be pervasively bioturbated (mainly vertical burrows), trough cross-laminated with mud drapes and well cemented with a striking white colour
FA4.1	Shoreface	Upper shoreface	B, C, F, N, O, (H, G, L)	Cross-bedded sandstones with interbedded bioclastic-bearing beds Bioclastic-rich packstones and grainstones Occasional intense biturbation by marine ichnotaxa
FA4.2	Shoreface	Proximal lower shoreface	F, G, E, M, (C, L, B, O)	HCS, low-angle cross-bedding and wave-rippled top beds can be locally abundant Locally common rippled-laminated fine-grained sandstones Occasional thin interbedded muds to fine-grained sandstones Mudstones-wackestones with occasional floating bioclasts in carbonate-dominated successions
FA4.3	Shoreface	Distal lower shoreface	F, L, (H, C, E, G)	Usually coarsening-upwards packages of interbedded muds and fine-grained sandstones up to 5 m thick Occasional thin interbeds to lenses of rippled-laminated fine- to medium-grained sandstones Bioclasts from absent to common Marls with thin interbeds of sandstones with current ripples or HCS usually capped by wave ripples
FA5	Offshore		L, (H, B, G, C)	Black clays Occasional interbeds of silts and fine-grained sandstones, including rippled top surfaces

3.5.1.3 Fluvial floodplain

This FA is mainly made of mottled silts to very fine-grained sandstones (lithofacies K, Figure 3.6C) with occasional interbeds of cross-bedded, massive and rippled-laminated sandstones (lithofacies B, C and H). Packages are up to 2.5 m thick, do not show a clear grain size trend but they usually exhibit a striking red colour. Iron crusts, calcretes and gypsum nodules may be present.

Interpretation. The fine grain size of the sediment and occasional sandstone beds suggest deposition in a low-energy environment with intermittent higher energy flows. Development of palaesols and chemical precipitation of sulphates, carbonates and iron suggest high rates of evaporation and long times of sub-aerial exposure.

3.5.1.4 Peritidal bar and channel fill

This FA is mainly made of fining-upwards packages of cross-bedded sandstones and subordinated normally-graded massive sandstones (lithofacies B and C) up to 7 m thick (Figure 3.6D). Scarce coarsening-upwards packages up to 2.5 m thick are also observed. This FA exhibits an overall striking white to light grey colour in outcrop. Current and wave ripples are uncommon (lithofacies H and G). Palaesols red/green/yellow in colour may develop on thin interbeds of mottled silt to very fine-grained sandstones (lithofacies K). Sedimentary structures suggest approximately N-S bidirectional currents, but with N being the dominant sediment transport direction. Soft sedimentary deformation can be locally common. Bioturbation, mainly by vertical burrows is locally abundant in the fine-grained sandstones (lithofacies F). Rare bivalve bioclasts may be present at the top of coarsening-upwards packages.

Interpretation. The coarse grain size, cross-bedding and overall fining-upward grain size profile suggests subaqueous dunes filling channels or migrating bar forms. The presence of bioturbation and occasional bidirectional palaeoflows registered indicates tidal-influenced channel fills.

Infrequent coarsening-upwards packages of cross-bedded sandstones crop out in the upper part of the thick peritidal successions (see m 50-57 at Hassi Oum Esbed outcrop in Figure 3.5). Occasional abundant bioturbation at the base, bivalves at the top and the vertical relationship with other sedimentary facies suggest an interpretation of intertidal bars.

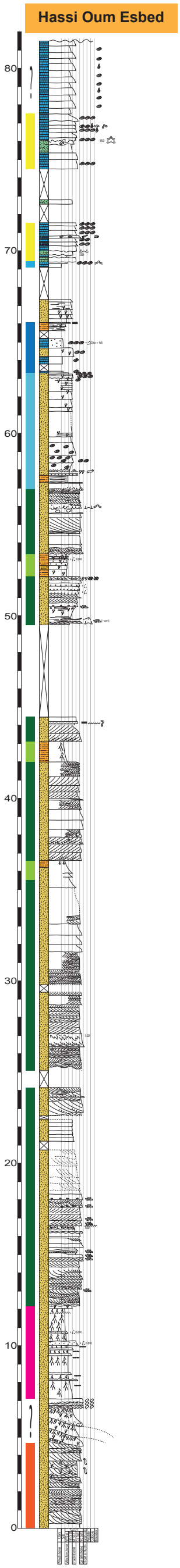

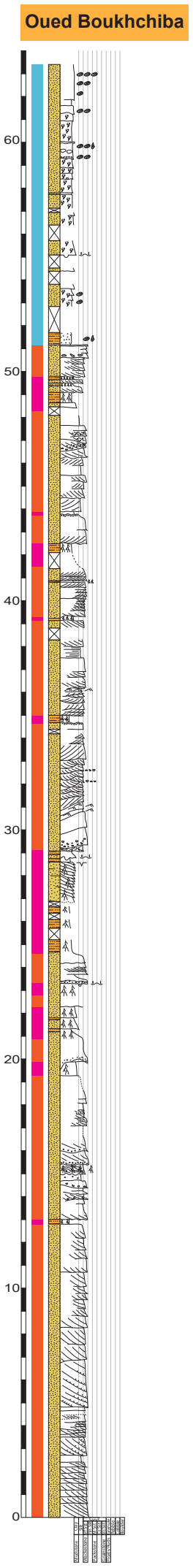

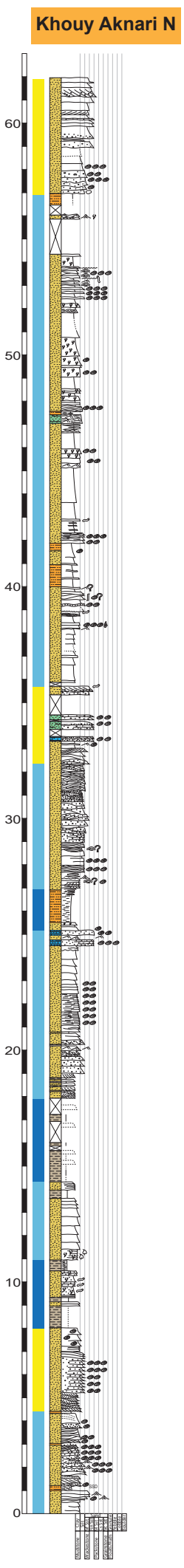

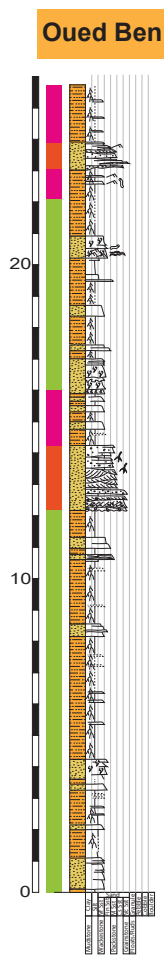

LITHOLOGY

- Limestone
- Sandy limestone
- Silty limestone
- Calcareous sandstone
- Sandstone
- Calcareous siltstone
- Siltstone
- Clay

SEDIMENTARY STRUCTURES

- Ripple lamination
- Hummocky cross stratification
- Wave ripples
- Parallel bedding
- Fine lamination
- Flaser bedding
- Wavy/irregular lamination
- Wavy/irregular bedding
- Erosive contact
- Channels
- Slump
- SSD Soft sedimentary deformation
- Dewatering structures
- Loading surface
- Scattered/banded granules-fine pebbles
- (cm) Rip up clasts (maximum size)
- Carbonate clasts
- Sandstone clasts

FOSSILS

- Gastropods
- Bivalves
- Unidentified shells
- "Belemnites"
- Plants/organic matter

TRACE FOSSILS

- Bioturbation
- Bioturbation by burrows
- Bioturbation by roots
- Palaeosol

FACIES ASSOCIATIONS

- Offshore
- Distal lower shoreface
- Proximal lower shoreface
- Upper shoreface
- Peritidal
- Fluvial
- Alluvial fans

Figure 3.5 (Previous page). Example of four graphic sedimentary logs showing main lithology, sedimentary structures, fossil content and interpreted depositional environments.

3.5.1.5 Peritidal flats

This FA is mainly composed of mottled red (occasionally green and grey) muds (lithofacies K) with subordinated massive, cross-bedded, current and wave ripple-laminated and/or bioturbated sandstones (lithofacies C, B, H, G and F; Figure 3.6E). Packages do not show a clear grain size trend or weak fining-upward trends, reaching up to 7 m in thickness. The red facies are generally muds to very fine-grained sandstones and can be bioturbated or have developed palaeosols. Tabular, laterally continuous, well cemented prominent white sandstones (lithofacies F) stand out over the red muddy background in some outcrops at the base of fining-upwards packages. These sandstones may show mud drapes on the cross laminae and are intensely bioturbated.

Interpretation. The cross-bedded, bioturbated and mud-draped sandstones were deposited in a relatively energetic environment probably in a shallow subtidal to intertidal environment. The red colour and development of palaesols suggests intermittent exposure. with low sedimentation rates in the intertidal to supratidal flats. An overall fining-upwards trend displaying the subtidal sandstones to the supratidal palaesols is characteristic of progradation in a peritidal environment.

Thin sandstone levels interbedded within the muds represent storms or higher tides.

3.5.1.6 Upper shoreface

This FA is mainly made of coarsening-upwards packages up to 5 m thick of cross-bedded, frequently bioclastic, and bioturbated sandstones (lithofacies B and F; Figure 3.6F). Carbonate-dominated successions are represented mainly by bioclastic packstones and grainstones (lithofacies N and O). Subordinated lithofacies include current and wave ripple-laminated sandstones and muds/marls. Marine bioturbation by *Thalassinoides* can be locally pervasive in sandstones.

Interpretation. Sedimentary structures, fossil content and bioturbation suggest deposition in a subtidal marine environment under the action of unidirectional currents modulated by the oscillatory flow produced by wave action.

3.5.1.7 Proximal lower shoreface

This FA is dominated by massive fine-grained yellow sandstones (lithofacies F). The massive appearance is probably due to weathering and complete destratification by

intense bioturbation. Occasionally, less intense weathering allows identification of discrete bioturbation (Figure 3.6G) or remnants of sedimentary structures (i.e. ripples). Subordinate lithofacies include hummocky cross-stratified, current and wave ripple-laminated and cross-bedded sandstones, micritic mudstones to wackestones with occasional bioclasts and muds (lithofacies E, H, G, B, M and L). Bioclastic grainstones or coquina beds (lithofacies O) can be present, spaced throughout the succession, some of them very prominent and laterally-extensive. A wide assortment of fossil groups may be found in an individual bed with bivalves (*Trigoniids* mainly; Figure 3.6H) being the dominant group. Subordinated groups include gastropods, bulbous corals, and scarce brachiopods (*Terebratulids*).

Interpretation. The presence of hummocky cross-stratification overlain by wave-rippled tops is diagnostic of storms (ref). Coquinas with cosmopolitan fossil assemblages are interpreted as shell lags, the result of storms reworking shallower sediments. The preservation of these two features indicates deposition below the fair weather wave base, allowing preservation.

3.5.1.8 Distal lower shoreface

This FA is usually made of interbedded fine-grained yellow sandstones and muds (lithofacies F and L) in coarsening-upwards packages up to 5 m thick. The amount of mud interbeds is higher than in the previous FA. Subordinated lithofacies include occasional thin interbeds or lenses of massive, rippled-laminated, hummocky cross-laminated and wave ripple-laminated fine- to medium-grained sandstones (lithofacies C, H, E and G). Bioclasts can range locally from absent to common.

Interpretation. The higher proportion of muds indicates a more distal and deeper depositional setting. Preservation of HCS interbedded in muds puts it between the storm and the fair weather wave base.

3.5.1.9 Offshore

This FA is almost entirely made of clay-sized clastics and marls (lithofacies L). Thin interbeds of silts and fine-grained sandstones are infrequent (lithofacies H, B, G and C).

Interpretation. The fine grain of the sediment suggests mainly suspension settling in an offshore setting below the storm wave base. The scarce interbeds of coarser sediment represent small-scale turbidites probably related with storms affecting the shallower part of the shelf.

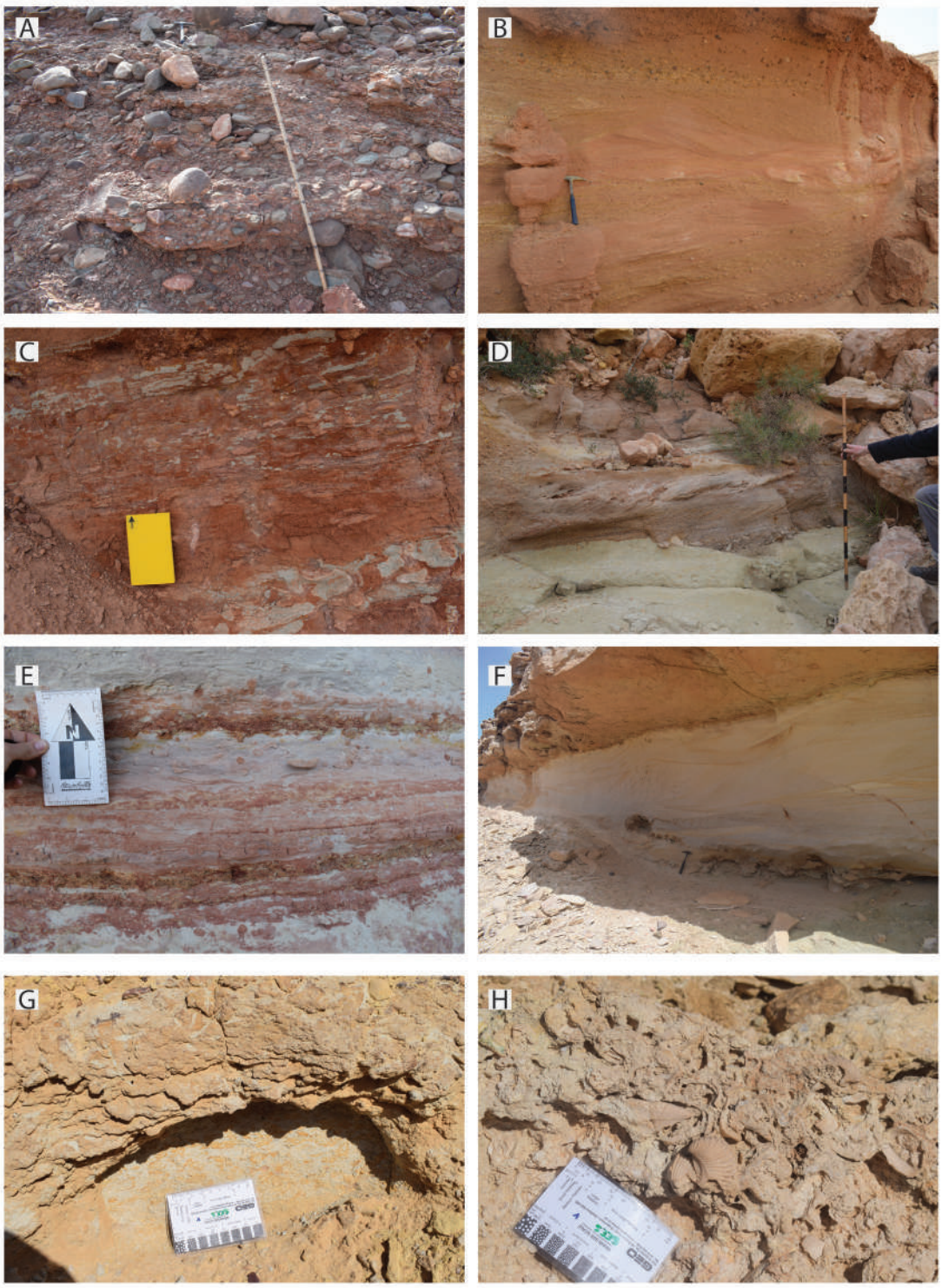

Figure 3.6. Examples of facies associations in the field. A) Alluvial fan conglomerates at Pont Sur l'Oued Draa outcrop. Note poor sorting and absence of sedimentary structures. B) Fluvial cross-bedded sandstones and pebbly sandstones at Old Tafnidilt. C) Laminated mottled floodplain silts and fine-grained sandstones at Old Tafnidilt outcrop. D) Coarse-grained cross-bedded peritidal bar at Wizard's Hat south outcrop. Note the erosive base and reworking of sandstone clasts from the underlying unit. E) Intensely bioturbated and rippled alternation of fine-grained sandstones and silts at New Tafnidilt outcrop. Red levels are related with longer exposure and incipient palaeosols. F) Cross-bedded fine- to medium-grained upper shoreface sandstones. G) Intensely burrowed fine-grained sandstones interpreted as proximal lower shoreface at El Hamairat outcrop. H) Field

photograph of a coquina along Oued Chebeika. Trigonids (center of image) are the most abundant group together with various unidentified bivalve groups.

3.5.2 Biostratigraphy

Marine facies in the area are rich in bivalve faunas. Among the bivalves along Oued Draa, several specimens belong to the group of *Plicatula placunea* Lamarck, *Plicatula radiola* Lamarck and *Plicatula inflata* Sowerby. Those taxa are in need of a modern taxonomic revision but their known stratigraphic range is strictly restricted to the Aptian to Lower Albian (Kotetishvili et al., 2005). *Plicatula inflata* was reported from the Tantan Fm. at Cap Dra by Freneix (1972) and according to Collignon (1967, 1966), the associated ammonite fauna indicates a late Aptian age. It should also be noted that in the Essaouira Agadir Basin, *Plicatula placunea* and *Plicatula radiola* are very common in the Tamzergout and Lemgo formations (Ambroggi, 1963; Rey et al., 1986a, 1986b). It is now clearly established that these formations are of early Upper Aptian to early Albian age (Luber et al., 2017).

In higher stratigraphic levels, at Oued Chebeika outcrop (Figure 3.4) a specimen of *Cymatoceras albense* (Figure 3.7A) was found dating this part of the succession as late Albian. At the topmost section visited, at Foum Chebeika outcrop, samples of black shales processed for palynological examination yielded dinoflagellates, spores and pollen of latest Albian to Cenomanian in age. Age diagnostic palynomorphs include the presence of at least two species of *Afropollis* (including *A. kahramanensis* described by (Schrank and Ibrahim, 1995) from the mid-late Cenomanian of Egypt and several rare specimens of elaterate pollen which are diagnostic of the Albian-Cenomanian Elaterates Province defined by (Herngreen et al., 1996).

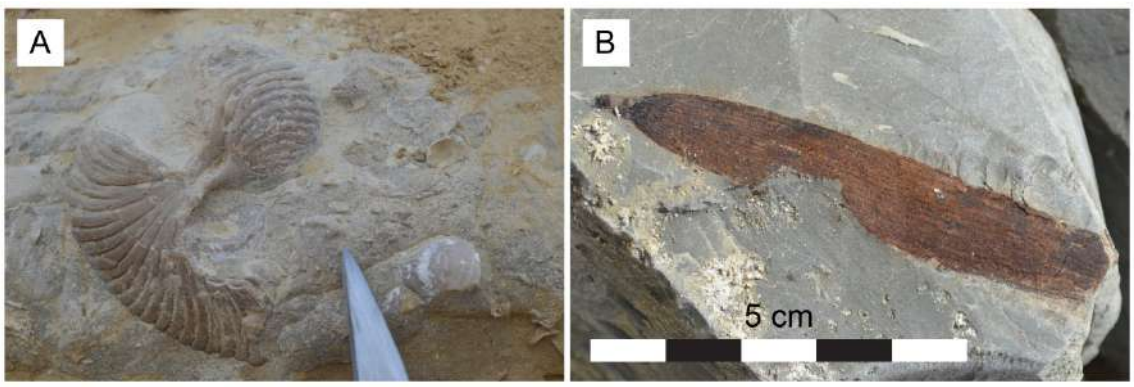

Figure 3.7. Field photographs of fossils found along Oued Chebeika. A) Nautiloid (*Cymatoceras albense*) from Oued Chebeika outcrop. B) Unidentified plant leaf from Foum Chebeika outcrop.

Stratigrapphic ranges inferred from new specimens collected and from the literature are shown on the correlation panel in Figure 3.9.

3.5.3 Lithostratigraphy

Previous work:

The stratigraphy covered during the present work belongs to the Tantan Fm. and the lower part of the Aguidir Fm. (Figure 3.2). From the descriptions and type section of Martinis and Visintin (1966) four main lithological intervals can be distinguished within the Tantan Fm (Figure 3.2). Despite of this, only a sixty five meter thick interval of interbedded marls and limestones was ranked as a Member (Figure 3.2; *member des Marnes du Draa* - Draa Marls Member). The interpreted main depositional environment for this succession is continental with intercalated marine episodes, mainly towards the upper part, and better developed during deposition of the Draa Marls Member interpreted as neritic facies (Martinis and Visintin, 1966).

This study:

Along the transect at Oued Chebeika, from Oued Boukhchiba to Foum Chebeika outcrops (Figure 3.3 and Figure 3.4), striking changes in lithology, sedimentary structures and/or interpreted depositional environments can be observed at outcrop scale. These differences become even more obvious at a larger scale, where striking changes in colours on the exposed slopes coincide with the previously mentioned lithological changes. Systematic changes in colour of different sedimentary units can be used as an excellent mapping tool.

Following recommendations compiled by Whittaker et al. (1991) the Tantan Fm. has been sub-divided into six members. These subdivisions integrate the previously proposed Draa Marls Member of Martinis and Visintin (1966). The contacts between these units are often sharp, making them mappable units in the field. Several of these lithostratigraphic units can be also distinguished along the Oued Draa.

Some characteristic facies have proved key for regional correlation: i) The continental alluvial fan conglomerates (FA1) display an intense red colour, and usually comprise fine-grained clastics with mottling and the development of palaeosols (FA3 and sometimes FA5). ii) A characteristic yellow colour was linked with marine deposits (FA6, 7 and 8). iii) A very distinctive laterally continuous white sandstone unit (FA4), approximately 45 m thick, is exposed in the central part of Oued Chebeika transect.

FA4 is also found along the Oued Draa, where it crops out in isolated outcrops passing laterally to a more distal facies association, but it does not present a laterally extensive unit.

Since the units are better exposed along the Oued Chebeika, this section has been used to subdivide the Tantan Fm. in Members, incorporating the previous one.

3.5.3.1 Red Conglomerates Member (RC)

This lithostratigraphic unit is exposed on both sides of the Oued Draa, at its exit from the Anti-Atlas into the ATB (Figure 3.8). It has an approximate thickness of 50 m. It is composed of red conglomerates with clasts up to cobble size (FA1) and no apparent sedimentary structures (Figure 3.6A).

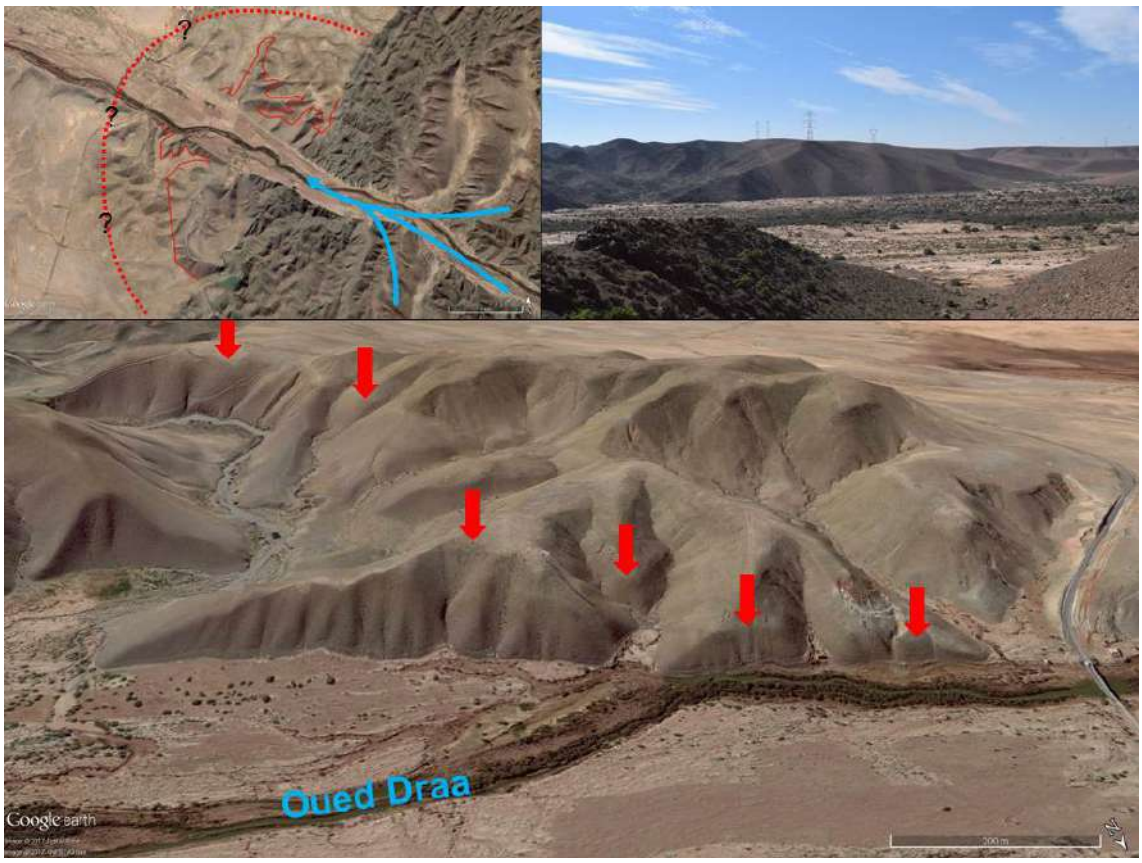

Figure 3.8. Red conglomerates exposed at Oued Draa along the faulted contact between the Anti-Atlas and the Aaiun-Tarfaya Basin (see Pont Sur l'Oued Draa outcrop in Figure 3.4 for location). The red vertical arrows indicate the sharp erosive contact between the conglomerates and the overlying fluvial sandstones interpreted as a sequence boundary at this location (see Figure 3.9 for more details).

The conglomerates have a faulted contact with the Anti-Atlas basement (Figure 3.8; Hollard et al., 1985) and its base is not exposed. The conglomeratic facies crop out only in the proximity of the Pont Sur l'Oued Draa outcrop, where the Oued Draa enters the

ATB. Mapping in photo-imagery suggests a fan shape geometry, in part a combination of the regional tilting of the Mesozoic succession together with the erosion (Figure 3.8). The present Oued Draa may have been active in the early Cretaceous, acting as the conduit for the alluvial conglomerates into the basin.

3.5.3.2 Red Basal Sandstone Member (RBS)

This lithostratigraphic unit makes up the lower 49 m of the section exposed at Oued Boukhchiba outcrop. It has light reddish to whitish colour in outcrop. It is mainly composed of cross-bedded fluvial sandstones (FA2) with intercalated flood plain reddish silts and sands (FA3). The main palaeoflow direction is towards the NNE. The base of this unit is not exposed in the area, but it probably onlaps the Palaeozoic which crops out approximately 750 m to the SE of the outcrop. Its lateral equivalent along the Oued Draa are fluvial sandstones ~ 250 m thick overlain by more than 50 m of peritidal red sands and silts.

3.5.3.3 Draa Marls Member (Martinis and Visintin, 1966)

This unit was originally defined along Oued Draa. Despite the name originally assigned to this member, the unit is composed of heavily bioturbated fine-grained sandstones with interbedded bioclastic-rich sandstones/limestones (FA6, 7 and 8) and occasional clays to silts levels (FA9). It has a striking yellow colour and regional extent allowing mapping even in satellite imagery across the DLT Basin. It is exposed in the upper 14 m of the Oued Boukhchiba, Oued Lassaal east and the lower part of the Oued Lassaal west outcrops with a total thickness of ca. 30 m and around 50 m at Oued Draa transect. It sharply overlies the fluvial sandstones at Oued Chebeika transect and the fluvial to peritidal sandstones and silts at Oued Draa transect belonging to the Red Basal Sandstone Member.

3.5.3.4 Red Upper Sandstone Member (RUS)

The basal contact with the previous member is poorly exposed. The best exposure is recorded in the upper part of the Oued Lassaal east outcrop. The first occurrence of pebble lags in cross-bedded sandstones, grain size increase and loss of marine fauna have been used to place the contact with the underlying member. The unit has an estimated thickness of ~ 120 m and its sedimentological features are characterized in the Oued Lassaal west outcrop. Facies are typified by cross-bedded sandstones and mottled silts and sands (FA2 and 3) recording a return to a continental setting very similar to the

Red Basal Sandstone Member. The main palaeoflow direction of this unit is towards the NW. This Member does not have an equivalent along the Oued Draa transect as the White Sandstone Member (see below) is overlying directly on the Draa Marls Member.

3.5.3.5 White Sandstone Member (WS)

This unit is not uniformly exposed across the study area. Along Oued Chebeika transect, this member is ca. 55 m thick and the contact with the underlying member is relatively sharp and well exposed at the base of the Hassi Oum Esbed outcrop, where the whole unit is exposed. Along Oued Draa transect this member is not continuous and interfingers with the overlying member.

It is a sand-dominated interval with abundant cross-bedding white to light grey in colour. Palaeocurrents are bi-directional and occasional intense bioturbation by invertebrates can be present even in coarse-grained sandstones. These features suggest interaction with a standing body of water and it has been interpreted as a tidal-influenced fluvial system (estuary) or tidal sand flats.

3.5.3.6 Yellow Upper Sandstone Member (YUS)

This yellow in colour unit is exposed at Wizard's Hat south and north, Hassi Oum Esbed, Oum Esbed and Oued Chebeika outcrops with an estimated thickness of ca. 65 m (Figure 3.4). The contact with the underlying member is sharp and in some cases very erosive. The overall lithology and depositional settings represented are similar (FA6, 7 and 8) to the Draa Marls Member, although carbonates are more abundant. The fauna includes groups that were not observed in the Draa Marls Member, such as oysters, scarce domal corals and cephalopods (ammonoids, nautiloids and belemnoids) and occasional gastropod-monospecific beds. The erosive base unit is interpreted to be represented by a tempestite. Along Oued Draa transect the top is not exposed and the thickness reaches at least 150 m. Towards the inland it interfingers with the White Sandstones Member.

3.5.3.7 Oued Chebeika Clay Member (Martinis and Visintin, 1966)

This unit is exposed around the mouth of Oued Chebeika. The contact with the underlying member is not well exposed. It is mainly made of dark grey clay-sized clastics and marls with interbedded fine-grained rippled- and hummocky cross-stratified sandstones (FA8 and 9). Plant fragments are common in the clay-sized clastics and marls (Figure 3.7B), with scarce body fossils (gastropods, bivalves and cephalopods).

This unit is correlated with the base of the *Membre des Argiles de l'Oued Chebeika* (Oued Chebeika Clay Member), which is the lowermost subdivision of the Aguidir Limestone Fm. (Martinis and Visintin, 1966).

Figure 3.9 (Next page). Correlation panels of the two transects along the Oued Draa (right) and Oued Chebeika (left) showing facies associations and position of sections logged. Both transects are parallel and oriented NW-SE. Stratigraphic intervals are from literature (see text) and new dating from new specimens. FS: flooding surface; P: parasequence; SB: sequence boundary; TS: transgressive surface; MFS: maximum flooding surface; SB + TS: amalgamated sequence boundary and transgressive surface.

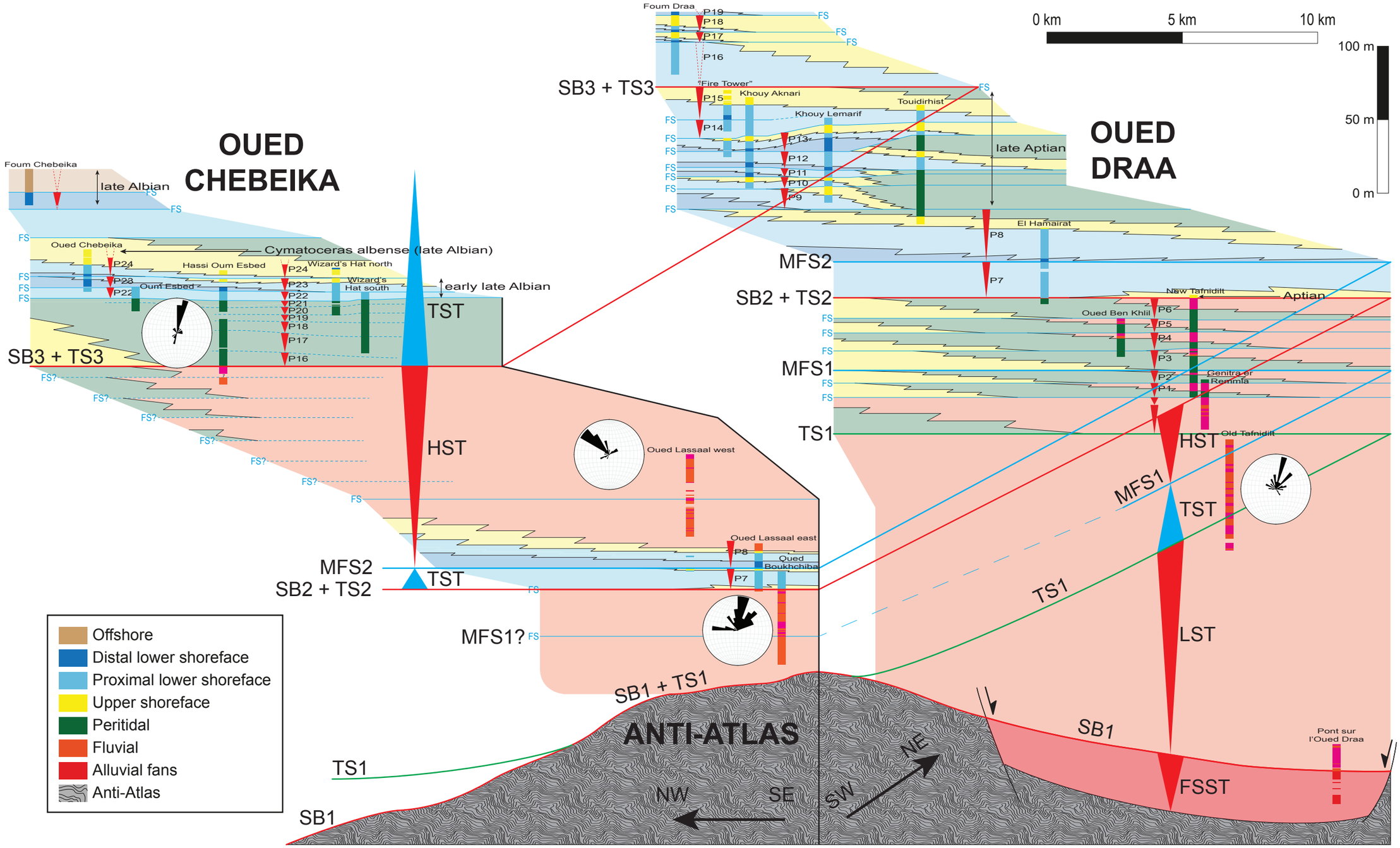
OUED CHEBEIKA
OUED DRAA
0 km
5 km
10 km
100 m
50 m
0 m
Foum Chebeika
late Albian
Oued Chebeika
Cymatoceras albense (late Albian)
Hassi Oum Esbed
Wizard's Hat north
Oum Esbed
Wizard's Hat south
early late Albian
TST
SB3 + TS3
HST
Oued Lassaal west
MFS2
SB2 + TS2
TST
Oued Lassaal east
Oued Boukhchiba
MFS1?
SB1 + TS1
ANTI-ATLAS
TS1
SB1
NW
SE
SW
NE
Foum Draa
"Fire Tower"
Khouy Aknari
Khouy Lemarif
Touidirhist
late Aptian
El Hamairat
MFS2
SB2 + TS2
New Tafnidilt
Aptian
Oued Ben Khlil
MFS1
Genitra er Remmla
TS1
HST
Old Tafnidilt
MFS1
TST
TS1
LST
SB1
FSST
Pont sur l'Oued Draa
Offshore
Distal lower shoreface
Proximal lower shoreface
Upper shoreface
Peritidal
Fluvial
Alluvial fans
Anti-Atlas

3.6 Discussion

3.6.1 Correlations and sequence stratigraphy

The acquisition of a complete stratigraphic record for the Tantan Fm. in the study area is challenging, relying on two partial transects, while some stratigraphic intervals are not recorded. To overcome this, several sections have been logged along both rivers, Oued Chebeika and Oued Draa (Figure 3.3, Figure 3.4 and Figure 3.9). The strata have a small overall regional dip towards the W, and the vertical size of the exposed sections ranges from 26 to 84 m. Correlation between time-equivalent sedimentary units over long distances was sometimes not possible due to lack of exposures and there was limited overlap between some of the sections. Biostratigraphic constraint for the Tantan Fm. is not of a high enough resolution to afford a detailed correlation in many areas; however age-diagnostic fossils, either from the literature or new data from this study have been used to improve the final correlation in the study area.

A sequence stratigraphic panel for both transects and a correlation between them is presented in Figure 3.9. Both transects are oriented SE-NW and the most representative sections logged have been projected on them. A sequence model with four systems tracts has been adopted for this study. To the classic model with lowstand, trasgressive and highstand (Posamentier and Vail, 1988; Vail, 1987; van Wagoner et al., 1988) the falling stage system tract (Plint and Nummedal, 2000) has been added.

The datum for the correlation is the Draa Marls Member, marking the first occurrence of marine facies in the Tantan Fm. This unit is present at both transects and it is traceable on satellite imagery at least until the Smara region for more than 200 km to the south. The lithostratigraphic units recognized along the Oued Chebeika have been correlated based on identification of flooding surfaces identified in Oued Draa. Age-diagnostic fossils, although sparse, were used to improve the final correlation in the study area, either from those reported in the literature or found in the study area.

The correlation presented in this work provides the opportunity to recognize in outcrop the early Cretaceous overall transgression expression in the Tantan Fm. into the lowermost part of the Aguidir Fm. This trend is, nevertheless, slightly masked by the fact that progressively higher stratigraphic levels are also exposed in more distal positions in the basin (see Figure 3.9).

Due to the absence of laterally-equivalent logged sections in continental sediments and the inherent difficulty of precisely identify flooding surfaces in continental successions, definition of parasequences have not been performed. Nevertheless, abrupt vertical changes in facies associations within continental environments have been interpreted as a possible effect of flooding events in distal areas.

Four depositional sequences have been interpreted based on correlations between the two transects. The Red Conglomerates Member is the lowermost unit exposed in the area, only exposed at the Oued Draa transect. Conglomerates belonging to the base of the Tantan Fm. have also been reported in the Cheb-1 and EA-1 onshore wells (Figure 3.3). They are exposed next to a faulted contact on the margin of the basin with the Palaeozoic of the Anti-Atlas (Figure 3.8), that is interpreted to have created the topography that developed the alluvial fan. This is cut by the present day Oued Draa. Alluvial fans at the toe of the slopes of the Anti-Atlas are interpreted as a result of a sea-level fall. A lowstand wedge developed on the Jurassic slope of the continental margin has been interpreted from seismic as a result of the same event. An age of Berriasian (Wenke et al., 2011) or Valanginian (Todd and Mitchum, 1977) has been proposed for that event. A sand-porne cycle in the turbidites of Fuerteventura has been dated as Berriasian, and interpreted as progradation of lower to middle deep sea fans (see Chapter 4). During the Berriasian, alluvial fans locally sourced from the Anti-Atlas developed during the sea-level lowstand. Possible incised valleys cut the exposed shelf as a result of bypass and erosion although this could not be confirmed due to non-exposure. At the same time deep water fans prograded at the platform margin reaching Fuerteventura. This moment represents the maximum progradation of the shoreline, interpreted as a FSST and capped by a sequence boundary (Figure 3.9). The SB has been placed at a sharp erosive contact between the conglomerates and fluvial sandstones.

The Red Conglomerates Member is overlain by fluvial sandstones and silts belonging to the Red Basal Sandstone Member. Although the contact is not exposed, Palaeozoic rocks of the Anti-Atlas are exposed close to the base of the Oued Boukhchiba outcrop, and it is assumed the Tantan Fm. onlaps the SB1 + TS1 in this area (Figure 3.9). Recorded palaeocurrents in the fluvial successions at Oued Boukhchiba and Old Tafnidilt outcrops yield a consistent transport direction towards the NNE. The upper ca. 60 m of this member at the Oued Draa transect represent deposition in a transitional

setting interpreted as interfingering distal flood plain and tidal flats (FA3 and 5; Figure 3.9). These peritidal sections have a striking red colour punctuated by dm-thick prominent white sandstone beds. These beds represent the base of individual parasequences that can be correlated between the logs taken at Genitra er Remla, New Tafnidilt and Oued Ben Khlil (Figure 3.9). The parasequences have the typical fining-upwards profile, characteristic of peritidal progradation (Daidu et al., 2013). Occasional fining-upwards packages of cross-bedded sandstones less than 4 m thick punctuate this silt-dominated interval, and are interpreted as tidal creeks. Six progradational parasequences (P1-P6) are identified in this upper interval. The base of P3 marks the transition from a retrogradational parasequence set to progradational, being interpreted as a maximum flooding surface (MFS1; Figure 3.9) and the limit between the TST and the HST. The lateral-equivalent of this peritidal interval along Oued Chebeika transect are fluvial sandstones and silts at Oued Boukhchiba outcrop. Despite the study of parasequences has not been performed on continental successions the MFS1 has been tentatively placed at a position with abundant floodplain deposits (Figure 3.9). A Valanginian to Barremian interval is interpreted for deposition of this sedimentary sequence. The upper limit is defined by the overlying Marls Draa Member dated as Aptian with bivalve and ammonite faunas (see section 1.5.2 Biostratigraphy).

The next depositional sequence is composed by a TST and the subsequent HST. Along Oued Chebeika transect, it includes marine sandstones, silts and carbonates belonging to the Draa Marls Member overlain by fluvial sandstones of the Red Upper Sandstone Member. In a more distal position along Oued Draa the marine facies are overlain by interstratified packages of marine and peritidal facies. The Red Upper Sandstone Member is absent at this location.

This third depositional sequence is bounded at the base by an amalgamated SB2 + TS2 that put marine transgressive sandstones overlying fluvial and floodplain sandstones and silts. Distal lower shoreface deposits at the base of P8 represent the deepest facies, where the MFS2 has been placed (Figure 3.9). Parasequences P8-P15 along Oued Draa transect exhibit an overall aggradational stacking pattern belonging therefore to an early stage of a HST. P9 to P13 exhibit a SE to NW transition from a more proximal sand-dominated peritidal setting to upper shoreface and proximal lower shoreface marine sandstones, with subordinated distal lower shoreface mudstones, siltstones and sandstones in the most distal outcrop at Khouy Aknari. The base of P13 and P14

represent flooding events of slightly higher magnitude and the facies recorded in all the outcrops are completely marine. At the most distal position along Oued Draa, at the Fire Tower outcrop, the final parasequence P15 comprises FA8. This package is 3.4 m thick and mainly covered, with only minor silt levels exposed. This has been correlated with the Khouy Aknari outcrop where lenticular and flaser bedding and hummocky cross-stratified is observed in very fine- to fine-grained sandstones. Evidence of a flooding surface at the base of P15 could not be clearly found in a more proximal location at Touidirhist outcrop. This suggests the flooding event did not have a clear expression in proximal locations. Lateral equivalent, more proximal facies along Oued Chebeika record red fluvial sandstones. One significant difference with the lower fluvial interval is that the cross-bedded sandstones here have a dominant palaeoflow towards the NW, as opposed to NNE for the Red Basal Sandstone Member.

The last depositional sequence is incomplete and represented only by a TST bounded at the base by a SB3 + TS3. The succession is more complete along Oued Chebeika with at least nine parasequences (P16-P24; Figure 3.9). The base of the Oued Chebeika Clay Member is also included in this TST. The White Sandstone Member is well exposed along Oued Chebeika. Its lower base shows peritidal cross-bedded sandstones overlying fluvial channel fill and flood plain deposits representing the transgressive surface. This basal contact can be followed for ca. 12 km along Oued Chebeika. The upper surface of the White Sandstone Member is defined by the presence of peritidal sandstones and muds (FA4 and 5) overlying proximal lower shoreface deposits (FA7). Six parasequences (P16-P21) have been identified in the White Sandstone Member, recorded across four outcrops. Only at the Hassi Oum Esbed outcrop (Figure 3.5) is the member completely exposed. Most of the parasequences exhibit a fining-upwards profile typical of progradation (Daidu et al., 2013) from peritidal to fluvial channel fill and abandonment. Palaeocurrent measurements show an asymmetric bidirectional flow NNE-SSW, which supports the peritidal interpretation. The base of parasequences P16 to P19 are marked by a sharp increase in grain size, erosive surfaces and occasionally abundant mud clasts. Parasequences P20 and P21 show a coarsening-upwards grain size trend that has been interpreted to be developed by tidal bars (Olariu et al., 2012).

Along the Oued Draa transect the base of parasequence P16 is not exposed due to a gap in exposure between the top of the Fire Tower and the base of Foum Draa outcrops. Only four parasequences have been recognized at Oued Draa until the end of the

exposure. The overlying Yellow Upper Sandstone Member could not be logged entirely along Oued Chabeika. Three parasequences (P22-P24) have been identified in the lower part, comprising shoreface sediments (FA6, 7 and 8) that overall describe a progradational stacking pattern. P22 starts with a very prominent, erosive based, fining-upwards 3 m thick unit that can be correlated across outcrops. This package has a variable thickness, decreasing towards the NW. In proximal settings (such as the Wizard's Hat north outcrop) this marker unit starts with a basal matrix-supported conglomerate with quartz pebbles and mud clasts up to 10 cm, resting on an erosive contact. It is overlain by medium- to coarse-grained hummocky cross-stratified sandstones, which in turn are overlain by fine- to medium-grained sandstones with wave ripples. The upper part contains shelly lags and interbedded sandstones capped by bioclastic sandy grainstones. Based on the vertical evolution of lithofacies this unit has been interpreted as a tempestite.

The lower part of the Foum Chebeika outcrop is made of clays, marls and interbedded hummocky cross-laminated and wave-rippled fine-grained sandstones. Due to missing section between the Oued Chebeika and Foum Chebeika outcrops, the uppermost parasequence has not been numbered in Figure 3.9. Some patchy oucrops contain fine-grained sandstones and numerous bioclastic-rich levels, including abundant oysters. Based on the average parasequence thickness in the area, two or three FS are expected, but this interval is patchy and not very well exposed and will need further investigation to construct a composite log through the missing interval.

3.6.2 Sediment provenance

The provenance of the lower Cretaceous siliciclastics of the Tantan Fm. has been located at the Precambrian Reguibat Shield and Palaeozoic Mauritanides (Ali et al., 2014a, 2014b) based on geochemical and radiogenic isotope analyses. Nevertheless, the sampling for those studies was not representative for the entire formation and concentrated only at the Oued Boukhchiba outcrop.

Analysis of the sedimentology and palaeocurrents throughout the entire Tantan Fm. has confirmed a provenance from the West African Craton, south of the study area, but has evidenced also the Anti-Atlas played a role as a source of sedimen. The varied lithologic composition of clasts (i.e. quartzites, rhyolites) in the Red Conglomerates Member is characteristic from the Palaeozoic terrains of the Anti-Atlas. Despite suggested subsidence or relative stability of the western Anti-Atlas during most of the

early Cretaceous (Gouiza et al., 2017b), the presence of alluvial fans suggest local uplift pulses of the Palaeozoic basement due to increased subsidence of the basin accommodated locally by normal faulting.

Dominant NNE sediment transport direction in the Red Basal Sandstone Member along both transects, supports the WAC sediment provenance from Ali et al. (2014a, 2014b). A major cooling event in the western Reguibat Shield during Barremian and possibly early Aptian (Gouiza et al., *in press.*) may be the main responsible for deposition of the this member.

A net change in palaeocurrents towards the NW is recorded in the Upper Red Sandstone Member. A combination of autocyclic processes and reconfiguration of the drainage area due to local tectonics of the western Anti-Atlas is a plausible explanation. Nevertheless, the significant thickness of clastics recorded during this interval and the consistency of the palaeocurrents throughout it, favours an allocyclic, long-term tectonic control.

During deposition of the White Sandstones Member palaeocurrents, although dominated by the tidal influence, return to the previous NNE (and SSW) direction. Volumes of sediment eroded from the Reguibat Shield are interpreted to have decreased dramatically (Charton et al., *in prep.*) suggesting the contribution is mainly coming from the Anti-Atlas.

3.6.3 Tectonostratigraphic evolution of the early Cretaceous section

The distribution and vertical evolution of facies associations suggests that the Tantan Fm. in the study area was deposited under fluctuating sediment supply, changing source areas and variable subsidence, linked with tectonics in the Anti-Atlas and Reguibat Shield (Gouiza et al., 2017a) and an overall relative sea-level rise during most of the early Cretaceous (Haq et al., 1987; Snedden and Liu, 2010). The combined interplay of these processes resulted in a progradational deltaic system that was subsequently dismantled by wave and tide action during transgression associated with relative increase in accommodation. A strong basin subsidence is needed paired with the eustatic sea-level rise in order to accommodate more than 500 m of sedimentary sequence exposed in a proximal location of the basin. The effect of tectonic pulses inland is interpreted to have modulated the overall trend switching uplifted areas and rerouting sediment.

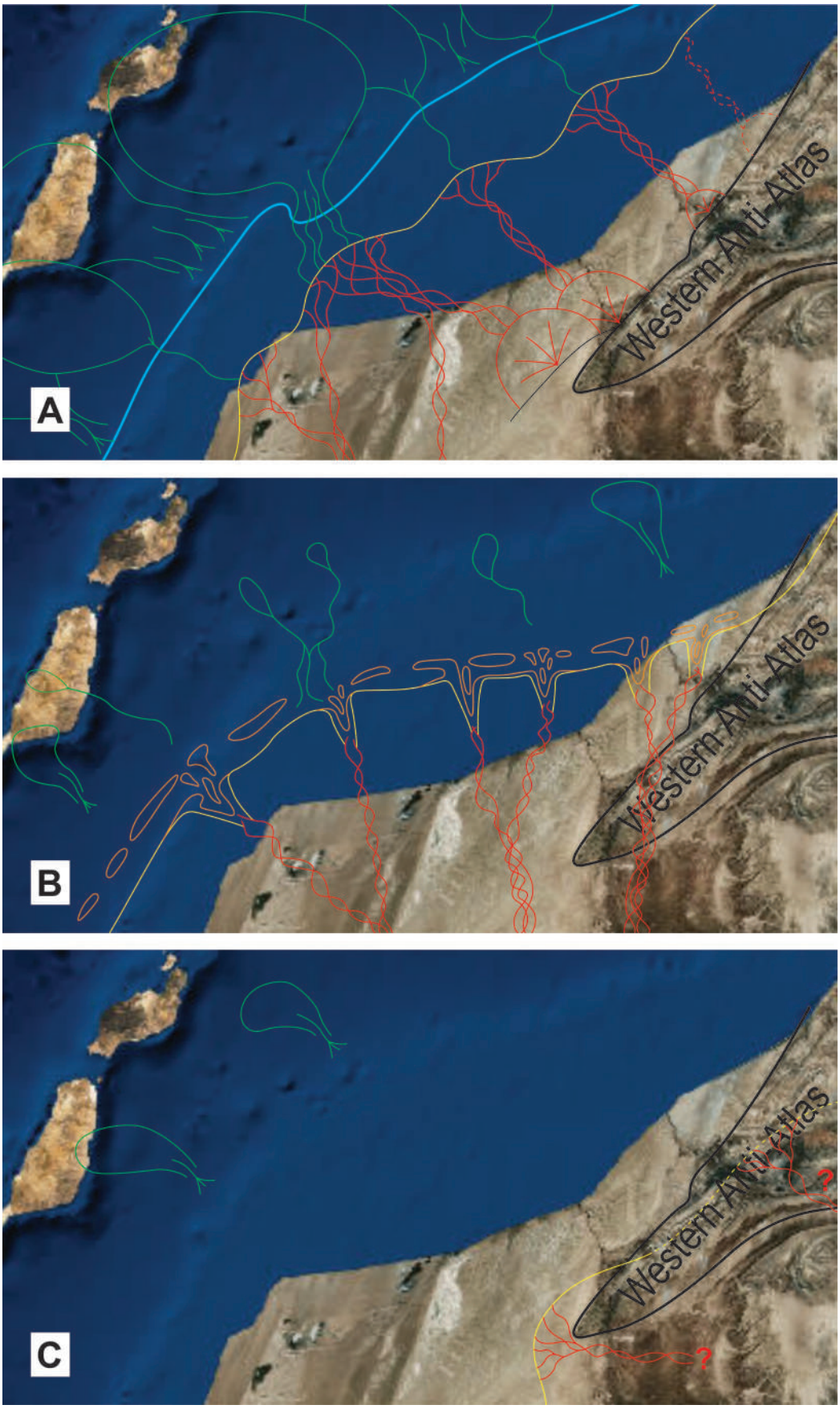

(Continue next page)

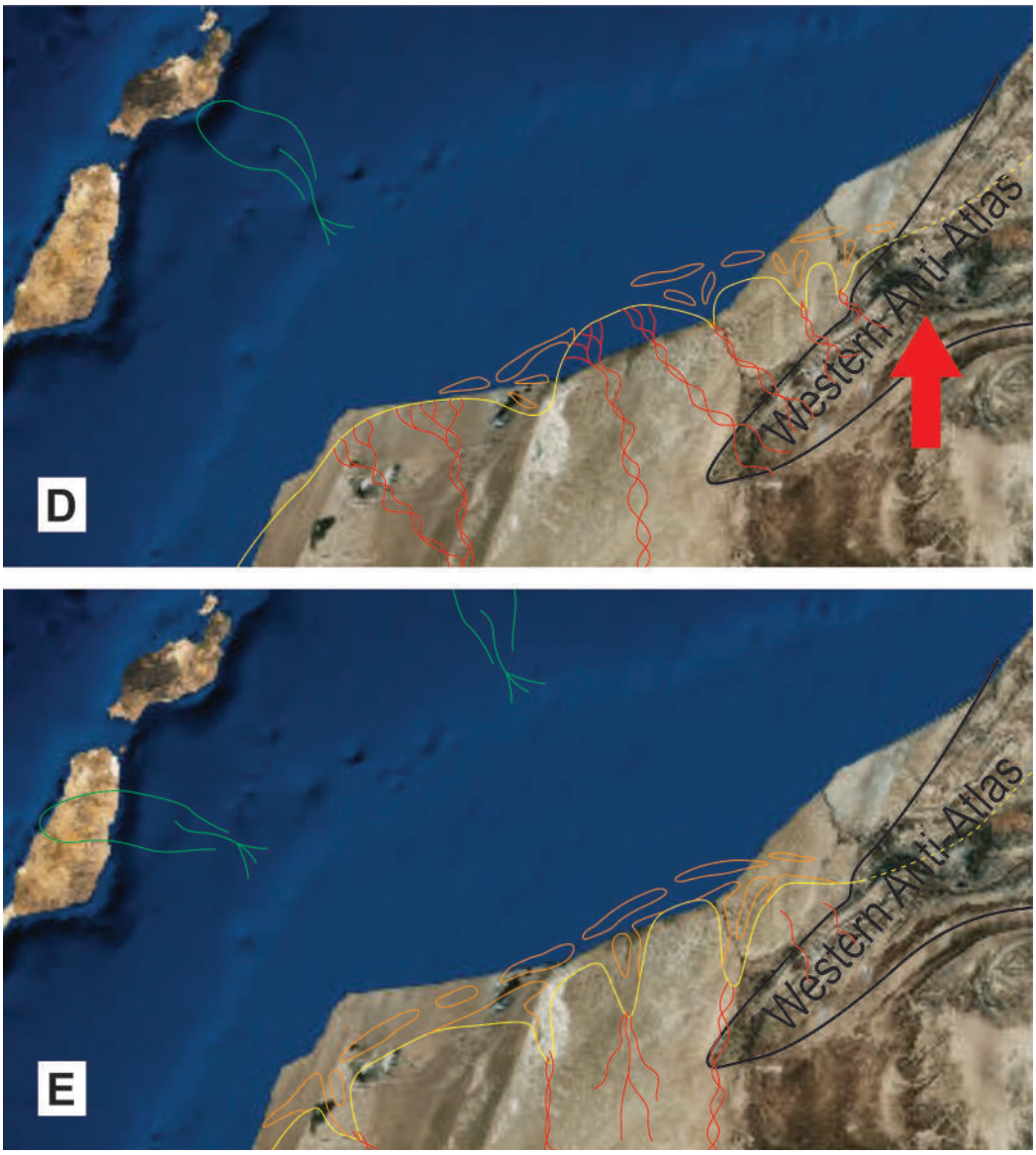

Figure 3.10. Reconstructions of the position of the shoreline at five stages during the evolution of the Tanta system. A) Reconstruction during deposition of the Red Conglomerates Member, during Berriasian. B) Reconstruction at the MFS1. C) Reconstruction at the MFS2. D) Reconstruction at the top of parasequence P12. E) Reconstruction during deposition of the White Sandstone Member of Albian age. Blue line: Jurassic shelf edge; Red lines: rivers and streams; Yellow lines: shoreline; Orange lines: tidal sand flats and barriers; Green lines: deep water fans; Red arrow: uplift of the basementof the Anti-Atlas.

The lowermost unit of the Tantan Fm. in the study area is the Red Conglomerates Member. This unit is on the flank of the Anti-Atlas and in the Oued Draa area can be related with a faulted contact that was probably responsible for creating the topography necessary for the deposition of the alluvial fans. Red conglomerates were also found at the base of lower Cretaceous continental successions in the proximal onshore well EA-1 (Figure 3.3). Deposition of these facies is related with topographic highs in the Anti-Atlas created by tectonic uplift and faulting, together with a relative sea-level fall. The available exposures integrated with well data allow a reconstruction of the

palaeogeography onshore (Figure 3.10A). In this interpretation the coastal plain and inner shelf would be areas of mainly bypass and possibly incision. A thin shallow marine succession is deposited close to the edge of the Jurassic carbonate platform (Wenke et al., 2011). Submarine canyons and associated slope fans develop at the front of the slope.

The main Tantan delta is interpreted to have prograded out mainly during the LST (Figure 3.9). The main source of sediment during this period of time was probably from the Reguibat Shield. A transgressive surface (TS1) marking the beginning of the TST is amalgamated with the SB at Oued Chebeika (SB1 + TS1; Figure 3.9). The uppermost part of the Red Basal Sandstone Member represents a valley fill, deposited in a transgressive regime in a very proximal setting. As a result, the sediments are back-stepping and onlapping onto the Anti-Atlas (Figure 3.10B).

A significant transgression occurred in the area in the Aptian, with thick marine mudstone deposited over a wide area. The extension inland is unknown, but it is possible that the westernmost part of the Anti-Atlas was covered by this event (Figure 3.10C).

Significant volumes of sediment were delivered during deposition of the HST represented by the Red Upper Sandstone Member. The accommodation was filled by significant amount of sand onshore and mud offshore. Discharge patterns suggest sediment was eroded from an uplifted Western Anti-Atlas and possibly the Reguibat Shield, (Figure 3.10Figure 3.10D).

The transgression continued through the Early Albian and the Tantan delta had retreated significantly. The time-equivalent sections exposed along the Oued Draa are made of marine facies. Along the Oued Chebeika transect extensive peritidal sand flats developed (Figure 3.10Figure 3.10E).

3.7 Conclusions

An outcrop-based study of the Tantan Fm., and lowermost Aguidir Fm., of the northern Aaiun-Tarfaya Basin has been performed for the first time since it was originally described in the late 1960's. Several sections have been logged along two sub-parallel transects, following the main two rivers in the area (i.e. Oued Draa and Oued Chebeika). Correlation shows that lateral equivalent lithounits represent more distal depositional environments at Oued Draa (north) than at Oued Chebeika (south).

An outcrop-based sequence stratigraphic framework has been established with four depositional sequences, and used to correlate with the distal offshore. Available new biostratigraphic data have been fed into this framework in order to better constrain the main episodes in the evolution of the Tantan system. Accumulation of sediment in the basin has been controlled by the interplay between basin subsidence, vertical movements in the basement and eustacy. An updated and more refined lithostratigraphic subdivision in six members is proposed, incorporating the members originally defined by Martinis and Visintin in 1966:

i) *Red Conglomerates Member*. Composed of red conglomerates derived from the Western Anti-Atlas and deposited as alluvial fans as result of differential subsidence of the basement and the basin accommodated by normal faults. These facies are also identified in wells drilled onshore farther south of the study area. Correlation with seismic interpreted offshore and sedimentary trends in the distal turbidites of Fuerteventura give a Berriasian age for deposition of this member. It represents the falling stage systems tract (FSST) and it is capped by a sequence boundary (SB1).

ii) *Red Basal Sandstone Member*. Crossbedded sandstones and silts deposited as fluvial bars, channels and flood plain deposits. The upper part at Oued Draa transect is represented by peritidal sandstones and muds correlated with fluvial facies at Oued Chebeika. The sediment provenance area for this unit is located to the south, at the Reguibat Shield and Mauritanides. Strong differential subsidence from north to south has accommodated more than 300 m of sediments in the north and less than 80 m in the south. This member represents a complete depositional sequence with a thick LST overlain by a TST and HST. Its lower boundary is the SB1 at Oued Draa and, an amalgamated sequence boundary and transgressive surface at Oued Chebeika (SB1 + TS1). A Valanginian to Barremian age is assumed for this member.

iii) *Draa Marls Member*. It is composed of marine sandstones, silts and limestones with variable fossil content. The age inferred from new faunas and literature is Aptian. This unit represents an important flooding event in the area, well recorded by marine facies along both transects. Its base it is delimited by an amalgamated sequence boundary and transgressive surface (SB2 + TS2). A maximum flooding surface within this unit marks the limit between the TST and the overlying HST.

iv) *Red Upper Sandstone Member*. Similar sedimentary facies to the Red Basal Sandstone Member along Oued Chebeika transect and more distal peritidal to shallow marine along Oued Draa. It was deposited during the Aptian when an exhumation pulse uplifted the Western Anti-Atlas to the SE. The Anti-Atlas sediment source is supported by a consistent change in

palaeocurrents. It constitutes a thick (>100 m) HST, capped by an amalgamated sequence boundary and transgressive surface (SB3 + TS3).

v) *White Sandstone Member*. Peritidal crossbedded sandstones and minor silts along Oued Chebeika passing into marine clastics and minor carbonates at Oued Draa were deposited probably during early Albian. It is the beginning of the last depositional sequence that starts with the TST and extends until the end of the sections exposed along the river.

vi) *Yellow Upper Sandstone Member*. Marine clastics and carbonates of late Albian age only exposed along Oued Chebeika. It is the last member of the Tantan Fm.

vii) *Oued Chebeika Clay Member*. It belongs to the overlying Aguidir Fm. Made of black clays and marls deposited in an offshore environment during latest Albian to Cenomanian.

3.8 References

Ali, S., Stattegger, K., Garbe-Schönberg, D., Frank, M., Kraft, S., Kuhnt, W., 2014a. The provenance of Cretaceous to Quaternary sediments in the Tarfaya basin, SW Morocco: Evidence from trace element geochemistry and radiogenic Nd–Sr isotopes. J. African Earth Sci. 90, 64–76. doi:10.1016/j.jafrearsci.2013.11.010

Ali, S., Stattegger, K., Garbe-Schönberg, D., Kuhnt, W., Kluth, O., Jabour, H., 2014b. Petrography and geochemistry of Cretaceous to quaternary siliciclastic rocks in the Tarfaya basin, SW Morocco: Implications for tectonic setting, weathering, and provenance. Int. J. Earth Sci. 103, 265–280. doi:10.1007/s00531-013-0965-6

Ambroggi, R., 1963. Étude géologique du versant méridional du Haut Atlas occidental et de la Plaine du Souss. Notes Mém. Serv. Géol. Maroc 157, 1–321.

Choubert, G., Faure-Muret, A., Hottinger, L., 1966. Aperçu géologique du bassin côtier de Tarfaya, in: Le Bassin Côtier de Tarfaya (Maroc Méridional). Notes et Mém. Serv. Géol. Maroc, 175.

Collignon, M., 1967. Les ammonites crétacées du bassin côtier de Tarfaya, Sud marocain. C. R. ACAD. Sc. PARIS 264, 1390–1392.

Collignon, M., 1966. Les céphalopodes crétacés du bassin côtier de Tarfaya: relations stratigraphiques et paléontologiques, in: Notes et Mém. Serv. Géol. Maroc, 175. pp. 10–149.

Daidu, F., Yuan, W., Min, L., 2013. Classifications, sedimentary features and facies associations of tidal flats. J. Palaeogeogr. 2, 66–80.

doi:10.3724/SP.J.1261.2013.00018

El Mostaine, M., 1991. Evaluation du potentiel pétrolier du bassin de Tarfaya-Laayoune onshore.

Freneix, S., 1972. Les mollusques bivalves crétacés du bassin côtier de Tarfaya (Maroc méridional). Notes Mémoires du Serv. géologique du Maroc 228, 49–255.

Gouiza, M., Bertotti, G., Andriessen, P., 2017a. Mesozoic and Cenozoic thermal history of the western Reguibat Shield (West African Craton). Terra Nov.

Gouiza, M., Charton, R., Bertotti, G., Andriessen, P., Storms, J.E.A., 2017b. Post-Variscan evolution of the Anti-Atlas belt of Morocco constrained from low-temperature geochronology. Int. J. Earth Sci. 106, 593–616. doi:10.1007/s00531-016-1325-0

Haq, B.U., Hardenbol, J., Vail, P.R., 1987. Chronology of fluctuating sea levels since the triassic. Science 235, 1156–1167. doi:10.1126/science.235.4793.1156

Herngreen, G.F.W., Kedves, M., Rivina, L.V., Smirnova, S.B., 1996. Palynology: Principles and Applications, in: Jansonius, J., McGregor, D.C. (Eds.), Cretaceous Floral Provinces: A Review. American Association of Stratigraphic Palynologists Foundation, pp. 1157–1188.

Hollard, H., Choubert, G., Bronner, G., Marchand, J., Sougy, J.M.A., 1985. Carte géologique du Maroc; Echelle: 1/1000 000. Notes Mém. Serv. Géol. Maroc 260.

Kotetishvili, E.V., Kvantaliani, I.V., Kakabadze, M.., Tsirekidze, L.R., 2005. Atlas of early Cretaceous fauna of Georgia. Georgian Academy of Sciences, Proceedings, New Series 120.

Luber, T.L., Bulot, L.G., Redfern, J., Frau, C., Arantegui, A., Masrour, M., 2017. A revised ammonoid biostratigraphy for the Aptian of NW Africa: Essaouira-Agadir Basin, Morocco. Cretac. Res. doi:10.1016/j.cretres.2017.06.020

Martinis, B., Visintin, V., 1966. Données géologiques sur le bassin sédimentaire côtier de Tarfaya (Maroc méridional), in: Reyre, D. (Ed.), Bassin Sedimentaires Du Littoral Africain. Union Internationale des sciences géologiques, Paris, pp. 13–26.

Miall, A.D., 2006. The geology of fluvial deposits; sedimentary facies, basin analysis, and petroleum geology, 4th ed. Springer Verlag Berlin Heidelberg.

Olariu, C., Steel, R.J., Dalrymple, R.W., Gingras, M.K., 2012. Tidal dunes versus tidal bars: The sedimentological and architectural characteristics of compound dunes in a tidal seaway, the lower Baronia Sandstone (Lower Eocene), Ager Basin, Spain. Sediment. Geol. 279, 134–155. doi:10.1016/j.sedgeo.2012.07.018

Plint, A.G., Nummedal, D., 2000. The falling stage systems tract: recognition and importance in sequence stratigraphic analysis, in: Hunt, D., Gawthorpe, R.L. (Eds.), Sedimentary Responses to Froced Regressions. Geological Society, London, Special Publications, pp. 1–17. doi:10.1144/GSL.SP.2000.172.01.01

Posamentier, H.W., Vail, P.R., 1988. Eustatic controls on clastic deposition II - Sequence and systems tract models, in: Sea-Level Changes. pp. 125–154. doi:10.2110/pec.88.01.0125

Rey, J., Carenot, B., Peybernès, B., Taj-Eddine, K., Rahhali, I., Thieuloy, J.P., 1986a. Le Crétacé inférieur de la région d'Essaouira: données biostratigraphiques et évolutions sédimentaires. Rev. la Fac. des Sci. Marrakech, Numer. spécial 2 413–439.

Rey, J., Carenot, B., Rocher, A., Taj-Eddine, K., Thieuloy, J.P., 1986b. Le Crétacé inférieur sur la versant nord du Haut-Atlas (région d'Imi n'Tanout et Amizmiz) données biostratigraphiques et évolutions sédimentaires. Rev. la Fac. des Sci. Marrakech, Numer. spécial 2 393–441.

Schrank, E., Ibrahim, M.I.A., 1995. Cretaceous (Aptian-Maastrichtian) palynology of the foraminifera-dated wells (KRM-1, AG-18) in northwestern Egypt. Berliner Geowissenschaftliche Abhandlungen 177, 1–44.

Snedden, J.W., Liu, C., 2010. A Compilation of Phanerozoic Sea-Level Change , Coastal Onlaps and Recommended Sequence Designations. Am. Assoc. Pet. Geol. Search Discov. Artic. 40594 40594, 2004–2006.

Todd, R.G., Mitchum, R.M., 1977. Seismic Stratigraphy and Global Changes of Sea Level: Part 8. Identification of Upper Triassic, Jurassic, and Lower Cretaceous Seismic Sequences in Gulf of Mexico and Offshore West Africa, in: Applicaton of Seismic Reflection Configuration to Stratigraphic Interpretaton. pp. 145–163.

Vail, P.R., 1987. Seismic Stratigraphy Interpretation Using Sequence Stratigraphy Part I : Seismic Stratigraphy Interpretation Procedure. AAPG Stud. Geol. 27, Vol. 1 Atlas Seism. Stratigr. 1, 1–10. doi:-

van Wagoner, J.C., Posamentier, H.W., Mitchum, R.M., Vail, P.R., Sarg, J.F., Loutit, T.S., Hardenbol, J., 1988. An overview of the fundamentals of sequence stratigraphy and key definitions, in: Wilgus, C.K., Posamentier, H.W., Ross, C.K., Kendall, C.G.S.C. (Eds.), Sea-Level Changes: An Integrated Approach. SEPM Society for Sedimentary Geology, Tulsa, pp. 39–45. doi:10.2110/pec.88.01.0039

von Rad, U., Einsele, G., 1980. Mesozoic-Cainozoic Subsidence History and Palaeobathymetry of the Northwest African Continental Margin (Aaiun Basin to D. S. D. P. Site 397). Philos. Trans. R. Soc. A Math. Phys. Eng. Sci. 294, 37–50. doi:10.1098/rsta.1980.0010

Wenke, A.A.O., Zühlke, R., Jabour, H., Kluth, O., 2011. High-resolution sequence stratigraphy in basin reconnaissance: example from the Tarfaya Basin, Morocco. first Break 29, 85–96.

Whittaker, A., Cope, J.C.W., Cowie, J.W., Gibbons, W., Hailwood, E.A., House, M.R., Jenkins, D.G., Rawson, P.F., Rushton, A.W.A., Smith, D.G., Thomas, A.T., Wimbledon, W.A., 1991. A guide to stratigraphical procedure. J. Geol. Soc. London. 148, 813–824. doi:10.1144/gsjgs.148.5.0813

Chapter 4

Predicting Early Cretaceous deepwater turbiditic successions in the offshore Aaiun-Tarfaya Basin, southern Morocco: constraints from new data from Fuerteventura

Predicting Early Cretaceous deepwater turbiditic successions in the offshore Aaiun-Tarfaya Basin, southern Morocco: constraints from new data from Fuerteventura

A. Arantegui, T. Luber, J. Redfern, L. Bulot

Keywords: Turbidites, Ammonite, Tarfaya Basin

4.1 Abstract

This paper re-examines the sedimentology and biostratigraphy of the Early Cretaceous Main Clastic Unit (Steiner et al., 1998) exposed in Fuerteventura, and provides a correlation to the proximal equivalent of the system onshore Morocco, in order to assess the implications for the petroleum system and potential reservoir distribution.

Lower Cretaceous coarse clastic-dominated continental to shallow-marine successions are extensively exposed in the onshore Aaiun-Tarfaya Basin, Morocco. The deep-water distal counterpart of these systems are less well-documented, and only exposed on Fuerteventura, where they have been exhumed by tectonic uplift associated with volcanism that built the islands. The studied section is dated as pre-late Berriasian based on previous work and the discovery of a well-preserved ammonite as part of this study. It is made of thin bedded clastic turbidites with occasional coarser and thicker bedded intervals exposed in a succession of overturned and sub-vertical outcrops, intruded by igneous bodies, with local repetitions of the succession due to tectonic folding.

Three large-scale cycles can be identified; two coarsening-upward, interpreted to represent the progradation of lower and middle lobes of a large submarine fan and an overall fining-upward cycle with increasing contribution of calciturbidites and limestone beds. The latter is interpreted to reflect the sea-level rise during Aptian and Albian times and the associated development of carbonates on the shelf, resedimented into the deep basin as calciturbidites.

The sand content in the lower of the three cycles can reach up to 95%, deposited as high density turbidites. This can be correlated with the lowstand wedge seen in seismic attached, draping the older Jurassic carbonate platform. Detailed logging and new biostratigraphy further constrains understanding of these depositional systems and their evolution, helping to reduce uncertainty in exploration for these important reservoir systems that are targets for offshore.

4.2 Introduction

The early Cretaceous is a time of significant clastic delivery in southern Morocco associated with the Tantan delta. Thick clastic-dominated continental and shallow marine succession of the Tantan Fm. (Martinis and Visintin, 1966) are well exposed onshore and have also been drilled by exploration wells. On the present day shelf, seismic and wells drilled during decades of hydrocarbon exploration also provide data on the sedimentology.

Although there are three non-commercial discoveries in the offshore basin, suggesting an effective petroleum system, the distribution, quality and potential of associated deep marine clastic reservoirs is poorly understood. The Mesozoic succession offshore in the Aaiun-Tarfaya Basin exceeds 10 km (Hinz et al., 1982; Ranke et al., 1982). Record of the lower Cretaceous distal equivalents of the onshore and shallow shelf deposits is limited to a few wells drilled by the IODP/DSDP program, partial penetrations by commercial wells on the continental slope and the Mesozoic succession exposed in the volcanic island of Fuerteventura (Canary Archipelago, Spain).

The Cretaceous sequence on Fuerteventura was first recognised in the 19th century (e.g. Hartung, 1857) and its stratigraphy and true deep-marine origin established by Robertson and Stillman, (1979) and Robertson, Alastair and Bernoulli, (1982). Due to the challenges posed by the high level of igneous intrusions and thermal metamorphism, a detailed stratigraphy was not presented until Steiner et al., (1998) defined five units ranging from Toartian to Campanian in age.

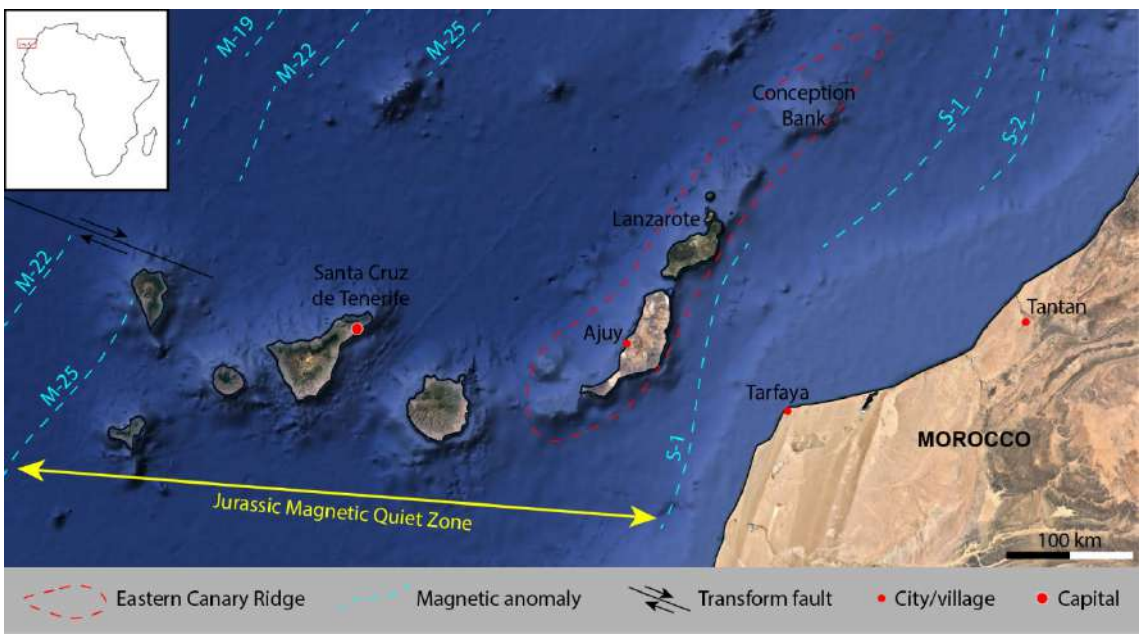

Figure 4.1 (Previous page). Location map and main tectonic elements of the Canary Islands. Satellite image taken from GoogleEarth™. Magnetic anomalies and oceanic transform faults after Steiner et al., 1998.

The aim of this paper is revisiting the lower Cretaceous interval of the succession (Main Clastic Unit of Steiner et al., 1998) in order to improve the sedimentology, biostratigraphy, its link with the proximal equivalent of the system offshore Morocco and its importance as a potential reservoir.

4.3 Study area

The Canary Islands is an archipelago composed of seven volcanic islands off the west coast of Morocco (Figure 4.1.) stretching for 450 km along an E-W direction. The archipelago sits on the passive margin within the Jurassic Magnetic Quiet Zone. Four main hypotheses have been invoked to explain the genesis of the Canary archipelago; propagating oceanic fractures (Anguita and Hernan, 1975), local extensional ridges (Fúster, 1975) or uplifted tectonics blocks (Araña, V., Ortiz, 1986) hypotheses and a mantle plume hypothesis (Morgan, 1971) that has been invoked extensively for the Canary Islands (e.g. (Carracedo et al., 1998; Holik et al., 1991). All of these hypotheses have limitations and most recently Anguita and Hernán (2000) combined some of them into an integrated model (Figure 4.2).

A feature that the Canaries share with other volcanic islands groups is that in the most complete sections up to three genetic units can be identified, i) turbiditic basal complexes, intruded by swarms of dykes, ii) shield edifices and iii) post-shield cones. Each one of these units is consistently older in the eastern islands of the archipelago than their comparable units on the west.

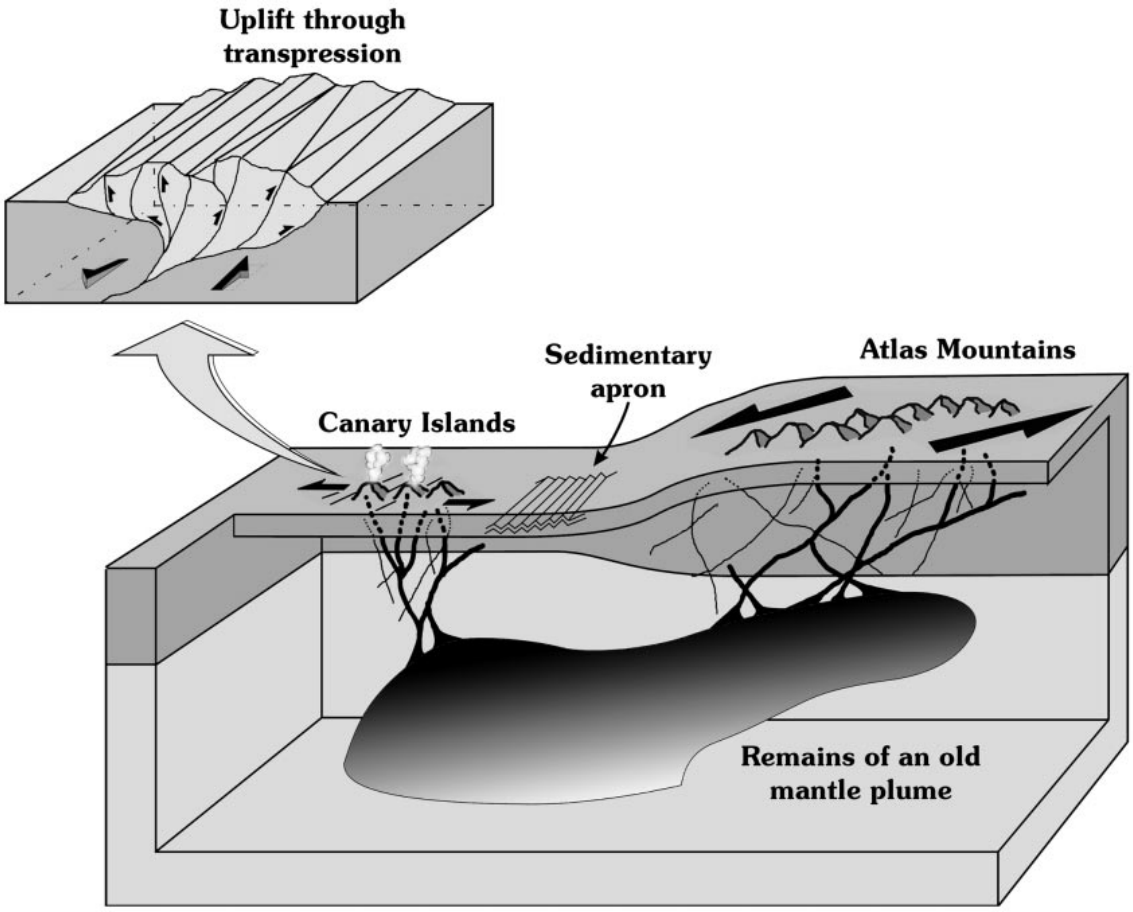

Figure 4.2. Genetic model for the formation of the Canary archipelago. From (Anguita and Hernán, 2000).

The closest island to the African continent is Fuerteventura, which lies approx. 100 km ENE from the coastal city of Tarfaya (Figure 4.1.). It is the second largest island in the archipelago with an elongated NE-SW shape aligned with the island of Lanzarote extending into the submarine structure of Conception Bank. Together they form the volcanic structure of the Eastern Canary Ridge (Figure 4.1.). The volcanic history of Fuerteventura can be traced to the Late Cretaceous (80 my; Le Bas et al., 1986).

The Basal Complex of Fuerteventura (Stillman et al., 1975) is best exposed on the central west side of the island, in the Betancuria Massif (Figure 4.3). They consist of a Mesozoic deep marine sedimentary succession (Robertson, Alastair and Bernoulli, 1982; Robertson and Stillman, 1979; Steiner et al., 1998) intruded by several generations of dykes, sills and plutons, unconformably overlain by volcanics.

The pre-volcanic sedimentary succession of Fuerteventura has been studied since the 19th century (e.g. Hartung, 1857; von Fritsch, 1868). Initially interpreted as Palaeozoic shallow-water sediments, the age of the sedimentary succession was later revised to

Mesozoic and placed within a shallow continental shelf environment (Rothe, 1968). The succession was thought to be repeated by a major east-west-trending isoclinal syncline (Figure 4.4). The succession was reinterpreted in the last decades of the 20th century as representing deep-water sedimentation (Robertson, Alastair and Bernoulli, 1982; Robertson and Stillman, 1979; Steiner et al., 1998). The succession crops out in a series of subvertical and overtuned outcrops (Figure 4.4 and Figure 4.5). Polarity of sedimentary structures and dating with microfossil assemblages and ammonites has demonstrated that the succession youngs towards the north (Renz et al., 1992; Robertson, Alastair and Bernoulli, 1982; Steiner et al., 1998). The exposed Mesozoic succession exceeds 1500 m in thickness and has been subdivided into several units (Robertson and Stillman, 1979; Rothe, 1968; Steiner et al., 1998). Five sedimentary units (Figure 4.3 and Figure 4.5) were defined by Steiner et al., (1998) and summarised below:

Basal unit: This is the lowermost unit and mainly crops out in the SW part of the area near the Playa de los Muertos and the Barranco del Aulagar (Figure 4.3). It is subdivided in a basalt- and a sediment-dominated sub-unit. The cumulative thickness of basalt in the lower sub-unit, interbedded with siltstones and claystones, was reported to range between 63 m and 320 m.

The upper sub-unit is 130-150 m thick and composed of thinly bedded dark claystones and yellow siltstone, interpreted to represent turbidite deposition from the lower lobes of a deep-sea fan. The siliciclastic succession is punctuated by limestone beds in the lower part, which are absent in the middle and then replaced by calcareous turbidites towards the upper 30 m.

Pelagic Bivalve Limestone Unit: This unit consist of 120 to 150 m of limestones, claystones and marlstones. Bioclastic or nodular limestones are recorded to alternate with green marls in the lower 50-60 m. Up-section, distal turbidites, with a SE-NW palaeoflow direction, become more frequent. The uppermost interval is dominated by marlstones and claystones. This unit is interpreted to have been deposited between the lower slope and abyssal plain above the CCD. This unit has been dated as Toarcian to Oxfordian based on the presence of *Bositra buchi* (Roemer, 1836).

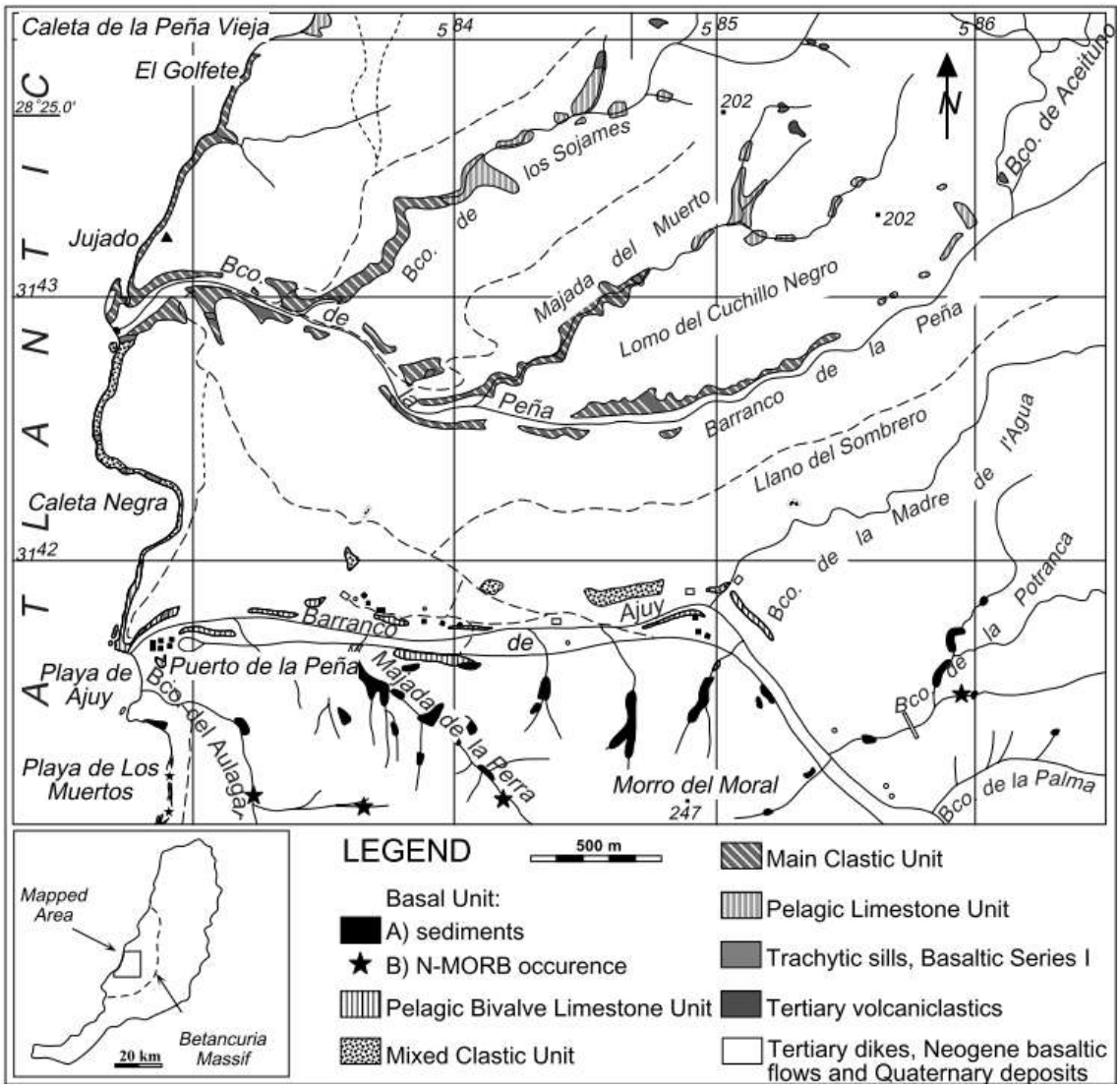

Figure 4.3. Main depositional and igneous units in the Betancuria Massif. (From Steiner et al., 1998)

Mixed Clastic Unit: This is exposed along the coast and it is reported by Steiner et al., (1998) to be 470 m thick. Sedimentation is dominated again by clastic sandy turbidites and claystones with occasional green marlstones and black shales. Two calciturbidites are intercalated in this unit. The overall deposional environment was interpreted to exhibit a progradation from a lower fan at the base to upper fan and slope at the top. Steiner et al., (1998) suggests a Tithonian to early Valanginian age based on the age of the base of the overlying unit, fauna and flora assemblages and facies correlation with the DSDP Site 370/416.

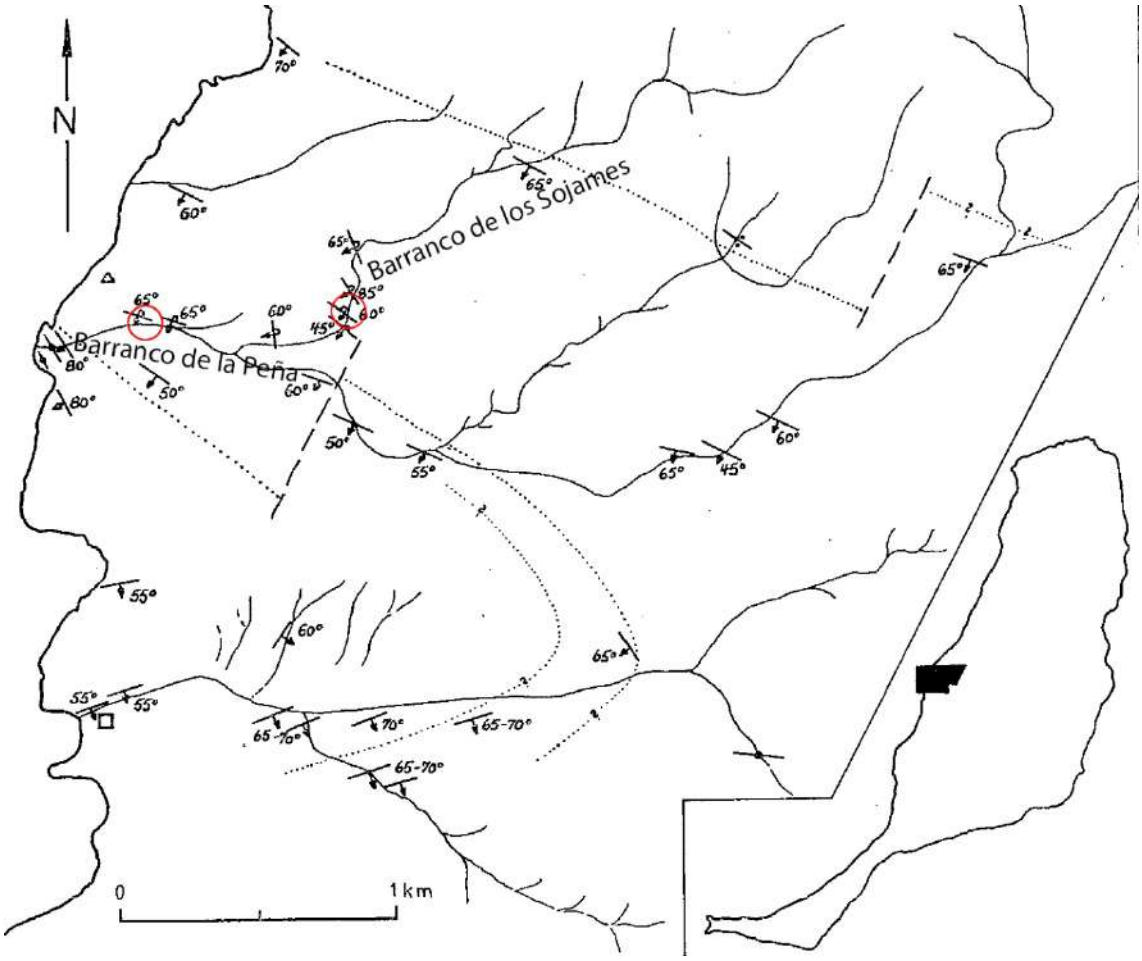

Figure 4.4. Map of the study area showing previous interpretation of repeated succession by overturned syncline. Red circles indicate the approximate locations where folds have been found in the present study. Modified from (Rothe, 1968).

Main Clastic Unit: This unit is mainly exposed along the Barranco de la Peña and Barranco de los Sojames. The unit is made of 600 m of sandy turbidites subdivided in two sub-units.

The lower sub-unit is made of poorly developed fining- and thinning-upward cycles, approx. 10 m thick, of facies C, D and E (*sensu* Howell and Normark, 1982) interpreted as middle fan fringe to outer fan. Upsection, both beds and cycles get thicker and coarser. The trend changes to coarsening- and thickening-upward cycles around 30 m thick representing progradation of sand lobes. A 40 m thick cycle of amalgamated sandstones showing a fining- and thinning-upward trend represents the filling of a middle fan channel. The unit is capped by 100 m of thinly bedded claystones, siltstones and sandtones of interchannel or outer fan fringe setting. The overall evolution of the

subunit shows progradation from lower fan into middle fan and return to quiet sedimentation of outer fan or interchannel.

The upper sub-unit represents more proximal upper and middle fan facies. One meter thick amalgamated turbidites are interpreted as an upper fan feeder channel. Intercalated thin-bedded turbidites and slumps with small cm-scale channel are characteristic of levee deposits. This interval is capped by sandy debris-flow or shale-clast conglomerates. The last 100 m is made of claystone and siltstone with occasional thin sandy turbidites.

The age of the base of the unit is constrained by the presence of a *Neocomites* Uhlig, 1906, Valanginian to Hauterivian in age (Renz et al., 1992). The top, by the Albian to Cenomanian next unit.

Pelagic Limestone Unit: This unit is made of 150 m of Albian to Cenomanian slope chalk deposits.

4.4 Methodology

The Mesozoic turbidites of Fuerteventura have been studied along two easily accessible transects along the Barranco de la Peña and Barranco de los Sojames (Figure 4.3). Data collection involved detailed sedimentary logging of the upper part of the Mixed Clastic Unit, the Main Clastic Unit and the base of the Pelagic Limestone Unit. The thickness of the main dykes and % of small-scale intrusions was recorded. Samples for biostratigraphy were also collected.

4.5 Results and discusion

A 1182 m thick stratigraphic log has been produced. This includes a high density of igneous intrusions that have increased the true thickness of the sedimentary succession considerably. The record of the main igneous units along with an estimation of the density of smaller bedding-parallel igneous dykes has been taken into account in order to calculate the true thickness of the section of 708 m (see details below).

Our observations confirm the previous overall interpretation of the stratigraphy and main depositional environments. The Main Clastic Unit has been subdivided into smaller “Divisions” based on the amount of igneous intrusions and sand/mud ratio along. The density of intrusions is uneven along the succession, ranging from negligible to up to 100%. Several generations of dykes, with different orientations, intrude the sediments, ranging from parallel to perpendicular to the bedding, generating different

rates of expansion in the sedimentary host. Swarms of smaller cm-scale dykes may also have a significant effect on the total thickness, but these are difficult to measure accurately in the field.

The estimated thickness of each "Division" has been calculated by subtracting the thickness of dykes from the total thickness measured in the field. A structural map with the main outcrops mapped is presented on Figure 4.5. The stratigraphic log presented in Figure 4.6 represents the total thickness measured in the field, including the igneous intrusions.

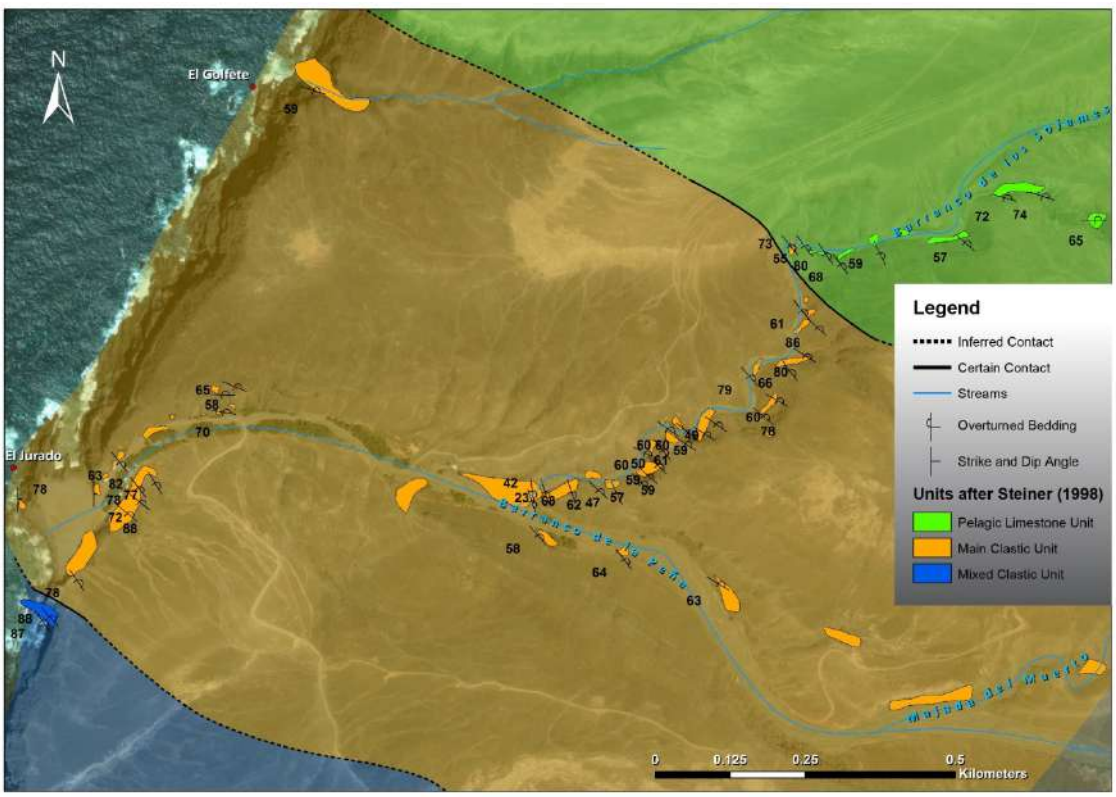

Figure 4.5. Sedimentary units mapped and structural information collected during fieldwork for the present study

Figure 4.6 (Next page). Stratigraphic log along Barranco de la Peña and Barranco de los Sojames. Divisions are explained in the text. Palaeoflow directions based mainly on current marks and minor crossbedding. Thicknesses shown corresponds to the total thicknesses measured in the field including the igneous intrusions

Mixed Clastic Unit

Subunit1 | Subunit 2 | Subunit 3 | Subunit 4 | Subunit 5 | Subunit 6

0 50 100 150 200 250 300 350 400 450 500 550 568

clay
silt
vf sand
f sand
m sand
c sand
vc sand
pebble

Subunit 7 | Subunit 8 | Subunit 9 | Subunit 10 | Subunit 11 | Subunit 12

568 600 650 700 750 800 850 900 950 1000 1050 1100 1126

clay
silt
vf sand
f sand
m sand
c sand
vc sand
pebble

Pelagic Limestone Unit

1126 1150 1183

clay
silt
vf sand
f sand
m sand
c sand
vc sand
pebble

N:G - CARBONATES

- Carbonate-prone
- 0-25% sand
- 26-50% sand
- 51-75% sand
- >75% sand

MAIN LITHOLOGY

- Mud-dominated
- Mud-prone
- Mud/Sand
- Sand-prone
- Sand-dominated
- Sand
- Sand/limestone
- Sand/mud/limestone
- Igneous intrusions

LEGEND

- Channel
- Erosion
- Flaser bedding
- Lenticular bedding
- Cross-bedding
- Ripples
- Current marks
- Undulating lamination
- Horizontal lamination
- Load casting
- Dewatering
- Mud clasts
- Granules/pebbles
- Bioturbation
- Ammonite
- Tectonic fold

4.5.1 Stratigraphy and sedimentology of the lower Cretaceous turbidites

4.5.1.1 Mixed Clastic Unit:

Only the uppermost 5 m of this Unit were logged. It is composed of cm thick rippled-laminated and occasionally parallel-laminated fine-grained calcareous sandstones, siltstone and claystone, displaying Tbcde turbidite divisions (Bouma, 1962), interpreted to be deposited by low density turbidity currents (*sensu* Lowe, 1982). Flute marks and small channels (Figure 4.7A) are relatively common. Interbedded debris-flows are scarce. The calciturbidites are interpreted as redeposited material derived from a carbonate platform, and deposited in an upper fan to slope setting.

Fossil assemblages yield an age ranging from Tithonian to early Valanginian for the top of this Unit, and suggest a Berriasian age (Steiner et al., 1998).

4.5.1.2 Main Clastic Unit:

The new study suggests the Main Clastic Unit, including igneous intrusions, is about 950 m-thick. Estimation of the igneous intrusions present in the section (as % of total thickness) yields an estimated total depositional thickness for this unit of 708 m (see details for each division below). The total thickness of this unit is about 15% higher than previously reported, which, due to the complexity induced by the level of intrusions, we consider within the error margin. It has been subdivided in 12 subdivisions, annotated in the stratigraphic log with a colour code (Figure 4.6).

Subunit 1

A 60 m thick igneous intrusion marks the base of this subunit from the underlying Mixed Clastic Unit. The gross measured thickness is 25 m, with a calculated true thickness of 22 m. It is highly affected locally by dyke swarms, but only about 10% of them have an influence on the thickness of the sedimentary deposits. Net sand content is 25%.

It is mainly made of cm-thick light to dark mudstones interbedded with very fine- to fine-grained sandstones, occasionally up to 15 cm thick. Bouma units Tcd, occasional Tb and rare Ta can be identified, suggesting deposition by low density turbidity currents. Sedimentary structures include mud rip-up clasts, slumps, parallel-, wavy- and ripple-laminations. It is organized in two m-scale coarsening-upwards cycles with Tcd more common at the base and Tabc more common towards the top, suggesting

progradation of lobes (*sensu* Prelat et al., 2009). Sedimentation is interpreted to have taken place as overbank or levee deposits on a deep-water lobe fringe.

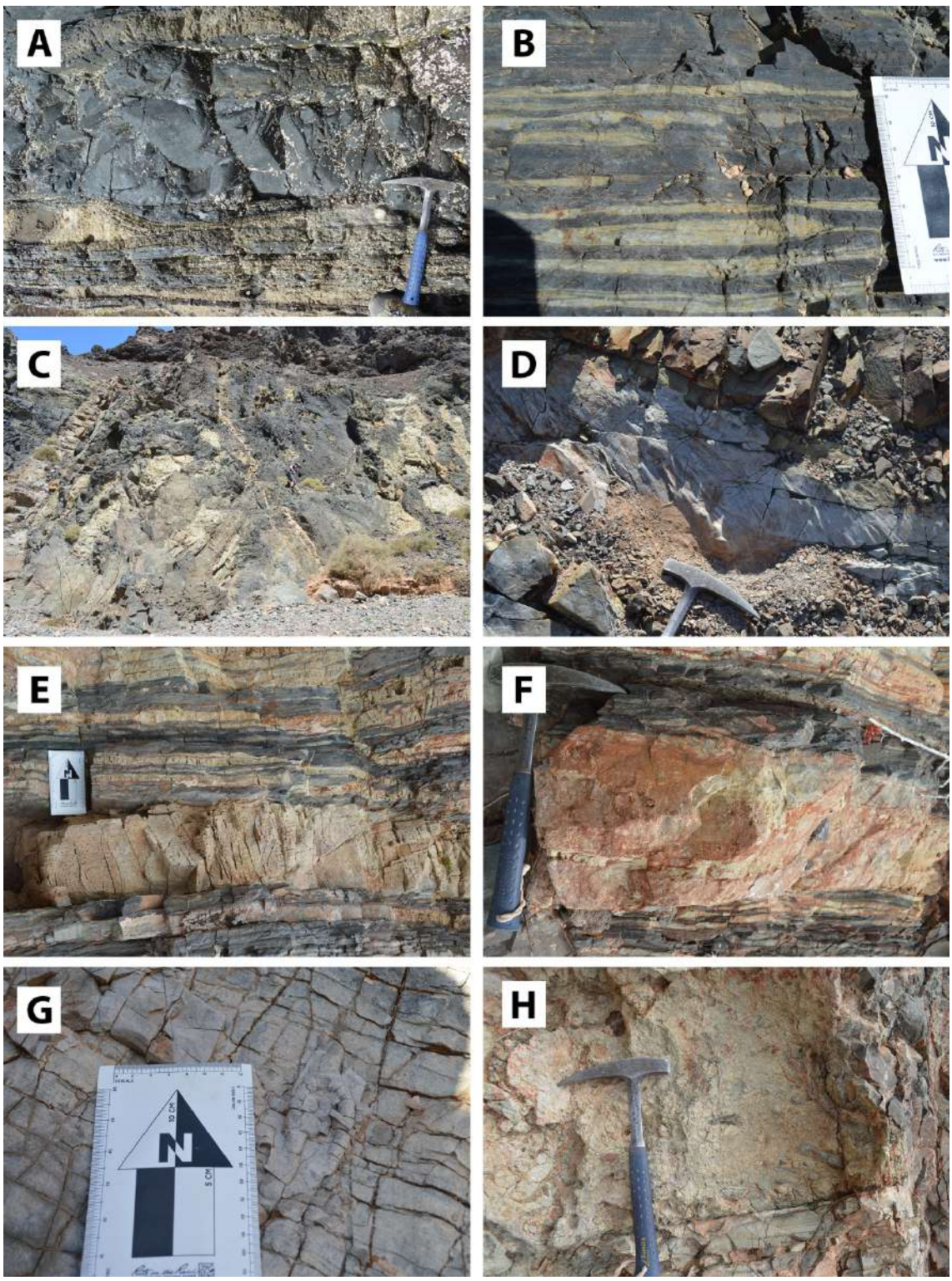

Figure 4.7. Field photographs of several details throughout the succession. A) Small-scale channel from the uppermost Mixed Clastic Unit. B) Mud-dominated interval of thinly bedded turbidites of subunit 2 with ripples and lenticular bedding. C) Outcrop photograph of subunit 3. Note the high degree of igneous intrusions and discontinuity of outcrops. Mean stratigraphy-up is towards the right of the image. D) Detail of palaeocurrent indicators preserved as a positive relief on the base of an overturned bed.

Subunit 2

The base of this subunit is a 3.7 m-thick dyke. About 35% is composed of igneous rocks, that increases the true thickness of 125m up to a measured thickness of 193 m. Occurrence of thick dykes between 2.5 and 20 m-thick becomes more frequent toward the top of the division. The average sand content in the whole unit is about 50%.

It is composed mainly of dm- to m-scale thinning- and fining-upward packages in the lower part and thickening- and coarsening-upward packages towards the top. These can be grouped in coarsening- and frequently thickening-upwards m-scale packages up to 23 m thick.

The lower half is mainly made of thin turbidites, displaying Tcde units, comprising intervals of very fine-grained yellow sandstone interbedded with 1 to 6 cm-thick grey to black (occasionally greenish) mudstones. Minor slumps, flaser, lenticular and ripple lamination (Figure 4.7B) and erosion surfaces resembling small-scale channelized flow structures can be observed. It is interpreted to represent deposition in a lower to middle fan setting of unconfined to poorly confined flows.

The upper half becomes slightly more calcareous and displays a coarser grain size. Sedimentary structures present include flute marks and load casts, ripple lamination, soft sedimentary deformation, channels and fossil traces. The thickness of intermittent sandy pulses increases towards the top from 20-30 cm thick beds in the lower and middle part of the division to metre scale beds in the upper part. Palaeocurrents in this interval show a flow direction towards the NW (Figure 4.6). The coarsening-upward trend is interpreted to record progradation of a middle fan over the lower fan and small scale channel sedimentation.

Figure 4.8. Field photographs. A) Mud drapes on cross-lamina. B) Thin-bedded turbidites with lenticular bedding and soft sediment defomation.

Subunit 3

This subunit (Figure 4.7C) has a gross thickness of 75 m. It is intensely intruded by igneous dykes. Intrusions sub-parallel to the bedding reach 70% of the total outcrop reducing the gross thickness of the interval to a true sedimentary thickness of 23 m. The net sand content is 95%.

The subdivision comprises several m-scale fining- and thinning-upward cycles of thick bedded to massive fine- to medium-grained calcareous sandstones. Bouma cycles observed are restricted to Ta. Bed thickness can reach m-scale.

The sedimentary features observed are interpreted to record deposition from high density turbidity currents (*sensu* Lowe, 1982). The high density of igneous intrusions does not allow confident identification of larger-scale trends, however individual fining- and thinning-upward trends probably record the fill of small channels that amalgamate to form a leveed-channel (Arnott, 2010) although the expected fining- and thinning-upward overall trend is not clear. The channel may have constituted a feeder of an active lobe in a middle fan position.

Subunit 4

This subdivision has a gross thickness of 35 m, with a density of igneous dykes of 50%. The true thickness is estimated at 18 m, with a net sand content of 75-80%.

The subunit contains two smaller sub-cycles. The lower one is a thinning- and fining-upward alternation of siltstones and very fine- to fine-grained sandstones, each up to 20 cm-thick. The upper cycle consists of thickening- and fining-upward medium- to fine-grained sandstones, with thicker individual beds than the underlying sub-cycle.

The fining-upward trend is interpreted as small channel fills that form part of a leveed-channel unit. The presence of thinner beds, intervening silts and a higher position in the leveed-channel fill than that interpreted in subunit 3, suggest a more marginal position within the channel unit (Arnott, 2010). Due to the limited extent of the outcrop the base of the channel or channel fill/levee contact is not exposed.

The age of subunits 1 to 4 is constrained to Berriasian by an age-diagnostic ammonite found at the base of subdivision 5 (see below). These subdivisions have the highest sand content in the entire section, and together represent an overall progradation of lower fan into middle fan. A lowstand sedimentary wedge attached to the Jurassic carbonate platform, Berriasian in age (Wenke et al., 2011) represents the more proximal upper fan

to slope setting of this part of the succession exposed in Fuerteventura (Figure 4.10). Onshore Morocco, the continental proximal equivalent is represented by the Red Conglomerates Member exposed at Oued Draa (see Chapter 3). Together, these deposits are the expression of the Berriasian sea-level fall (Haq et al., 1987; Snedden and Liu, 2010) at different locations of the Aaiun-Tarfaya Basin.

Subunit 5

The subdivision has a gross thickness of 33 m and comprises an overall thickening- and coarsening-upward trend. It is not heavily affected by igneous intrusions (estimated 15%) and the estimated true thickness of this interval is 28 m, with a relatively low 15% net sand content

It is mostly made of thinly bedded dark silts and clays with minor sandstones laminae, exhibiting mainly Tde units (Bouma, 1962). These are interpreted to be deposited by low density turbidity currents and suspension fallout. The upper 3m are made of alternating medium- to coarse-grained sandstones and dark siltstones/mudstones, interpreted as Tcde and occasional Tbcd Bouma units. Bioturbation is common and flute casts are also observed, mainly in the finer sub-units.

The change to a coarsening-upward trend, together with the predominance of Tde turbidites suggest overbank deposition in a middle fan position or deposition of unconfined low density turbiditic flows in a lower fan.

An ammonite (*Neocomites* sp.) was reported by Renz et al., (1992) the Main Clastic Unit (Unit D of Robertson and Stillman, 1979), which, together with lithological correlation to the DSDP Site 370/416 (Renz et al., 1992; Steiner et al., 1998) suggested a Valanginian age to be assigned to the base of the Main Clastic Unit. In this current study an ammoniate was found close to the base of this subunit 5, which has been identified as *Tirnovella* sp., (Figure 4.9). The shorter stratigraphic range of this new ammonite, restricted to Late Berriasian, allows us to refine the age of the top of Subdivision 4 to late Berriasian and therefore we suggest a maximum early Berriasian age for the base of the Main Clastic Unit.

Figure 4.9. Field photograph of the *Tirnovella* sp. (late Berriasian).

Subunit 5

The contact with the underlying subunit is a 10 m thick igneous intrusion. Gross measured thickness is 108 m, consisting of mainly grey to greenish clays and silts with subordinate thinly bedded very fine- to fine-grained cm-thick sandstones. The division is moderately affected by dykes (making up 30% of the section) yielding an estimation of the real thickness of 76 m, with overall net sand content of 30%.

Four coarsening- and thickening-upward cycles up to 37 m thick can be identified. Occasional individual heterolithic very fine- to fine-grained sandstone beds can be up to 15 cm-thick. Tcde Bouma divisions dominate this interval, exhibiting ripples, flaser bedding, with erosional contacts and soft sedimentary deformation, abundant sole casts (Figure 4.7D). Bioturbation is more frequent in the lower few metres of the unit.

One thickly-bedded fine-grained sandstone in the lower part of this unit has a variable thickness between 50 to 70 cm, and cuts into the underlying heterolithic bedding. This is interpreted as a small channel cutting into overbank/levee deposits. Another massive to thickly-bedded sandstone, 1.5 m thick, in the middle part of the division is also interpreted as a small channel fill but exposure did not allow observations of cross-cut relationships with the host sediments. The top of this unit includes occasional medium-

to coarse-grained sandstones beds up to 20 cm thick with granules and well developed low angle planar cross-bedding (Figure 4.7E).

Each one of the four cycles is interpreted to represents overbank progradational episodes in the middle fan, occasionally interrupted by small-scale distributive channels feeding more distal lobes.

According to the position of the *Neocomites* sp. described by Renz et al., (1992) we assign a probable Valanginian to Hauterivian age to Subunit 6.

Subunit 7

The Subunit has a gross thickness of 53 m thick and is composed of four thickening- and coarsening-upward packages. The overall trend of the subdivision is fining-upwards and individual cycles thin-upwards. The subdivision is intruded by two thick dykes (in total 3.5 m thick) and a number of smaller dykes, making up an estimated 15% of the interval. The true thickness of sedimentary thickness is 45 m and it has a net sand content of 25%.

The four individual thinning-upward cycles range from 17.5 to 5.5 m thick. Individually they are interpreted to represent discrete episodes of progradation, of an overall retrograding fan. They are composed of a thicker lower interval, dominated by dark grey cm-thick Tde Bouma divisions, and minor thinly bedded fine-grained sandstones. The upper part is made of slightly thicker turbidites incorporating thicker and more frequent sandy layers exhibiting bouma Tcde divisions. Occasional medium- to coarse-grained sandstones with granules and pebbles up to 35 cm thick may exhibit the lower elements of the Bouma sequence (Figure 4.7F). Occasional flute casts, bioturbation, slumps and loading surfaces are observed throughout the Subunit. The uppermost 5 m of the Subunit are made of turbidites exhibiying Tde units.

The reduction of thickness of the cycles, together with homogeneous thin bedding of silts and muds, suggest a progressive reduction of sedimentation rate. This could be due to a decrease in sediment input associated with a rise in relative sea-level or to autocyclic migration of the active lobe. Sand-rich intervals, including coarse-grained beds, indicate overspill from the active channel into the overbank/levee. Overall sedimentation is interpreted to have occurred in a middle fan location, but perhaps in a more distal position than previous Subunits.

Subunit 8

This Subunit comprises 136 m of sand-prone sediments forming three thickening- and coarsening-upward cycles. The cycles themselves get thicker too. The division is not highly intruded by igneous rocks. The density of intrusions affecting the thickness of the sedimentary sequence is about 15%, including two 5 m thick dykes. The real thickness of sediments is 116 m. The net sand content in the division is 65%.

Sandstones are fine- to medium-grained, dm-thick and an alteration of yellow to reddish in colour, with interbedded grey muds. Well-developed bioturbation (Figure 4.7G) and current marks can be found especially in the lower cycle. The higher proportion of coarser sand content of this Subunit indicates a more proximal setting compared to the underlying subdivision. The entire Subunit is interpreted to be part of a lobe complex (Prelat et al., 2009) and the overall sand-prone facies could indicate deposition in a lobe axis position.

Subunit 9

This Subunit has a gross measured thickness of 125 m, and compriese three alternating decametric-scale mud-dominated and sand-dominated intervals. Each interval is quite homogeneous and no cyclicity is evident. Two thick dykes, 2 m and 3.5 m-thick, along with a number of small dykes, results in a reduction by 20% to give a the true thickness of 100 m. The net sand content in the unit is 40%.

One structureless breccia (Figure 4.7H), 0.5 m thick, with mud rip-up clasts up to 7 cm in size, scattered pebbles and very sharp base is intercalated within the upper mud-dominated interval. Occasional bioturbation and flute casts can be found through the whole unit.

The base of the middle sand-prone interval within this sudivision exhibits an erosive contact onto the lower mud-dominated interval (Figure 4.6), interpreted to represent the migration of a lobe complex, sandwiched between two mud-dominated interlobe complexes (Prelat et al., 2009). The absence of a clear trend suggests an aggradational lobe complex.

Subunit 10

This subdivision has a gross thickness of 60 m and composed of two thick sandstone- and mud-dominated packages. It has a dyke density of 50%, giving a true thickness of about 30 m and net sand content is 30%.

Rippled- and small-scale trough cross-bedded, fine-grained sandstone beds dominate the lower package of the unit and can individually be up to 8 cm thick. Mud drapes on the cross-lamination may be present (Figure 4.8A). These are interpreted as turbidites, usually exhibiting Tcd Bouma divisions. The hemipelagic mud is sometimes not preserved and occasionally the parallel-laminated sandstone division is deposited at the base of some of the turbidites. The Subunit exhibits bioturbation in the finer layers at the base of the package. Mudstones in the upper half of the Subunit are dark and massive towards the top and sandstone layers are rarely deposited.

The larger-scale trend is very similar to the underlying division, showing a dominantly aggradational pattern. This is also interpreted as a migrating lobe complex. In this case, the clear erosive base of the sand-prone cycle is missing.

Subunit 11

This gross 28 m thick unit comprises a thinning- and fining- upward mud-dominated subdivision. The majority of the dykes strike north, so the density of intrusions affecting the thickness of the sedimentary sequence is very low and the true thickness is ~ 25 m. Net sand content is about 20%.

This interval is dominated by thinly (mm- to cm-scale) bedded silts and muds with minor interbeds of very fine-grained, calcareous sandstones. Frequent lenticular bedding and sandstone lenses are affected by soft-sediment deformation.

Fine-grained sedimentation and thin bedding suggest quiet overbank deposition in the lower fan.

Subunit 12

With a gross thickness of 115 m, this unit comprises m-scale cycles composed of alternating limestones and very fine-grained calcareous sandstones and cycles of alternating mudstone and calcareous sandstones. The base of this sudivision is in contact with a 40 m-thick igneous intrusion. The density of the dykes is not very high, but some of them run parallel to the bedding, mainly in the lower part of the cycle, so the true thickness is estimated to be reduced to 100 m. Net sand content is 40%.

The finer material in the lower cycle shows rare bioturbation and soft sedimentary deformation. Calcareous sandstone beds can be up to 2 m-thick. The cycles become more calcareous towards the top.

According to the figures provided in previous work of Steiner et al., (1998), this Subunit corresponds to the upper part of the *Main Clastic Unit*; the *Sandstone-Siltstone-Shale Unit of* Robertson, Alastair and Bernoulli, (1982) and Robertson and Stillman (1979) or the *Siltstones and Sandstones with clayey partings* of Rothe (1968). These units are described entirely as clastic in the previous work, with no mention of carbonate components made. We identify an increasing carbonate content, which started in the previous subunit and suggests a gradational evolution into the overlying Pelagic Limestone Unit.

The presence of calciturbidites in this division is interpreted to be due to redeposition of carbonates developed on the shelf, suggesting clastic sediment input from the continent has lowered. Rothe, 1968; Steiner et al., 1998 suggested an age for this part of the Mixed Unit of Albian, linked with a rising sea-level at this time that may have reduced the delivery of clastics to deep basin and favoured carbonate production on the shelf.

Three large-scale sedimentary cycles are interpreted in this study (Figure 4.6) that we interpret as tectonostratigraphic units resulting from the interplay between eustacy and the complex post-rift tectonics in the Aaiun-Tarfaya Basin. These cycles can be correlated with the sedimentary sequences interpreted onshore Morocco (see Chapter 3; Figure 3.9). We interpret the last cycle, fining-upward and increasing carbonate components, can be correlated with the trangressive event registered onshore above SB2 + TS2. The increase in accommodation space in the proximal basin trapped large volumes of sediment and allowed carbonates to develop on the distal shelf.

4.5.1.3 Pelagic Limestone Unit:

The base of this Unit is defined by a 30 m-thick igneous intrusion, after which there is a notable facies change to limestone dominated sediments. Scarce dykes running parallel to the bedding within the unit reduce the true sedimentary estimated thickness down to 36 m, and net sand content (mostly calcareous) is about 50 %.

This study has logged the lower 40 m of this unit, exhibiting stacked decimetre-scale cycles of alternating calcareous sandstones, siltstones and limestones. Micritic limestones frequently appear nodular. The limestones are variable, sometimes replaced by very fine-grained non calcareous sandstones.

This unit is interpreted to be the lower part of the Pelagic Limestone Unit (Steiner et al., 1998). The upper part of the unit was not investigated.

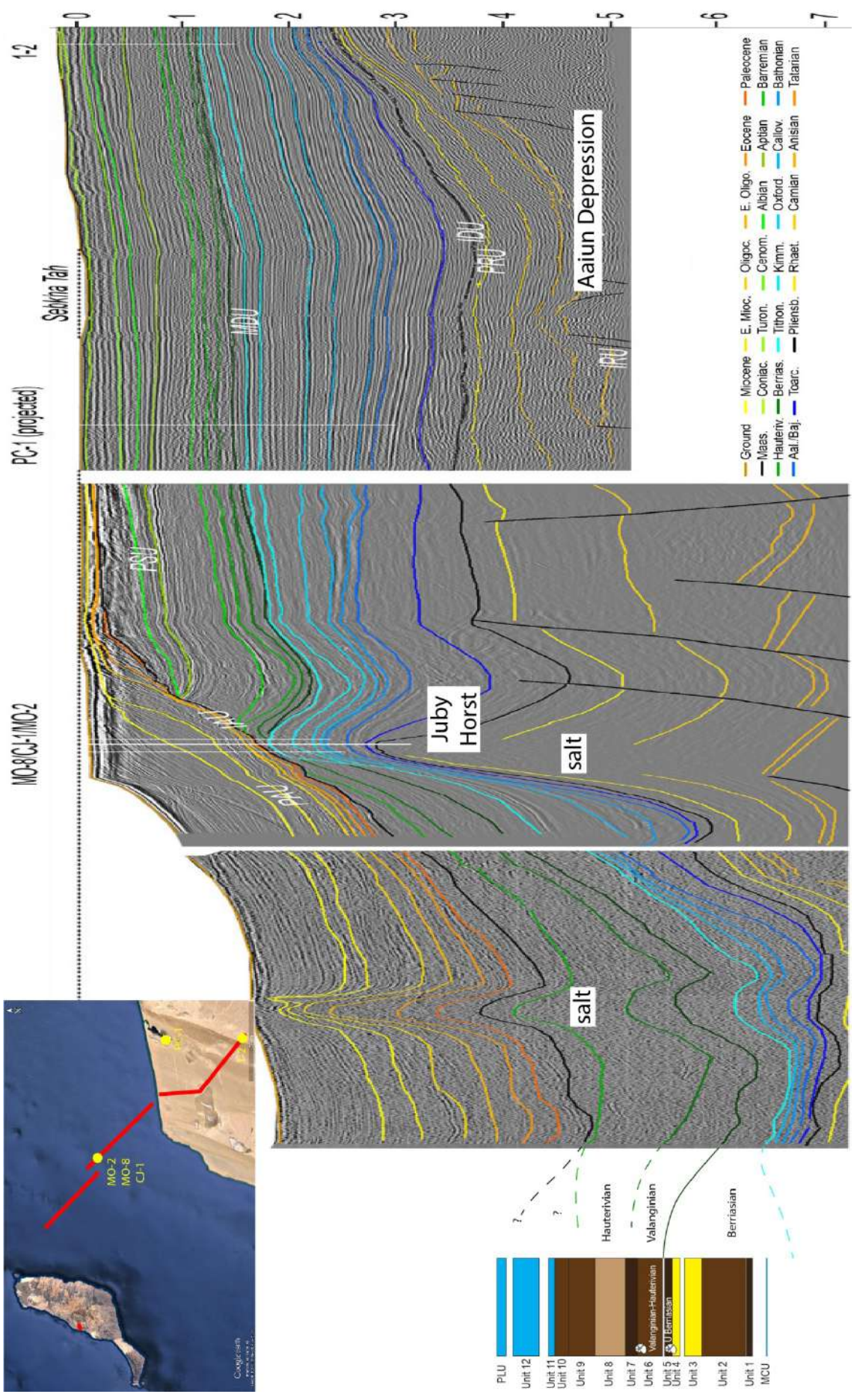
1-2
Sebkha Tah
PC-1 (projected)
MO-8/CJ-1/MO-2
Aaiun Depression
MBU
PRU
PLU
Juby
Horst
salt
salt
Ground
Miocene
E. Mioc.
Oligoc.
E. Oligo.
Eocene
Paleocene
Maas.
Coniac.
Turon.
Cenom.
Albian
Aptian
Barremian
Hauteriv.
Berrias.
Tithon.
Kimm.
Oxford.
Callov.
Bathonian
Aal./Baj.
Toarc.
Pliensb.
Rhaet.
Carnian
Anisian
Tatarian
MO-2
MO-8
CJ-1
Hautervian
Valanginian
Berriasian
Valanginian-Hautervian
U Berriasian
PLU
Unit 12
Unit 11
Unit 10
Unit 9
Unit 8
Unit 7
Unit 6
Unit 5
Unit 4
Unit 3
Unit 2
Unit 1
MCU

Figure 4.10. Correlation of lower Cretaceous turbidites of Fuerteventura with seismic interpreted on the shelf and onshore Morocco. Seismic interpretation modified after (Wenke, 2015). Same horizontal and vertical scale for seismic and schematic succession.

4.5.2 Repetition of stratigraphy

Large-scale folding of the succession was first proposed by Rothe (1968) who interpreted the whole Mesozoic succession exposed in the Betancuria Massif to part of an E-W isoclinal overturned syncline and therefore partially repeated (Figure 4.4). Later work by Robertson and Stillman, (1979) suggested the succession uniformly youngs towards the north. This study supports an overall complete succession, with the presence of only small-scale folding (Figure 4.11). The folding could be later tectonics or related to syn- or early post-depositional sliding.

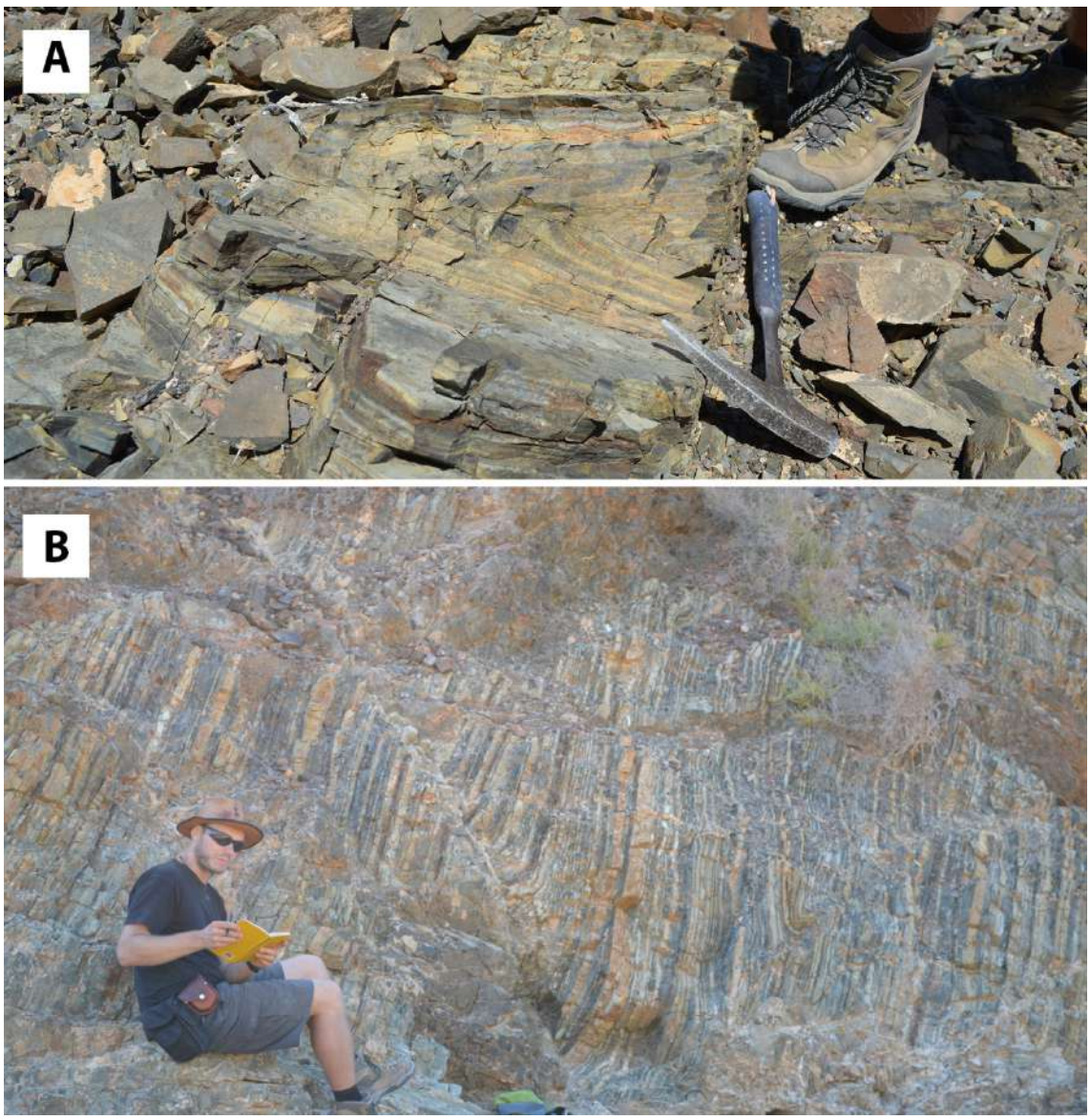

Figure 4.11. Field examples of isoclinal fold at Barranco de la Peña (A) and folds and associated fault at Barranco de los Sojames (B).

At Barranco de la Peña, within Subunit 5, a small tight isoclinal fold was observed (Figure 4.11A) with a subvertical axial plane. The geometry of the fold, class 2 or 3 of Ramsay (1967), suggests a tectonic origin, produced during uplift of the sediments to the present location. At Barranco de los Sojames, a small outcrop exhibits several small-scale folds and associated thrusts (Figure 4.11B). The fractures indicate a post-depositional event when the sediment was already lithified. Furthermore, restoration to horizontal of the hinge lines of these features, using the average bedding of their surroundings, yields an azimuth of 350N and 040N. These directions would correspond with the line of smallest σ3 stress. A hypothetical syn-sedimentary displacement of sediments would be expected at about 90 degrees to these directions, which seems unlikely in a fan system being fed from the SE. In the absence of larger exposures that allow a better assessment of these structures we interpret these folds as tectonic-generated during the construction of the island.

This implies that, although repetition of large parts of the stratigraphy has been ruled out, repetitions at a smaller scale are likely. This fact requires further study and should be considered when estimating the total thickness of the succession.

4.6 Conclusions

The Mesozoic turbiditic succession of Fuerteventura have been re-logged, with the main focus on the lower Cretaceous Main Clastic Unit of Steiner et al., (1998). An updated, more detailed stratigraphic log is presented. A new ammonite discovery and correlation with onshore sections allows further constraint of the age of main sedimentary cycles and transition between the Mixed Clastic Unit, Main Clastic Unit and Pelagic Limestone Unit.

The abundant evidence from the lithologies, sedimentary structutes, bioturbation and stacking pattens, suggest sedimentation took place in a deep marine fan / lobe environment initially dominated by terrigenous sediment, deposited dominantly by turbidity currents.

The early Berriasian is the period of time with higher proportion of sand deposited throughout the succession. Over 200 m of turbidites were logged, that exhibit a large-scale coarsening-upward trend, culminating in a large channel fill, about 50 m thick. This is interpreted to record the progradation of a lobe complex, related with a lowstand sedimentary wedge observed on seismic and developed to the east, at the slope of the

Jurassic carbonate platform and with alluvial fans recorded onshore in outcrop. An ammonite (*Tirnovella* sp.) of late Berriasian age occurring above the last sand-dominated interval has been used to date the termination of this pulse of terrigenous sediment.

A second big-scale progradational coarsening-upward cycle is 265 m thick has a lower sand content. Its base is dated as late Berriasian by the ammonite found in this study. The upper age can be established as pre-Albian based on correlation of big-scale trends with onshore successions.

The upper part of the section becomes increasingly carbonate-prone, with sedimentation of calciturbidites and occasional limestone beds among the clastic turbidites. This is interpreted to be related with a relative sea-level increase in the area during Aptian that triggered carbonate production on the shelf. These carbonates were resedimented by turbiditic currents in distal lobe complexes.

Although the entire succession seems continuous, small tectonic isoclinal folds produce local duplication of parts of the succession. Further mapping is needed in other to assess the effect of these structures on the total thickness of the sequence.

4.7 References

Anguita, F., Hernan, F., 1975. A propagating fracture model versus a hot spot origin for the Canary islands. Earth Planet. Sci. Lett. 27, 11–19. doi:10.1016/0012-821X(75)90155-7

Anguita, F., Hernán, F., 2000. The Canary Islands origin: a unifying model. J. Volcanol. Geotherm. Res. 103, 1–26. doi:10.1016/S0377-0273(00)00195-5

Araña, V., Ortiz, R., 1986. Marco geodinámico del volcanismo canario. An. Física (serie B) 82, 202–231.

Arnott, R.W.C., 2010. Deep marine sediments and sedimentary systems, in: James, N.P., Dalryrmple, R.W. (Eds.), Facies Models 4. Geological Association of Canada, pp. 295–322.

Bouma, A.H., 1962. Sedimentology of some Flysch deposits : a graphic approach to facies interpretation. Elsevier, Amsterdam.

Carracedo, J.C., Day, S., Guillou, H., Rodríguez Badiola, E., Canas, J.A., Pérez Torrado, F.J., 1998. Hotspot volcanism close to a passive continental margin: the

Canary Islands. Geol. Mag. 135, 591–604. doi:10.1017/S0016756898001447

Fúster, J.M., 1975. Las Islas Canarias: un ejemplo de evolucion espacial y temporal del vulcanismo oceanico. Estud. Geol. 31, 439–463.

Haq, B.U., Hardenbol, J., Vail, P.R., 1987. Chronology of fluctuating sea levels since the triassic. Science 235, 1156–1167. doi:10.1126/science.235.4793.1156

Hartung, G., 1857. Die geologischen Verhältnisse der Inseln Lanzarote und Fuerteventura. Neue Denkschriften der Allg. Schweizerischen Gesellschaft für die Gesammten Naturwissenschaften 15, 1–168.

Hinz, K., Dostmann, H., Fritsch, J., 1982. The continental margin of Morocco: seismic sequences, structural elements and geological development, in: von Rad, U., Hinz, K., Sarnthein, M., Seibold, E. (Eds.), Geology of the Northwest African Continental Margin. Springer Berlin Heidelberg, Berlin, Heidelberg, pp. 34–60. doi:10.1007/978-3-642-68409-8

Holik, J.S., Rabinowitz, P.D., Austin, J.A., 1991. Effects of Canary Hotspot volcanism on structure of oceanic crust off Morocco. J. Geophys. Res. 96, 12039–12067. doi:10.1029/91JB00709

Howell, D.G., Normark, W.R., 1982. Sedimentology of submarine fans. AAPG Mem. 31 Sandstone Depos. Environ. 365–404.

Le Bas, M.J., Rex, D.C., Stillman, C.J., 1986. The early magmatic chronology of Fuerteventura, Canary Islands. Geol. Mag. 123, 287–298. doi:10.1017/S0016756800034762

Lowe, D.R., 1982. Sediment gravity flows: II. Depositional models with special reference to the deposits of high-density turbidity currents. J. Sediment. Petrol. 52, 279–297.

Martinis, B., Visintin, V., 1966. Données géologiques sur le bassin sédimentaire côtier de Tarfaya (Maroc méridional), in: Reyre, D. (Ed.), Bassin Sedimentaires Du Littoral Africain. Union Internationale des sciences géologiques, Paris, pp. 13–26.

Morgan, W.J., 1971. Convection plumes in the lower mantle. Nature 230, 42–43.

Prelat, A., Hodgson, D.M., Flint, S.S., 2009. Evolution, architecture and hierarchy of distributary deep-water deposits: a high-resolution outcrop investigation from the Permian Karoo Basin, South Africa. Sedimentology 56, 2132–2154.

doi:10.1111/j.1365-3091.2009.01073.x

Ramsay, J.G., 1967. Folding and Fracturing of Rocks, Folding and Fracturing of Rocks. McGraw-Hill, New York. doi:10.1126/science.160.3826.410

Ranke, U., von Rad, U., Wissmann, G., 1982. Stratigraphy, facies and tectonic development of the On and offshore Aaiun-Tarfaya basin - a review, in: von Rad, U., Hinz, K., Sarnthein, M., Seibold, E. (Eds.), Geology of the Northwest African Continental Margin. Springer-Verlag, pp. 86–105.

Renz, O., Bernoulli, D., Hottinger, L., 1992. Cretaceous ammonites from Fuerteventura, Canary Islands. Geol. Mag. 129, 763–769.

Robertson, Alastair, H.F., Bernoulli, D., 1982. Stratigraphy, facies and significance of Late Mesozoic and Early Tertiary sedimentary rocks of Fuerteventura (Canary Islands) and Maio (Cape Verde Islands), in: von Rad, U., Hinz, K., Sarnthein, M., Seibold, E. (Eds.), Geology of the Northwest African Continental Margin. Springer Verlag Berlin Heidelberg New York, pp. 498–525.

Robertson, A.H.F., Stillman, C.J., 1979. Late Mesozoic sedimentary rocks of Fuerteventura, Canary Islands: Implications for West African continental margin evolution. J. Geol. Soc. London. 136, 47–60. doi:10.1144/gsjgs.136.1.0047

Rothe, P., 1968. Mesozoische Flysch-Ablagerungen auf der Kanareninsel Fuerteventura. Geol. Rundschau 58, 314–332. doi:10.1007/BF01820611

Snedden, J.W., Liu, C., 2010. A Compilation of Phanerozoic Sea-Level Change , Coastal Onlaps and Recommended Sequence Designations. Am. Assoc. Pet. Geol. Search Discov. Artic. 40594 40594, 2004–2006.

Steiner, C., Hobson, A., Favre, P., Stampfli, G.M., Hernandez, J., 1998. Mesozoic sequence of Fuerteventura (Canary Islands): Witness of Early Jurassic sea-floor spreading in the central Atlantic. Geol. Soc. Am. Bull. 110, 1304–1317. doi:10.1130/0016-7606(1998)110<1304

Stillman, C.J., Bennell-Baker, M.J., Smewing, J.D., Fúster, J.M., Muñoz, M., Sagredo, J., 1975. Basal complex of Fuerteventura (Canary Islands) is an oceanic intrusive complex with rift-system affinities. Nature. doi:10.1038/257469a0

von Fritsch, K., 1868. Reisebilder von den Canarischen Inseln. Petermanns Geogr. Mitt. 5, 1–44.

Wenke, A.A.O., 2015. Sequence stratigraphy and basin analysis of the Meso- to Cenozoic Tarfaya- Laâyoune Basins, on- and offshore Morocco. Ruprecht-Karls-Universität Heidelberg.

Wenke, A.A.O., Zühlke, R., Jabour, H., Kluth, O., 2011. High-resolution sequence stratigraphy in basin reconnaissance: example from the Tarfaya Basin, Morocco. first Break 29, 85–96.

Chapter 5

SYNTHESIS AND CONCLUSIONS

5.1 Synthesis

The aim of this thesis was to re-evaluate the sedimentology of the post-rift successions exposed onshore Morocco in the Aaiun-Tarfaya Basin. Initially, the focus was on the lower Cretaceous fluvio-deltaic system, represented by the Tantan Fm (Martinis and Visintin, 1966). For many decades, since the formation was first described in 1966, it has been assumed the entire section exposed onshore along the coast was early Cretaceous in age.

During the course of the project, new sampling and biostratigraphic dating of gastropods and bivalves, supported by benthic foraminifers and calcareous algae, revealed a Bathonian age (Middle Jurassic) for the sediments exposed in the northern margin of the basin, around the city of Sidi Ifni. Thus the sections in the north of the basin did not belong to the Tantan Fm. No middle Jurassic stratigraphy had previously been established for the basin, as the only Jurassic formation formally described to date in the basin was the upper Jurassic Puerto Cansado Fm (Martinis and Visintin, 1966). A new subdivision in three formations is been proposed for the Bathonian. The entire succession records an overall deepening, despite his being contemporary with a global Bathonian eustatic sea-level fall, suggesting a tectonic control on accommodation in the basin at this time. The implications for the hydrocarbon exploration in the area are significant as the new age of the outcrops represents an interesting new input parameter in depositional models for oil exploration.

No age dates were obtained from the underlying red beds, which are exposed from Sidi Ifni north to Gueriza Beach, but by superposition these are suggested to be Liassic or possibly Triassic in age.

The clastic-dominated Tantan Fm. was studied along two transects, at Oued Draa and Oued Chebeika. The original previously published work in the 1950's and 1960's focused on regional mapping and provided a broad sedimentological interpretation of depositional environments, without detailed vertical and lateral facies logs and no discussion of the evolution of the system. In addition, specific locations of logs, or exact collection points of age-diagnostic fossils were not documented.

The work for this project focused on collecting the complete detailed stratigraphy of the Tantan Fm. in order to compare, correlate and interpret vertical and lateral facies changes. The higher resolution and level of detail applied has allowed the delimitation of 16 facies, within 9 facies associations, that can be assigned to specific depositional

environments. These have been correlated between the two transects to elucidate lateral facies variations.

This study also identified a continental to peritidal sand-dominated unit more than 150 m thick, along the Oued Chebeika transect, sandwiched between two marine intervals, that had never been previously reported. Based on new age-diagnostic biomarkers found in the field, compiled with previous biostratigraphic data from the literature, an Aptian to early Albian age has been assigned for this interval. This contradicts the widespread belief of marine facies draping this part of the basin at that time.

The Tantan system has been traditionally interpreted as a large delta prograding towards the NW. Palaeocurrent measurements from sedimentary structures in the continental sections show an overall transport direction in the study area towards the north. Lateral facies variation between the two transects also suggest a palaeocoastline oriented approximately ENE-WSW in this part of the basin. Together, they suggest a provenance area mainly located from the south (i.e. the Reguibat Shield, WAC) with an occasional local sediment supply coming from the Western Anti-Atlas, as evidenced by punctuated changes in palaeocurrents in specific units. The location of source terranes from exhuming basement, and the alternation between a local supply from the Anti-Atlas and the more regional input from the large cratonic terranes of the Reguibat Shield are supported by recent studies of exhumation and subsidence episodes in the hinterland.

The entire Tantan Fm. exhibits an overall evolution from proximal continental to more distal marine depositional environments. Onshore sedimentary sequences hundreds of meters thick are recorded by the interplay between the early Cretaceous sea-level rise and an enhanced basin subsidence. Despite the overall early Cretaceous eustatic sea-level rise, the interpreted driving mechanism for this sedimentary filling is tectonic.

Preservation of km-scale sedimentary sequences was allowed by an enhanced post-rift subsidence of the basin coupled with pulsating exhumation periods of the Reguibat Shield and Western Anti-Atlas, with eustacy acting as a modulating factor. Despite the accommodation created, considerable volumes of sediment were delivered to the offshore basin, as demonstrated by thick successions imaged in seismic.

The wide shelf during the early Cretaceous is suggested to have acted as a sink for coarse clastic sediment in the proximal locations now exposed onshore, probably allowing little sand to reach distal parts of the shelf, where the drilling has been focused

for decades. Sand-prone facies are conspicuous onshore and possibly in the shallow shelf but scarcely encountered in the outer shelf.

The distal deep water equivalent of the Tantan Fm. is exposed in Fuerteventura. Three large-scale cycles are recorded in this part of the succession. The lower two are progradational cycles of lower to middle submarine fans of clastic turbidites. The last of the cycles is retrogradational recording a decrease in mud content and increase in calciturbidites upwards and linked with the eustatic sea-level rise during Aptian. A well-preserved ammonite (*Tirnovella* sp.) of late Berriasian age was found immediately above the interval with highest sand proportion. This is interpreted as the distal counterpart of the Berriasian lowstand wedge that has been mapped in seismic previously at the slope of the Jurassic platform, and correlated with the alluvial fan conglomerates at the base of the Tantan Fm. exposed onshore. The upper part of the succession could not be dated.

The increase in carbonate-rich turbidites suggests, re-deposition of carbonates being developed on the shelf under increasing sea-level conditions during Aptian. This is correlated with fluvial, peritidal and shallow marine intervals of the Red Upper Sandstone member onshore Morocco.

The increase in accommodation space reflects a combined effect of tectonic subsidence of the basin and the eustatic rise during this time. The lower Berriasian is the most promising interval in terms of reservoir facies although the high water depth and the thick sedimentary pile make it a high risk target.

5.2 Key questions

The main goal of this project was to improve the framework of the Tantan Fm. in terms of sequence stratigraphy, biostratigraphy and sedimentology and place it into a regional context. Five objectives were defined and the main findings are listed below.

5.2.1 Reinterpret the coastal sections in the northern tip of the Aaiun-Tarfaya Basin, next to Sidi Ifni, and sample extensively for biostratigraphy.

Thick successions of red conglomerates and sandstones in this area have been traditionally interpreted as part of the Tantan Fm. overlain by mixed limestones and fine-grained clastics assigned to the Aguidir Fm, all previously dated as Cretaceous.

Detailed sedimentary logging of the mixed system and extensive macrofossils sampling has allowed a complete reinterpretation of these sections.

- The new Bathonian dates for the Craima section (see objective 2) revises previous interpretations.
- Three new formations have been proposed for this interval.
- An outcrop-based high-resolution sequence stratigraphic framework has been developed for the first time in the basin.
- A pre-Bathonian age (Triassic to Liassic) has been established for the thick (~180 m) basal conglomeratic succession interpreted as alluvial fans fed from the Ifni inlier.
- An overall deepening-upwards succession is recorded during the Bathonian eustatic sea-level drop. Tectonics is the main driver for the deposition of these units. Basin subsidence combined with exhumation pulses in the Ifni inlier (Anti-Atlas) provided the accommodation space and topography for the sediment to be eroded and preserved.

5.2.2 Re-date the successions with new collections of macro and microfossils, pollen and spores.

The study has utilised fossil groups not commonly used for biostratigraphic purposes, such as gastropods and bivalves, used in the absence of “classical” species such as ammonites or foraminifera, which were not recovered from the sections or belonged to long-ranging groups. A summary of the findings for the three areas under study follows:

Ifni:

- The peritidal to shallow marine succession was definitely dated as Bathonian using bivalves and gastropods fossil assemblages.
- Long-ranging groups of benthic foraminifers and calcareous algae also supported the Jurassic age.

Tantan:

- The first marine transgression recorded inland was dated as Aptian by the presence of Plicatula-type oysters in shoreface deposits.

- The second marine transgression was dated as late Albian by the presence of one specimen of *Cymatoceras* albense.
- The upper part of the succession is dated as late Albian to Cenomanian based on the presence of dinoflagellates and palynomorphs in offshore clays.

Fuerteventura:

- One ammonite specimen (*Tirnovella* sp.) found in the turbiditic succession yielded a late Berriasian age.

5.2.3 Construct a vertical composite sedimentary log along two parallel transects, Oued Draa and Oued Chebeika and compare with the original descriptions and interpretations.

Despite good exposures, the onshore sections had not been re-examined during the last 5 decades and previous interpretations accepted without question and used for models for hydrocarbon exploration. The new results from this study provide high-resolution vertical composite sedimentary logs along two transects. Although they confirmed a similar evolution to that reported previously, the higher level of detail revealed significant differences on specific facies associations and identified important spatial shifts of the system. The most significant is a ~150 m thick sand-prone continental and peritidal interval along Oued Chebeika described in this thesis that had been previously considered as marine facies. This work also for the first time developed a regional depositional model through time and addressed the controls on the system, and its correlation offshore.

- The Tantan Fm. has been subdivided in six lithostratigraphic units that incorporate the previous *Draa Marls Member* of Martinis and Visintin (1966). Two basin-scale transgressive events are recorded during Aptian and Albian.
- The Tantan Fm. is made of four depositional sequences. The lower one is a Falling Stage systems Tract represented by alluvial fan facies.
- The overlying sequence is the most complete including a LST, TST and HST. It is bounded at the base by a SB at the northern sections and an amalgamated SB and transgressive surface at the southern sections. It is mainly made of continental facies that interfinger with peritidal fine-grained clastics towards the

top. Significant thickness variation is registered at this time. The age of this sequence is pre-Aptian, likely Valanginian to Barremian.

- The third sequence starts with a TST over an amalgamated SB and TS that floods the entire area of study. The succession evolves upwards in a continental (proximal) and peritidal/shallow marine (distal) HST more than 100 m thick.
- The last sequence exposed is incomplete and only a TST can be recognized. The contact with the underlying sequence is also through an amalgamated SB and TS.
- Correlation between transects and palaeocurrent measurements suggest advance and retreat of the system along an approximate NNW-SSE direction.
- Available biostratigraphic markers date the first marine incursion registered onshore as Aptian (see above).
- The thick successions recorded onshore and offshore are the result of combined sea-level rise and basin subsidence. The coarse fraction of the sediment was trapped in proximal locations of the basin depositing mainly fine-grained clastics and carbonates offshore. Pulsating uplifts in the Reguibat Shield and Western Anti-Atlas provided enough volume of sediment to develop km thick sequences offshore.

5.2.4 Correlate the two transects assisted by biostratigraphic markers and sequence stratigraphy.

The parasequences interpreted along both transects, assisted by the available biostratigraphic markers collected in the field (see objective 2) and compiled from the literature, allowed the first correlation between transects in the area and a better understanding of the evolution of the Tantan system through time. The main palaeogeographic implication of this correlation is that the northern Oued Draa transect represents more distal settings than along Oued Chebeika. This allows delineation of a shoreline with an approximate E-W orientation, contrary to the approximate NE-SW interpreted in the past. Improved palaeogeographic reconstructions and depositional model have been developed for this part of the basin.

5.2.5 Re-examine the distal deep-water equivalent of the Tantan Fm. exposed in Fuerteventura.

The overall interpretation of a Cretaceous turbiditic succession in Fuerteventura broadly confirms interpretations of previous work in the area. This study has improved the resolution by detailing two large-scale coarsening-upwards cycles with significant sand content overlain by fining-upward cycle with increasing carbonate content. The presence of an ammonite (see objective 2) constrained the age of the first of these cycles to early Berriasian, the interval with more sand. This can be linked with the eustaic sea-level drop that occurred in the Berriasian and reworked shelf material into deep-water fans. This interval can be linked with the alluvial fans exposed onshore interpreted as time equivalent.

The calciturbidites at the top of the succession were deposited by reworking of shelf carbonates during the Aptian and Albian retreat of the Tantan delta. Increasing sea-level coupled with basin subsidence trapped much of the clastic sediment in more proximal positions allowing the development of carbonates.

5.3 Future questions

5.3.1 Dating – early Cretaceous biostratigraphy of the Tantan Fm.

Extensive fieldwork during this project has evidenced that classical age-diagnostic marine fossil groups like ammonoids or planktonic foraminifers are scarce in the area. Nevertheless, gastropods and bivalves are extremely abundant in marine facies and have proven themselves a useful biostratigraphic tool at least to the stage level (see chapter 2). The new framework provided for the Tantan Fm. in this project could benefit greatly from a follow-up project with a strong palaeontological component. This would include tdating and refining the depositional environments interpretation using fossil assemblages and investigation of new outcrops not visited during this project.

5.3.2 Provenance

In order to understand better the basin context, size of drainage area and timing of sediment delivery to the basin, the provenance of clastic material should be addressed. A provenance from the Reguibat Shield during early Cretaceous has been already proposed (Ali et al., 2014). The significant post-rift vertical movements demonstrated in recent studies (e.g. Bertotti and Gouiza, 2012; Charton et al., 2017; Ghorbal et al., 2008;

Gouiza et al., 2017a, 2017b) in the area for different basement terranes are likely to have left different signatures in the sediments record. Systematic changes in palaecurrents recorded throughout the stratigraphy are interpreted as tectonic-induced rather than autocyclic evolution of the system. Abundant feldspars and heavy minerals observed in thin section indicate the feasibility of this project.

5.3.3 Sediment partitioning

Significant amount of sand is exposed onshore in both continental and marine successions. Oil and gas exploration offshore has only located thin clastic reservoir facies. Continuous exposures of marine units subparallel to depositional dip between Oued Chebeika in the south and Oued Draa in the north and beyond might reflect systematic variations in grain size and sub-depositional environments. This could be extrapolated and applied to well data offshore in order to understand how the sediment is partitioned in the basin and the influence in reservoir predictability.

5.3.4 Smara sections

A prolongation of the present PhD could be started 150 km to the south in the Smara region as a multidisciplinary project integrating outcrop and sub-surface data. Continuous, easily accessible lower Cretaceous outcrops exposed in the area would allow the development of an outcrop-based sequence stratigraphic framework to correlate with the Tantan area. Numerous onshore wells penetrating lower Cretaceous sediments in the area and vintage 2D seismic could be integrated in the project if access was granted. Understanding the evolution of the Boujdour delta and its relationship with the Tantan delta to the north would give a larger basin-scale dimension within a source-to-sink study for NW Africa.

5.3.5 Jurassic in the Aaiun-Tarfaya Basin

This PhD has proven the presence of Jurassic sediments exposed in the basin for the first time (chapter 2). The sediments at the Ifni inlier constitute the only Jurassic outcrops, south of the Agadir-Essaouira Basin, in the whole NW Africa. This provides a unique opportunity to get insight of the basin evolution during a period of time only known from wells so far. Besides the sedimentological point of view the project could benefit from a structural study of the Precambrian basement of the Ifni inlier and the tectonostratigraphic relationships with its sedimentary cover.

5.4 References

Ali, S., Stattegger, K., Garbe-Schönberg, D., Frank, M., Kraft, S., Kuhnt, W., 2014. The provenance of Cretaceous to Quaternary sediments in the Tarfaya basin, SW Morocco: Evidence from trace element geochemistry and radiogenic Nd–Sr isotopes. J. African Earth Sci. 90, 64–76. doi:10.1016/j.jafrearsci.2013.11.010

Bertotti, G., Gouiza, M., 2012. Post-rift vertical movements and horizontal deformations in the eastern margin of the Central Atlantic: Middle Jurassic to Early Cretaceous evolution of Morocco. Int. J. Earth Sci. 101, 2151–2165. doi:10.1007/s00531-012-0773-4

Charton, R., Bertotti, G., Arantegui, A., Bulot, L.G., 2018. The Sidi Ifni transect across the rifted margin of Morocco (Central Atlantic): Vertical movements constrained by low-temperature thermochronology. J. African Earth Sci.

Ghorbal, B., Bertotti, G., Foeken, J., Andriessen, P., 2008. Unexpected Jurassic to Neogene vertical movements in “stable” parts of NW Africa revealed by low temperature geochronology. Terra Nov. 20, 355–363. doi:10.1111/j.1365-3121.2008.00828.x

Gouiza, M., Bertotti, G., Andriessen, P., 2017a. Mesozoic and Cenozoic thermal history of the western Reguibat Shield (West African Craton). Terra Nov.

Gouiza, M., Charton, R., Bertotti, G., Andriessen, P., Storms, J.E.A., 2017b. Post-Variscan evolution of the Anti-Atlas belt of Morocco constrained from low-temperature geochronology. Int. J. Earth Sci. 106, 593–616. doi:10.1007/s00531-016-1325-0

Martinis, B., Visintin, V., 1966. Données géologiques sur le bassin sédimentaire côtier de Tarfaya (Maroc méridional), in: Reyre, D. (Ed.), Bassin Sedimentaires Du Littoral Africain. Union Internationale des sciences géologiques, Paris, pp. 13–26.